

University of Groningen

Vanadium complexes containing amido functionalized cyclopentadienyl ligands

Witte, Petrus Theodorus

IMPORTANT NOTE: You are advised to consult the publisher's version (publisher's PDF) if you wish to cite from it. Please check the document version below.

Document Version

Publisher's PDF, also known as Version of record

Publication date:

2000

[Link to publication in University of Groningen/UMCG research database](#)

Citation for published version (APA):

Witte, P. T. (2000). *Vanadium complexes containing amido functionalized cyclopentadienyl ligands*. [s.n.].

Copyright

Other than for strictly personal use, it is not permitted to download or to forward/distribute the text or part of it without the consent of the author(s) and/or copyright holder(s), unless the work is under an open content license (like Creative Commons).

The publication may also be distributed here under the terms of Article 25fa of the Dutch Copyright Act, indicated by the "Taverne" license. More information can be found on the University of Groningen website: <https://www.rug.nl/library/open-access/self-archiving-pure/taverne-amendment>.

Take-down policy

If you believe that this document breaches copyright please contact us providing details, and we will remove access to the work immediately and investigate your claim.

Downloaded from the University of Groningen/UMCG research database (Pure): <http://www.rug.nl/research/portal>. For technical reasons the number of authors shown on this cover page is limited to 10 maximum.

Front cover: De Schaduw

Copyright Dick Bruna ©



This research has been financially supported by the Council of Chemical Sciences of the Netherlands Organization for Scientific research (CW-NWO).

Rijksuniversiteit Groningen

Vanadium Complexes
Containing
Amido Functionalized Cyclopentadienyl Ligands

PROEFSCHRIFT

ter verkrijging van het doctoraat in de
Wiskunde en Natuurwetenschappen
aan de Rijksuniversiteit Groningen
op gezag van de
Rector Magnificus, Dr. D.F.J. Bosscher
in het openbaar te verdedigen op
vrijdag 8 december 2000
om 16.00 uur
door

Petrus Theodorus Witte

geboren op 4 maart 1970
te Den Burg, Texel

Promotor: Prof. Dr. J.H. Teuben

Co-promotor: Dr. B. Hessen

Beoordelingscommissie: Prof. Dr. R.M. Kellogg

Prof. Dr. G. van Koten

Prof. R. Poli

Contents

Dankwoord

Chapter 1 1
General Introduction

Chapter 2 13
Synthesis of vanadium(V) complexes containing amido functionalized
cyclopentadienyl ligands

Chapter 3 37
Generation of cationic vanadium(V) complexes

Chapter 4 59
Olefin coordination towards cationic d^0 vanadium complexes

Chapter 5 83
Synthesis of di-, tri- and tetravalent vanadium complexes

Samenvatting / Summary

Dankwoord

Voordat dit proefschrift "echt" begint, wil ik de mensen bedanken die geholpen hebben bij het tot stand komen ervan. Allereerst mijn promotor Jan Teuben. In het begin botsten we nog wel eens, maar ik kijk met plezier terug op mijn vijf jaar in Groningen. Nadat ik ongeveer een jaar in Groningen was, kwam Bart Hessen als UHD onze groep versterken. Zijn enthousiasme voor zijn oude jeugdliefde Vanadium heeft er voor gezorgd dat dit boekje een stuk dikker is geworden dan ik ooit gedacht had.

De leden van de beoordelingscommissie Prof. Dr. R.M. Kellogg, Prof. Dr. G. van Koten en Prof. R. Poli wil ik bedanken voor het doornemen van het manuscript en de suggesties die daaruit volgden.

Een proefschrift waarvan anderhalf hoofdstuk gebaseerd is op NMR-schaal reacties kan niet geschreven worden zonder een goed NMR-team. Henk Druiven, Wim Kruizinga, Jan Herrema en Klaas Dijkstra, bedankt voor jullie hulp bij alle LT, RT, HT, ^1H , ^{13}C , ^{19}F , ^{31}P , ^{51}V , COSY, NOESY en HETCOR metingen. En als het niet lukte met NMR, omdat de verbindingen paramagnetisch waren, dan stond Auke Meetsma paraat voor een kristalstrukturbepaling. Verder bedank ik alle vaste medewerkers voor hun ondersteunend werk, met name Harm Draaijer, Jan Ebels en Jannes Hommes voor het uitvoeren van de element analyses, Oetze Staal voor het doen van de polymerisatie-experimenten, Andries Jekel voor de GPC en GC-MS metingen, Jan Helmantel voor technische ondersteuning, Berend Kwant voor het gebruik van de dichtheidsmeter, en Peter Budzelaar voor de theoretische berekeningen en nuttige tips voor de discussie hierover.

Ook voor het praktische werk heb ik de nodige ondersteuning gekregen.

Allereerst mijn enige hoofdvakstudent Ton Hubregtse. Helaas heb ik hem een onderzoeksvorstel gegeven waarin vooral ligandvariaties voorgesteld werden die onduidelijke of instabiele verbindingen opleverden. Toch heeft hij veel

belangrijke informatie weten te krijgen over de niet gebrugde Cp-amido complexen. I would like to thank Hans Grablowitz and Stéphanie Catillion for their contributions to this thesis. Although both of them only stayed in the lab for a short time, their synthetic work was a big help for me.

Als ik iets geleerd heb tijdens mijn verblijf in Groningen, dan is het wel dat voor goed werk een goede sfeer noodzakelijk is. Patrick, jij bent er mede verantwoordelijk voor dat mijn sportieve uitspattingen nu alleen nog maar plaatsvinden in de kroeg. Al die avonden snookeren, darten, poolen en visueel-vrijgezellen deden mij veel goed. Maar ook de avonden met de klaverjasclub (Tessa, Loes, Marco1, Marco2, Patrick en Cindy) en de kookclub (Isabel, Sergio, Giansiro, Marco, Patrick, Cindy en Stéphanie) zal ik niet snel vergeten. Ik bedank verder alle zaal- en labgenoten voor goede discussies in de labzaal en foute in de koffiekamer: Bas, Beatrice, Bodo, Chris, Daan, Dirk, Edward, Erik, Esther, Geert-Jan, Hans, Helena, Jeannette, Jeroen, Johan, Joop, Kees, Koert, Luis, Marc, Marten, Menno, Minze, Nathalie, Patrick, Piet-Jan, Pietro, Reinder, Reinout, Stephan, Susanna, Thomas, Weidong, Winfried, Wolter en Wouter. Met een speciale vermelding voor Gerda, met wie ik menig sneakje heb meegepikt (en bedankt voor de tekeningen!).

Mijn ouders wil ik bedanken voor hun liefde voor en interesse in mij, ook als ik weer eens weken niets van me liet horen. Het is heerlijk om te weten dat ik altijd iemand heb om bij aan te kloppen.

Tot slot Judith. Bedankt, voor alles wat je in de afgelopen jaren voor me gedaan hebt, maar vooral omdat je tijdens mijn schrijfperiode kon tolereren dat ik bij je in kwam wonen, terwijl ik met mijn gedachten juist steeds verder weg ging.

A handwritten signature in black ink, appearing to read "Peter". The signature is stylized with a large, sweeping loop at the beginning and a horizontal line underneath.

Chapter 1

General Introduction

1.1 Ziegler-Natta catalysts for olefin polymerization

In the 1950's Ziegler *et al.* investigated the reaction of tri-ethyl aluminum with ethene. They found that traces of colloidal nickel change the course of the reaction to ethene dimerization, and almost exclusive formation of 1-butene.¹ This led to a systematic search of the use of other metal salts as possible catalysts in this reaction. The investigators found that traces of metal salts of the group 4, 5 and 6 metals in combination with aluminum alkyls catalyzed the polymerization of ethene to linear HDPE (High Density PolyEthylene), even at low pressures and temperatures,¹ while at that time industrial processes were only able to make branched LDPE (Low Density PolyEthylene).^{1,2} Shortly after Ziegler's discovery, Natta reported the stereospecific polymerization of propene to isotactic polypropene, using Ziegler's $\text{TiCl}_4/\text{AlEt}_3$ catalyst.³ Before this discovery polypropylene was of low molecular weight, had uninteresting properties and no commercial value.⁴

Nowadays, most commercial processes still use TiCl_4 based catalysts with aluminum alkyl cocatalysts, but with the current technology polymer yields exceed 20 kg of polymer per gram of catalyst, with an isotactic index of 95%.⁴ World wide, millions of tons of polyolefins are nowadays produced using Ziegler-type catalysts.⁵

1.2 Vanadium based catalysts

There are several differences between vanadium and titanium based Ziegler-Natta catalysts. Most importantly, vanadium based Ziegler catalysts are unique in their ability to incorporate comonomers in a random order, an important characteristic to produce an amorphous, elastomeric product.⁵ In

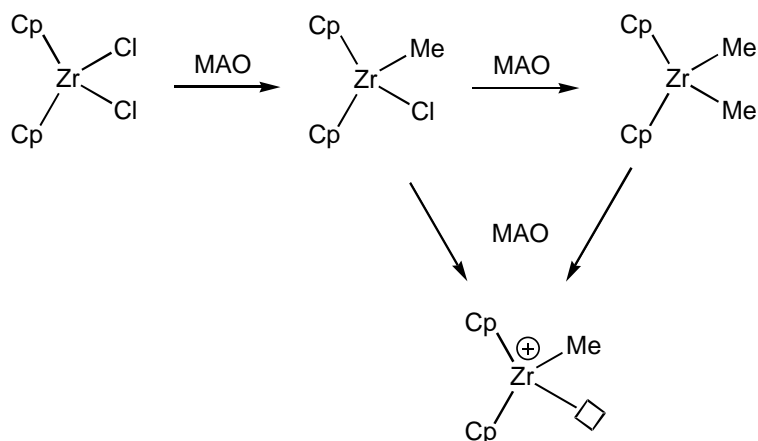
industry, vanadium based catalysts are generally used in the production of Ethylene-Propylene copolymers (EPM; M stands for saturated back-bone) and Ethylene-Propylene-Diene terpolymers (EPDM).⁵

Titanium based Ziegler catalysts form heterogeneous systems, which contain multiple active sites and therefore produce a polymer with a broad molecular weight distribution⁶ ($M_w/M_n = 3 - 7$).^{7,8} In contrast, vanadium based Ziegler systems are soluble and single-site, as indicated by the narrow molecular weight distribution of the produced polymer ($M_w/M_n < 3$).^{8,9}

A long standing question in the chemistry of vanadium based Ziegler catalysts is the oxidation state of the active species. Early studies already indicated that vanadium(0) and vanadium(I) species were inactive, but it was unclear whether the active species was in an oxidation state of +2, +3 or +4.¹⁰ Nowadays, the generally accepted idea is that the active species is formed by reduction of the vanadium(IV) or vanadium(V) catalyst precursor by the aluminum cocatalyst, to form a vanadium(III) alkyl species. However, since the vanadium appears to be further reduced to inactive vanadium(II) species, organic halides (for instance butyl-perchloro-crotonate ester) are added to the reaction mixtures to reoxidize the vanadium to the +3 oxidation state.¹¹

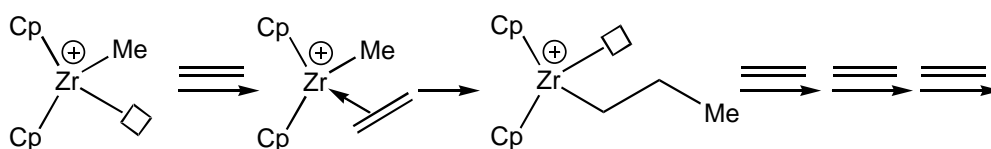
1.3 Single-site catalysts

Soluble catalysts based on group 4 metallocenes were initially used as simple model compounds for the heterogeneous Ziegler catalysts, but became an important and independent class of catalysts after the discovery of MAO (MethylAluminOxane, formally $[AlMeO]_n$) as a powerful cocatalyst. The narrow molecular weight distribution of the produced polymer ($M_w/M_n < 3$) indicates that these soluble catalysts, just as the soluble vanadium catalysts, are single site catalysts.¹²



Scheme 1

Studies on the activation of metallocenes by MAO reveal that high MAO/metallocene ratios are necessary to generate an active species. When the catalyst precursor Cp_2ZrCl_2 is treated with MAO, the metal is alkylated to generate Cp_2ZrMeCl and, when an excess of MAO is used, Cp_2ZrMe_2 . When the ratio Al/Zr exceeds 200, methyl or chloride abstraction generates the cationic species $[\text{Cp}_2\text{ZrMe}]^+$ (Scheme 1).¹³ This cationic species is now recognized as the active species in olefin polymerization.¹⁴ The polymerization is believed to take place by coordination of the olefin to the vacant side of the cationic metal center, and subsequent insertion into the metal-alkyl bond, as previously described for Ziegler-type catalysts (Scheme 2).¹⁵



Scheme 2

An advantage of the metallocene derived catalysts is that their properties can be tuned by rational ligand modifications. By connecting the two Cp moieties of the achiral metallocenes the ligand system becomes rigid (*ansa*-metallocenes, Figure 1A);¹⁶ after introduction of substituents on the Cp rings

stereoselective polymerization of propene is possible. When one Cp moiety is replaced by an amido group, the metal becomes more open and electron deficient (constrained geometry catalysts, Figure 1B);¹⁷ this catalyst shows a random incorporation of α -olefins in copolymerizations. Additional advantages of the constrained geometry catalysts over the *ansa*-metallocenes are the higher stability towards MAO, the higher thermal stability, and the higher molecular weight of the produced polymer. Recently, new catalysts have been developed based on late transition metals (Figure 1C);¹⁸ in general late transition metals are more tolerant towards functional groups.

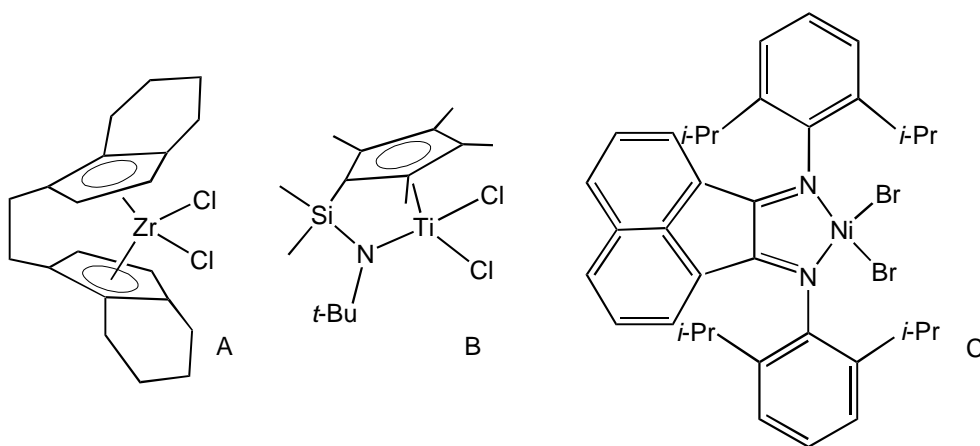
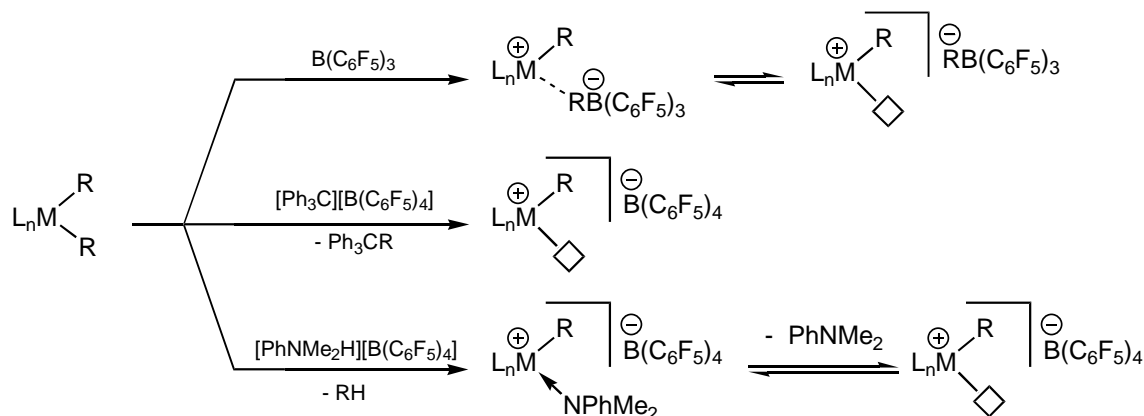


Figure 1: Examples of soluble catalyst precursors.

1.4 Well defined cationic complexes

Although the role of MAO in generating catalytically active cationic species is now reasonably well understood, the exact composition of MAO is still unknown.¹⁹ Furthermore, a large excess of the cocatalyst is necessary to generate the active species, which makes the study on these systems difficult. However, the development of alternative methods for the generation of cationic species has led to an extensive research in this field. Here we will describe three of these methods, all of which use neutral metal alkyl complexes (preferably methyl or benzyl species) as catalyst precursor.



Scheme 3

Alkyl abstraction from the di-alkyl complex L_nMR_2 ($R = \text{Me}$ or CH_2Ph) with the Lewis acidic borane compound $B(\text{C}_6\text{F}_5)_3$ generates $[L_nMR][\text{RB}(\text{C}_6\text{F}_5)_3]$ (Scheme 3).²⁰ The $[\text{RB}(\text{C}_6\text{F}_5)_3]^-$ anion can remain coordinated to the cationic metal center (by the methyl²⁰ or phenyl²¹ group), or dissociate, depending on the circumstances (for instance: solvent polarity, steric hinderance of L, ect.).

Alkyl abstraction with the trityl cation of $[\text{Ph}_3\text{C}][\text{B}(\text{C}_6\text{F}_5)_4]$ generates a cationic complex with a weakly coordinating anion, $[L_nMR][\text{B}(\text{C}_6\text{F}_5)_4]$ and Ph_3CR (Scheme 3).²² Although a weak interaction of the fluorine atoms of the anion with the cationic metal center in $[\text{Cp}^*\text{ThMe}][\text{B}(\text{C}_6\text{F}_5)_4]$ is observed in the solid state,²³ the anion is dissociated in solution.

Protonation of L_nMR_2 with the Brønsted acid $[\text{PhNMe}_2\text{H}][\text{B}(\text{C}_6\text{F}_5)_4]$ generates $[L_nMR][\text{B}(\text{C}_6\text{F}_5)_4]$, RH and PhNMe_2 (Scheme 3).²⁴ This last method generates a cationic metal center with the weakly coordinating $[\text{B}(\text{C}_6\text{F}_5)_4]^-$ anion, but the PhNMe_2 that is also generated can block the free coordination site on the metal. This can be overcome by using amines with large substituents.²⁵

1.5 Well-defined vanadium catalysts

The studies on ligand systems and cocatalysts described above have almost all been performed on group 4 metal complexes. Only relatively recently have well-defined catalysts based on middle and late transition metals been

described in literature.¹⁸ Despite the increasing number of metals used in olefin polymerization, the number of well-defined vanadium catalysts is very limited.

In analogy to the group 4 single-site catalysts, the vanadocene dichloride Cp_2VCl_2 was investigated as a catalyst precursor. The vanadium complex is activated by aluminum halo alkyls to generate an ethene polymerization catalyst, however, there are indications that the Cp_2V moiety does not remain intact.²⁶ This was further demonstrated by the generation of the cationic species $[\text{Cp}_2\text{VMe}]^+$, which is unreactive towards ethene under a variety of reaction circumstances (various counter anions, solvents, temperatures and ethene pressures).²⁷ Apparently the 14 valence electron species $[\text{Cp}_2\text{TiR}]^+$ is an active catalyst, while the 15 valence electron species $[\text{Cp}_2\text{VR}]^+$ is not. Probably, the extra electron in the vanadium complex occupies the orbital necessary for monomer coordination (Scheme 2). Similar differences are found between the isostructural Cp^*_2ScH and Cp^*_2TiH . While the 14 valence electron scandium species is active in olefin polymerization,²⁸ the 15 valence electron titanium species only reacts by a single ethene insertion.²⁹

The isolobal relationship between the group 4 metallocenes and the group 5 half-sandwich imido complexes (Figure 2A), has led to the investigation of these last species, and their isolobal hydrotris(pyrazolyl)borate (Tp) analogues (Figure 2B), as possible catalyst precursors.³⁰ Both type of complexes are activated by MAO to polymerize ethene, although the exact nature of the active species is unknown.

More recently, new non-Cp vanadium complexes have been investigated as possible catalyst precursors (Figure 2C - F).³¹ Although these complexes are active catalysts when activated by aluminum halo alkyls (complexes C and D) or MAO (complexes E and F), no significant activities were observed after activation of the di-alkyl species of complexes D - F with $\text{B}(\text{C}_6\text{F}_5)_3$.

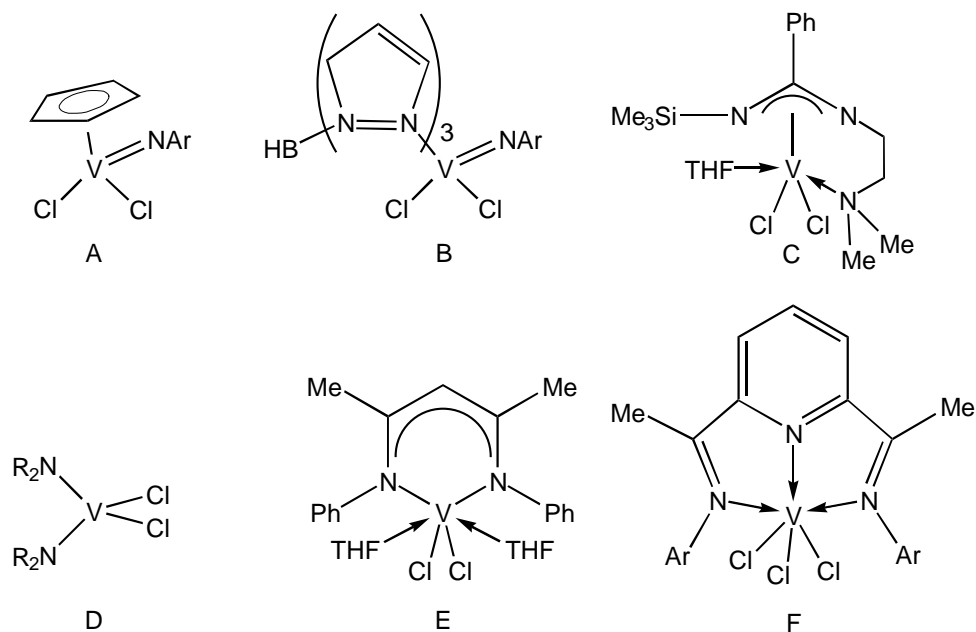


Figure 2: Example of soluble vanadium catalyst precursors.

Theopold *et al.* report that the cationic vanadium(III) alkyl complex $[LVMe(OEt_2)(THF)][B\{3,5-(CF_3)_2-C_6H_3\}_4]$ ($L = N,N$ -diphenyl-2,4-pentadiimine, Figure 3) is an active polymerization catalyst. Unfortunately, characterization of the catalyst and details about the polymerization experiments have not been reported so far.^{31d}

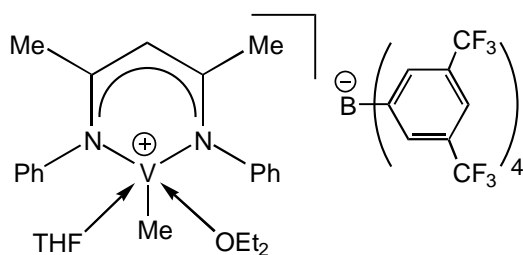


Figure 3: Cationic vanadium(III) alkyl complex.

1.6 Aspects of organo-vanadium chemistry

In general the organometallic chemistry of vanadium complexes is not as well developed as that of its group 4 neighbor, titanium. There are several reasons for this. First of all, vanadium has a more extensive redox chemistry than titanium, and oxidation states in organometallic compounds range from +5 to -1.³² Furthermore, most vanadium complexes are paramagnetic, which makes study by NMR spectroscopy difficult. Even complexes with an even number of d-electrons tend to have multiple unpaired electrons, unless the complexes are 18 valence electron species. Although IR spectroscopy and elemental analysis give valuable information about functional groups and stoichiometry, characterization often has to be based on single crystal X-ray diffraction.

For diamagnetic vanadium complexes (mostly d^0 vanadium(V) compounds), ^{51}V NMR spectroscopy is a much used tool (^{51}V nucleus: Spin number $I = 7/2$, natural abundance $> 99\%$). So far, it has mostly been used to observe trends within series of structurally related complexes,³³ and characterization based only on the chemical shift is not possible. Although ^{51}V NMR resonances are often broad, information about coupling constants (especially $J_{\text{V-N}}$) is reported.³³ The quadrupolar ^{51}V nucleus broadens ^1H , ^{13}C and ^{31}P NMR resonances of groups close to the metal center, which can be used in assigning resonances. However, much information about coupling constants in these spectra is lost, even though lowering the temperature can help to make resonances more narrow.³⁴

A limitation in the organometallic vanadium chemistry is the relatively low stability of vanadium alkyl complexes. Furthermore, vanadium in the +5 and +4 oxidation state is a strong oxidant, and often alkylation leads to reduction of the metal center. These features are especially important for the chemistry of well-defined vanadium catalysts, since this requires the synthesis of vanadium di-alkyl species. So far, only few vanadium di-alkyl species have been reported,³⁵ the most surprising is probably the bis-*n*-butyl complex, $\text{LV}(n\text{-Bu})_2$ ($\text{L} = N,N$ -diphenyl-2,4-pentadiimine), reported by Budzelaar *et al.*^{31c} This complex, which contains four β -hydrogens, can be crystallized from warm hexane (50°C), without significant decomposition.

1.7 Aim of the research

The aim of this research is (1) to develop the chemistry of vanadium complexes containing the amido functionalized cyclopentadienyl (Cp-amido) ligand; (2) to study the nature and reactivity of well-defined cationic vanadium species; (3) to synthesize Cp-amido vanadium complexes that are isostructural to known titanium complexes, and compare their properties in catalytic olefin polymerization.

The Cp-amido ligand $C_5H_4(CH_2)_nNR$ is chosen for this study, since the corresponding titanium complexes are active olefin polymerization catalysts. The 15 valence electron species $[Cp_2VR]^+$ is not active in olefin polymerization, but the cationic $[(Cp\text{-amido})VR]^+$ is a 13 valence electron species and could therefore be an active catalyst. This gives an opportunity to compare isostructural d^0 and d^1 catalyst systems.

1.8 Contents of the thesis

In Chapter 2 the synthesis of Cp-amido vanadium(V) complexes is described. Various ways to introduce the Cp-amido ligand on the metal center have been explored, and the synthesis and stability of a series of Cp-amido vanadium(V) alkyl complexes studied. An additional imido ligand is used to stabilize the high valence vanadium center.

Starting from neutral vanadium(V) methyl complexes, Chapter 3 describes the generation and characterization of well-defined cationic complexes. Although these complexes are not suitable as polymerization catalysts, since they lack a metal alkyl bond for olefin insertion, the study of their reactivity towards C-C unsaturated substrates provided useful information on the reactivity of these species. For instance, although the V-N(imido) bond is inert, the V-N(amido) bond shows the unprecedented insertion of non-activated di-olefins and alkynes.

Simple olefins like ethene and propene coordinate to the cationic vanadium(V) center, which is the first time that adducts of these olefins with d^0 metal centers were characterized. An extensive study of these adducts is found in Chapter 4.

Chapter 5 describes the synthesis of a Cp-amido vanadium(IV) dichloro complex, by a route which also gives entry to vanadium complexes in the oxidation state of +2 and +3. The vanadium(IV) complex is activated by MAO to generate an active catalyst for ethene polymerization, although the activity is lower than that of the isostructural titanium(IV) complex.

Parts of this research have been communicated: Witte, P.T.; Meetsma, A.; Hessen, B.; Budzelaar, P.H.M., *J. Am. Chem. Soc.*, **1997**, *119*, 10561. Witte, P.T.; Meetsma, A.; Hessen, B., *Organometallics*, **1999**, *18*, 2944.

1.9 References

- (1) Ziegler, K.; Holzkamp, E.; Breil, H.; Martin, H., *Angew. Chem.*, **1955**, *67*, 541.
- (2) Mülhaupt, R., in: Fink, G.; Mülhaupt, R.; Brintzinger, H.H. (Editors), *Ziegler catalysts, recent scientific innovations and technological improvements*, Springer report, Berlin, **1995**.
- (3) (a) Natta, G., *Angew. Chem.*, **1956**, *68*, 393. (b) Natta, G.; Pasquon, I.; Giachetti, E., *Angew. Chem.*, **1957**, *69*, 213.
- (4) Moore, E.P. Jr., *Polypropylene*, in: Salamone, J.C. (Editor), *The polymeric materials encyclopedia* (on CD-ROM), CRC Press, **1996**.
- (5) Parshall, G.W.; Ittel, S.D., *Homogeneous catalysis, the applications and chemistry of catalysis by soluble transition metal complexes*, 2nd Edition, Wiley & Sons inc., New York, **1992**, Chapter 4.
- (6) Polymer 'molecular weight': M_n = number average, M_w = weight average; Polydispersity = M_w/M_n . When the chain growth and termination are of a constant rate and independent of the chain length, $M_w/M_n = 2$. See: Parker, D.B.V., *Polymer chemistry*, Applied Science Publishers, London, **1974**, pp. 134 - 141.
- (7) Lee, D-H., *Olefin polymerization catalysts*, in: Salamone, J.C. (Editor), *The polymeric materials encyclopedia* (on CD-ROM), CRC Press, **1996**.
- (8) Sinn, H.; Kaminsky, W., *Adv. Organomet. Chem.*, **1980**, *18*, 99.

- (9) Davis, S.C.; Von Hellens, W.; Zahalka, H.A.; Richter, K-P., *Ethylene-propylene elastomers*, in: Salamone, J.C. (Editor), *The polymeric materials encyclopedia* (on CD-ROM), CRC Press, **1996**.
- (10) Henrici-Olivé, G.; Olivé, S., *Angew. Chem.*, **1971**, *83*, 782.
- (11) See for instance: Adisson, E.; Deffieux, A.; Fontanille, M.; Bujadoux, K., *J. Pol. Sci. A, Pol. Chem.*, **1994**, *32*, 1033.
- (12) Huang, B.; Tian, H., *Metallocene catalysts*, in: Salamone, J.C. (Editor), *The polymeric materials encyclopedia* (on CD-ROM), CRC Press, **1996**.
- (13) Kaminsky, W.; Bark, A.; Steiger, R., *J. Mol. Catal.*, **1992**, *74*, 109.
- (14) See for instance: Jordan, J.F., *Adv. Organomet. Chem.*, **1991**, *32*, 325.
- (15) (a) Cossee, P., *J. Catal.*, **1964**, *3*, 80. (b) Arlman, E.J.; Cossee, P., *J. Catal.*, **1964**, *3*, 99.
- (16) Ewen, J.A., *J. Am. Chem. Soc.*, **1984**, *106*, 6355. For a recent review see: Brintzinger, H.H.; Fischer, D.; Mülhaupt, R.; Rieger, B.; Waymouth, R.M., *Angew. Chem. Int. Ed. Eng.*, **1995**, *34*, 1143.
- (17) Shapiro, P.J.; Bunel, E.; Schaefer, W.P.; Bercaw, J.E., *Organometallics*, **1990**, *9*, 867. For a recent review see: McKnight, A.L.; Waymouth, R.M., *Chem. Rev.*, **1998**, *98*, 2587.
- (18) Johnson, L.K.; Killian, C.M.; Brookhart, M., *J. Am. Chem. Soc.*, **1995**, *117*, 6414. For a recent review see: Britovsek, G.J.P.; Gibson, V.C.; Wass, D.F., *Angew. Chem. Int. Ed. Eng.*, **1999**, *38*, 428.
- (19) Sinn, H., *Macromol. Symp.*, **1995**, *97*, 27.
- (20) Yang, X.; Stern, C.L.; Marks, T.J., *J. Am. Chem. Soc.*, **1994**, *116*, 10015.
- (21) Pellecchia, C.; Immirzi, A.; Grassi, A.; Zambelli, A., *Organometallics*, **1993**, *12*, 4473.
- (22) Chien, J.C.W.; Tsai, W-M.; Rausch, M.D., *J. Am. Chem. Soc.*, **1991**, *113*, 8570.
- (23) Yang, X.; Stern, C.L.; Marks, T.J., *Organometallics*, **1991**, *10*, 840.
- (24) Bochmann, M.; Lancaster, S.J., *J. Organomet. Chem.*, **1992**, *434*, C1.
- (25) Lin, Z.; le Marechal, J-F.; Sabat, M.; Marks, T.J., *J. Am. Chem. Soc.*, **1987**, *109*, 4127.
- (26) Karapinka, G.L.; Carrick, W.L., *J. Pol. Sci.*, **1961**, *55*, 145.
- (27) Choukroun, R.; Douziech, B.; Pan, C.; Dahan, F.; Cassoux, P., *Organometallics*, **1995**, *14*, 4471.
- (28) Parkin, G.; Bunel, E.; Burger, B.J.; Trimmer, M.S.; van Asselt, A.; Bercaw, J.E., *J. Mol. Catal.*, **1987**, *41*, 21.
- (29) Luinstra, G.A.; ten Cate, L.C.; Heeres, H.J.; Pattiasina, J.W.; Meetsma, A.; Teuben, J.H., *Organometallics*, **1991**, *10*, 3227.
- (30) (a) Coles, M.P.; Gibson, V.C., *Polym. Bull.*, 1994, *33*, 529. (b) Scheuer, S.; Fischer, J.; Kress, J., *Organometallics*, **1995**, *14*, 2627.
- (31) (a) Brandsma, M.J.R.; Brussee, E.A.C.; Meetsma, A.; Hessen, B.; Teuben, J.H., *Eur. J. Inorg. Chem.*, **1998**, 1867. (b) Desmangles, N.; Gambarotta, S.; Bensimon, C.; Davis,

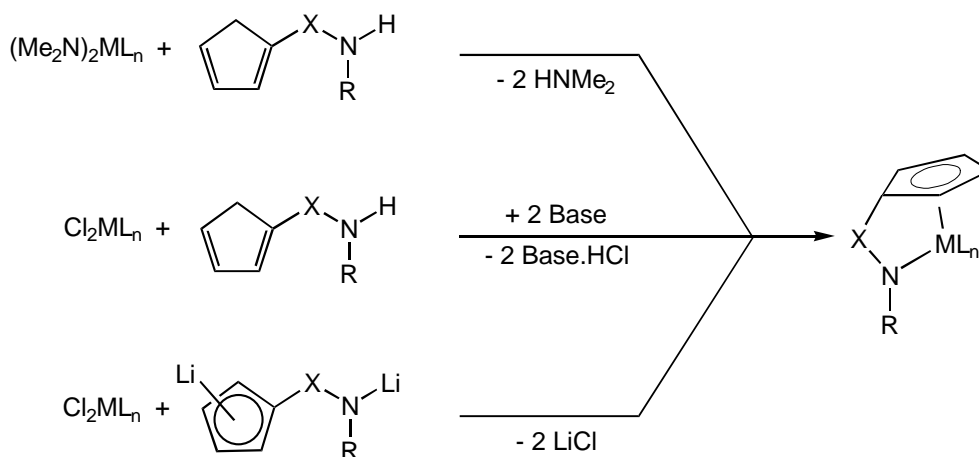
- S.; Zahalka, H., *J. Organomet. Chem.*, **1998**, 562, 53. (c) Budzelaar, P.H.M.; van Oort, A.B.; Orpen, G.A., *Eur. J. Inorg. Chem.*, **1998**, 1485. (d) Kim, W-K.; Fevola, M.J.; Liable-Sands, L.M.; Rheingold, A.L.; Theopold, K.H., *Organometallics*, **1998**, 17, 4541. (e) Reardon, D.; Conan, F.; Gambarotta, S.; Yap, G.; Wang, Q., *J. Am. Chem. Soc.*, **1999**, 121, 9318.
- (32) Berno, P.; Gambarotta, S.; Richeson, D., *Comp. Organomet. Chem.*, **1995**, 5, 1.
- (33) see for instance: (a) Maatta, E.A., *Inorg. Chem.*, **1984**, 23, 2560. (b) Preuss, F.; Steidel, M.; Vogel, M.; Overhoff, G.; Hornung, G.; Towae, W.; Frank, W.; Reiss, G.; Müller-Becker, S., *Z. Anorg. Allg. Chem.*, **1997**, 623, 1220.
- (34) Mann, B.E.; Taylor, B.F., *¹³C NMR data for organometallic compounds*, Academic Press, London, **1981**, pp 2-5.
- (35) (a) Wills, A.R.; Edwards, P.G., *J. Chem. Soc. Dalton Trans.*, **1989**, 1253. (b) Danopoulos, A.A.; Edwards, P.G., *Polyhedron*, **1989**, 8, 1339. (c) Hessen, B.; Teuben, J.H.; Lemmen, T.H.; Huffman, J.C.; Caulton, K.G., *Organometallics*, **1985**, 4, 946. (d) Hessen, B.; Meetsma, A.; Teuben, J.H., *J. Am. Chem. Soc.*, **1989**, 111, 5977. Vanadium tris-alkyl species have also been reported: (e) Buijink, J-K.F.; Meetsma, A.; Teuben, J.H., *Organometallics*, **1993**, 12, 2004. (f) Murphy, V.J.; Turner, H., *Organometallics*, **1997**, 16, 2495.

Chapter 2

Synthesis of vanadium(V) complexes containing amido functionalized cyclopentadienyl ligands

2.1 Introduction

Several methods have been reported to introduce amido functionalized cyclopentadienyl (Cp-amido) ligands on a metal center. Ligand introduction by amine elimination (starting from a metal-amido complex)¹ or HCl elimination (starting from a metal-chloro complex)² uses a neutral ligand precursor which is deprotonated by the metal-amido or metal-chloride group (Scheme 1). Lithiation of the neutral ligand precursor and subsequent reaction of the resulting di-anion with a metal chloride is probably one of the most frequently used methods (Scheme 1).³

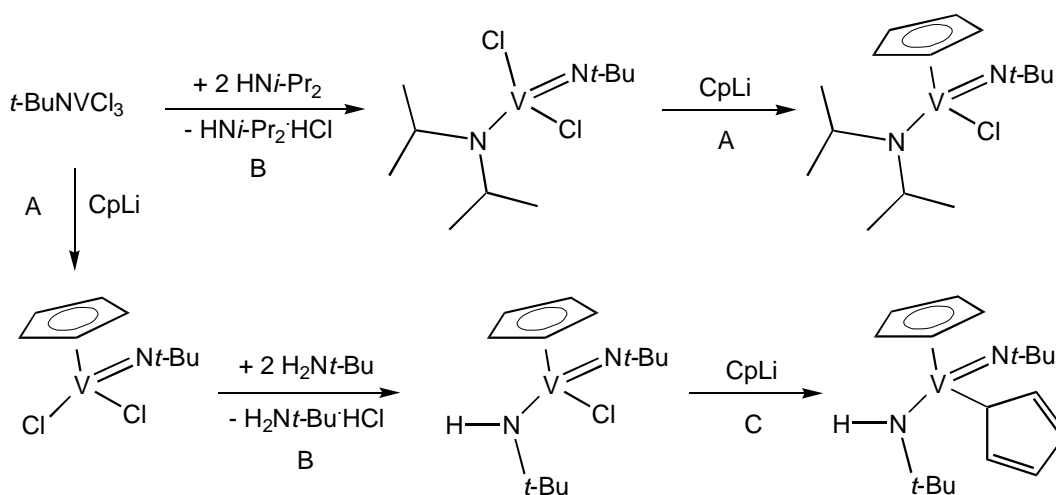


Scheme 1

So far, research on complexes with Cp-amido ligands has mainly been focussed on the group 4 metals.⁴ Research on Cp-amido complexes of group 5

metals is limited to the synthesis of $(\eta^5, \eta^1\text{-C}_5\text{H}_4\text{SiMe}_2\text{NPh})\text{M}(\text{NMe}_2)_3$ ($\text{M} = \text{Nb}$, Ta), and $(\eta^5\text{-C}_5\text{Me}_4\text{CH}_2\text{N}t\text{-Bu})\text{TaCp}^*$ ($\text{Cp}^* = \eta^5\text{-C}_5\text{Me}_5$).⁵ The NMe_2 complexes are synthesized by amine elimination from $\text{M}(\text{NMe}_2)_5$; the Cp^* complex is formed by intramolecular coupling of one of the Cp^* ligands of $[\text{Cp}^*_2\text{Ta}(\text{N}t\text{-Bu})][\text{B}(\text{C}_6\text{F}_5)_4]$ with the imido ligand. Related vanadium chemistry has not been reported.

Although no Cp-amido vanadium complexes are known, vanadium(V) complexes with both a cyclopentadienyl and an amido ligand, but without a link between them, have been reported (Scheme 2).⁶ The Cp ligand was introduced on vanadium(V) using CpLi (reactions A), the amido ligands by HCl elimination (reactions B). Since the Cp vanadium amido chloro complexes react with CpLi (reaction C), it is preferred to introduce the Cp ligand prior to the amido ligand.



Scheme 2

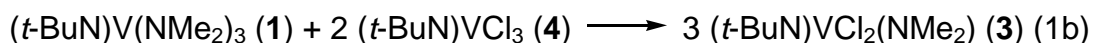
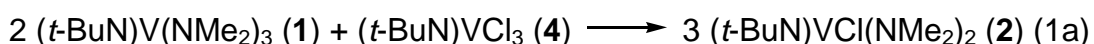
This chapter describes the synthesis and characterization of Cp-amido vanadium(V) complexes with an additional imido ligand. Imido ligands are often used in vanadium(V) chemistry, since the good π -donating capabilities of these ligands stabilize the high oxidation state of the metal center. Introduction of the Cp-amido ligand by amine elimination was investigated using the series of complexes $t\text{-BuNV}(\text{NMe}_2)_n\text{Cl}_{3-n}$ ($n = 1, 2, 3$) as starting materials. This yielded the complexes $(\text{Cp-amido})\text{VCl}(\text{N}t\text{-Bu})$, from which a series of alkyl complexes

was synthesized. Cp-amido vanadium(V) imido complexes with an aromatic substituent on the imido ligand were obtained by exchange of the imido ligand after introduction of the Cp-amido ligand. In addition, several Cp vanadium(V) amido complexes, without a link between the Cp and amido functionality, were synthesized, which can serve as comparison.

2.2 Results and discussion

2.2.1 Synthesis of imido vanadium(V) amido complexes

The imido tris-amido vanadium complex (*t*-BuN)V(NMe₂)₃ (**1**) is obtained by reacting (*t*-BuN)VCl₃ (**4**) with three equivalents of LiNMe₂. Complex **1** is an oil and can be purified by vacuum transfer. The di-amido and mono-amido complexes (*t*-BuN)VCl(NMe₂)₂ (**2**) and (*t*-BuN)VCl₂(NMe₂) (**3**) can also be synthesized by reaction of **4** with LiNMe₂ (using two and one equivalents of LiNMe₂ respectively) but in a low isolated yield (<50%). A more convenient route for their synthesis is by the comproportionation of **1** and **4** (Equations 1a, b). These ligand redistributions are fast: reactions in C₆D₆ on NMR tube scale show that full conversion is reached within five minutes at room temperature. For comparison, the comproportionation of the vanadium(IV) complexes VCl₄ and V(NEt₂)₄ takes five hours at 100°C to go to completion.⁷ A comproportionation reaction on preparative scale was performed for **2** and resulted in an 81% isolated yield.



The ¹H NMR spectra of **1** and **2** show only one singlet for the NMe₂ groups over the temperature range of -70 to +30°C, indicating rapid rotation of the NMe₂ fragment around the V-N(amido) bond. For **3** the NMe₂ resonance appears as two singlets at -70°C (both with the intensity of one Me-group), which coalesce at 80°C into one broadened resonance. Since no steric effects

influence the rotation around the V-N(amido) bond, the higher rotational barrier of **3** (compared to **1** and **2**) is probably caused by a stronger N(amido) to V π -donation due to the greater electron deficiency of the vanadium center in **3**.

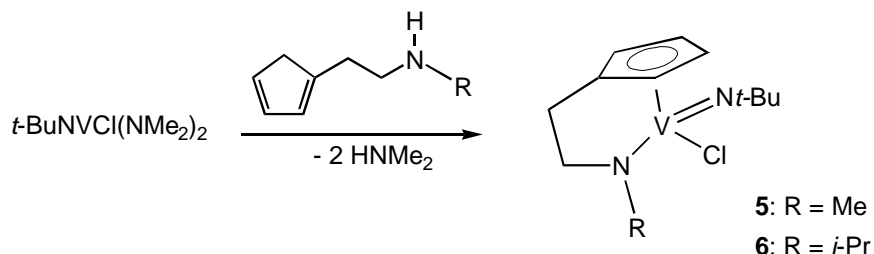
The ^{51}V NMR spectra of **1** - **4** show that substitution of a chloride by an amido ligand results in an upfield shift of the vanadium resonance. Starting from the imido vanadium tri-chloride **4** (^{51}V NMR: δ 3 ppm) substitution of one chloride for a NMe_2 group results in an upfield shift in the ^{51}V NMR of about 160 ppm (**3**: δ -153 ppm): substitution of a second chloride results in a further upfield shift of 130 ppm (**2**: δ -281 ppm). Comparable upfield shifts for the substitution of a chloride ligand for an amido ligand have been found in the series of vanadium(V) oxo complexes $\text{OV}(\text{NMe}_2)_n\text{Cl}_{3-n}$ ($n = 1, 2, 3$),⁸ and shows that the stronger π -donation of the amido group compared to the chloride increases the electron density on the metal.

2.2.2 Ligand introduction by amine elimination

We have introduced the Cp-amido ligand on vanadium(V) by amine elimination, using the vanadium(V) amido complexes **1** and **2** as starting materials. The reaction of **2** with $\text{C}_5\text{H}_5\text{CH}_2\text{CH}_2\text{N}(\text{H})\text{R}$ ($\text{R} = \text{Me}, i\text{-Pr}$) in refluxing pentane resulted in the formation of $(\eta^5, \eta^1\text{-C}_5\text{H}_4\text{CH}_2\text{CH}_2\text{NR})\text{VCl}(\text{N}t\text{-Bu})$ (**5**: $\text{R} = \text{Me}$; **6**: $\text{R} = i\text{-Pr}$, Scheme 3). The Cp-amido vanadium(V) complexes **5** and **6** crystallized readily from pentane solutions and were isolated in yields of 74 and 83% respectively.

The vanadium center in the complexes **5** and **6** is asymmetric and the four Cp protons and the four protons of the ethylene bridge all appear in the ^1H NMR as separate multiplets. The NMe resonance in **5** (4.0 ppm) appears downfield from the corresponding resonance in the ligand precursor $\text{C}_5\text{H}_5\text{CH}_2\text{CH}_2\text{N}(\text{H})\text{Me}$ (2.3 ppm). In **6** the two methyls of the $i\text{-Pr}$ group are inequivalent (1.01 and 0.98 ppm), with a chemical shift comparable to the corresponding resonance in the ligand precursor $\text{C}_5\text{H}_5\text{CH}_2\text{CH}_2\text{N}(\text{H})i\text{-Pr}$ (0.95 ppm). The methine proton of the $i\text{-Pr}$ group appears much more downfield in **6** than in the ligand precursor (6.0 ppm in **6**, 2.6 ppm in ligand precursor). Similar

downfield shifts are observed in the Cp-amido titanium(IV) complexes $[\text{C}_5\text{H}_4(\text{CH}_2)_n\text{N}i\text{-Pr}]\text{TiCl}_2$ ($n = 2, 3$).²



Scheme 3

Reaction of the imido vanadium tris-amido complex **1** with the ligand precursor $\text{C}_5\text{H}_5\text{CH}_2\text{CH}_2\text{N}(\text{H})i\text{-Pr}$ in C_6D_6 at 75°C showed rapid formation of HNMe_2 . After 3 hours, resonances of **1** and the ligand precursor were no longer observed in the ^1H NMR spectrum. Instead, the product $(\eta^5, \eta^1\text{-C}_5\text{H}_4\text{CH}_2\text{CH}_2\text{N}i\text{-Pr})\text{V}(\text{NMe}_2)(\text{N}t\text{-Bu})$ was observed, together with unknown impurities. Further heating at 75°C caused the product to decompose.

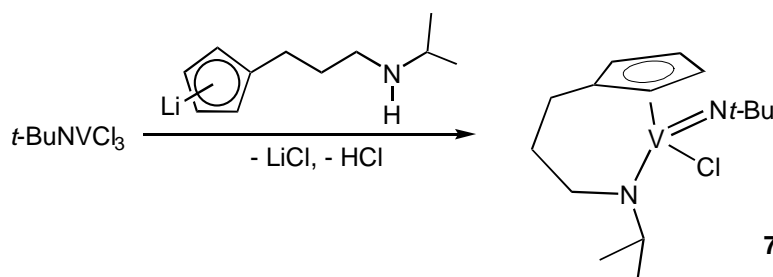
Ligand introduction can also be achieved by a combination of amine and HCl elimination, using the mono-amido complex **3** as a starting material. When the reaction of **3** with the ligand precursor $\text{C}_5\text{H}_5(\text{CH}_2)_2\text{N}(\text{H})i\text{-Pr}$ was performed in the presence of an extra added base (Et_3N , in C_6D_6), ^1H NMR showed the formation of the Cp-amido complex **6**. However, when we attempted this reaction on a preparative scale, **6** was obtained as an impure sticky solid, which could not be purified by crystallization.

2.2.3 Ligand introduction by salt metathesis

The Cp-amido ligand with an ethylene bridge between the Cp and amido functionality can easily be introduced on vanadium(V) by amine elimination from the bis-amido complex **2**. However, introduction of a Cp-amido ligand with a propylene bridge proved much more difficult. The reaction of **2** with $\text{C}_5\text{H}_5(\text{CH}_2)_3\text{N}(\text{H})i\text{-Pr}$ on NMR scale (C_6D_6) showed no conversion, even after prolonged heating at 75°C . Higher temperatures resulted in decomposition of

the ligand and **2**, therefore another method was used for the synthesis of Cp-amido vanadium(V) complexes with a propylene bridge.

When a THF- d_8 solution of the ligand precursor $C_5H_5(CH_2)_3N(H)i\text{-Pr}$ was treated with one equivalent of Me_3SiCH_2Li , 1H NMR showed the deprotonation of the Cp moiety (two triplets are observed for the four Cp protons) and Me_4Si was generated. Addition of an extra equivalent of Me_3SiCH_2Li generated more Me_4Si , but no resonances for the Cp-amido ligand were observed, instead, the solution became turbid. Although the deprotonation of the Cp moiety is fast (complete in less than five minutes), deprotonation of the amido functionality takes more than half an hour. Similar observations were made when the ethylene bridged ligand precursor $C_5H_5(CH_2)_2N(H)i\text{-Pr}$ was deprotonated by Me_3SiCH_2Li .



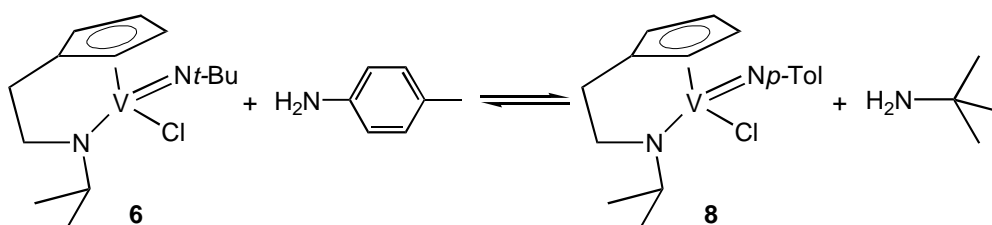
Scheme 4

For ligand introduction by salt metathesis the imido vanadium tri-chloride **4** was used as a starting material. Reaction of the mono-lithium salt $[C_5H_4(CH_2)_3N(H)i\text{-Pr}]Li$ with **4** resulted in the formation of $(\eta^5, \eta^1-C_5H_4CH_2CH_2CH_2Ni\text{-Pr})VCl(Nt\text{-Bu})$ (**7**), indicating the additional elimination of HCl (Scheme 4). The Cp-amido complex **7** was isolated as a red oil in a low yield (37%) after extraction with pentane. Large amounts of pentane-insoluble paramagnetic (by 1H NMR) compounds were formed as well. The yield of **7** did not improve when its synthesis was carried out in the presence of the base Et_3N .

2.2.4 Variation of the imido substituent

Introduction of the Cp-amido ligand on vanadium(V) bearing an imido ligand with an aromatic substituent could not be performed using the amine elimination route described above, since the synthesis of imido vanadium(V) amido starting complexes from (*p*-TolN)VCl₃ was unsuccessful. An alternative synthetic procedure is the exchange of the *t*-Bu imido ligand after introduction of the Cp-amido ligand.

It was reported that the reaction of (*t*-BuN)V CpCl₂ with one equivalent of the aniline ArNH₂ (Ar = 2,6-(*i*-Pr)₂-C₆H₃) yields (ArN)V CpCl₂ and *t*-BuNH₂, after heating at 75°C for 10 days (C₂H₄Cl₂).⁹ When the *t*-Bu imido vanadium complex **6** was reacted with *p*-TolNH₂ in a sealed NMR tube (C₆D₆), resonances for a new complex and *t*-BuNH₂ appeared after the mixture was heated to 75°C. However, even after prolonged heating full conversion was not observed. Apparently the reaction reaches an equilibrium where about 50% of **6** is converted.



Scheme 5

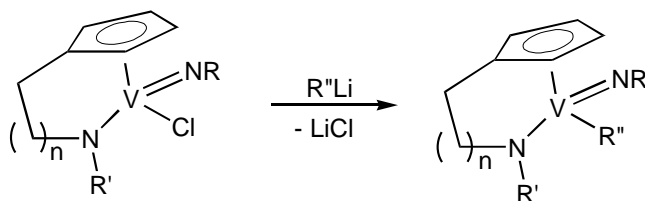
The complex (η^5, η^1 -C₅H₄CH₂CH₂N*i*-Pr)VCl(N*p*-Tol) (**8**, Scheme 5) was obtained on preparative scale from **6** and *p*-TolNH₂ in refluxing toluene in a 78% isolated yield. In this case the equilibrium shown in Scheme 5 could be driven to the right by using a small excess of *p*-TolNH₂ and by degassing the reaction mixture periodically to remove the volatile *t*-BuNH₂.

The imido exchange has little effect on the ¹H and ¹³C NMR resonances of the Cp-amido ligand. In the ⁵¹V NMR spectrum the *p*-Tol imido complex **8**

appears 95 ppm downfield from the *t*-Bu imido complex **6**, probably because of the better electron donating properties of the *t*-Bu substituent. The difference is much smaller than for the corresponding imido vanadium(V) tri-chlorides, where (*p*-TolN)VCl₃¹⁰ appears 300 ppm downfield from (*t*-BuN)VCl₃.¹¹

2.2.5 Synthesis of Cp-amido vanadium(V) alkyl complexes

Reaction of the Cp-amido vanadium(V) chloro complexes **5 - 8** with lithium alkyls that do not contain β-H atoms yielded the vanadium(V) alkyls (Cp-amido)VR'(NR) (Scheme 6). Only the *t*-Bu imido vanadium methyl complex **10** was obtained as a crystalline solid, all other complexes were isolated as highly soluble dark red or brown oils. The *p*-Tol imido vanadium methyl complex **13** crystallized when it was refrigerated at -30°C, however, the crystals melted upon warming.



n	R	R'	R''	compound
1	<i>t</i> -Bu	Me	Me	9
		<i>i</i> -Pr	Me	10
			CH ₂ CMe ₃	11
			CH ₂ CMe ₂ Ph	12
1	<i>p</i> -Tol	<i>i</i> -Pr	Me	13
2	<i>t</i> -Bu	<i>i</i> -Pr	Me	14

Scheme 6

The ¹H and ¹³C NMR spectra of the alkyl complexes show that the resonances for the imido and Cp-amido ligands do not change significantly upon alkylation. The resonances for the alkyl groups show a characteristic broadening caused by the quadrupolar vanadium nucleus (see Chapter 1, section 1.5). In the ¹H NMR spectra the V-CH₃ resonance appears as a broadened singlet around 0.8 ppm with a line width at half height (Δv_{1/2}) of 7 Hz,

the V-CH₂ group appears more downfield (multiplet, 1.6 ppm). In the ¹³C NMR spectra the V-C resonances are only observed at low temperatures, the V-CH₂ resonance also appears more downfield than the V-CH₃ resonance.

The alkyl complexes **10** - **12** were stable in C₆D₆ solution for several months at room temperature. However, heating the solutions led to slow decomposition as was seen by a color change of the solution from brown to purple (see below). The same product was formed for all three decompositions, however, the decompositions were not clean.

Attempts to synthesize a vanadium(V) alkyl complex by reaction of **6** with EtMgCl at low temperatures, led to the formation of a purple solution. After extraction of the reaction mixture with pentane, dark crystals were obtained which display the same ¹H NMR spectra as the thermolysis product described above. The product could not be purified by crystallization.

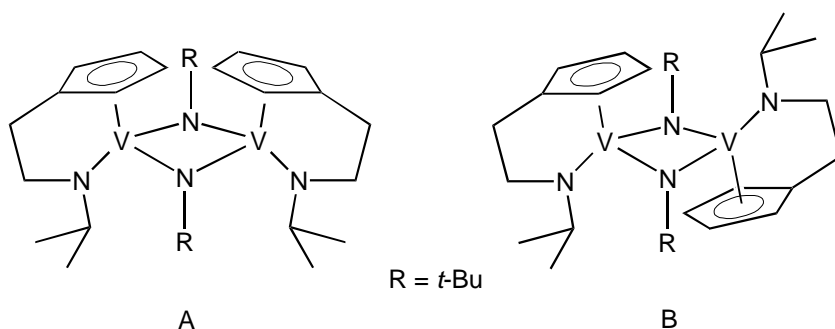


Figure 2: Two possible isomers of **15**.

In contrast to complexes **5** - **14** the thermolysis product has a plane of symmetry, as is seen from the ¹H and ¹³C NMR spectra. We propose that this product is the vanadium(IV) dimer [(η⁵,η¹-C₅H₄CH₂CH₂N*i*-Pr)V(μ-N*t*-Bu)]₂ (**15**). Similar vanadium(IV) dimers have been reported for the attempted alkylation of the vanadium(V) complexes (*t*-BuN)VCP(O*t*-Bu)Cl and (*p*-TolN)VCPCl₂.¹⁰ These products, [Cp(*t*-BuO)V(μ-N*t*-Bu)]₂ and [CpClV(μ-N*p*-Tol)]₂, show a downfield shift in the ⁵¹V NMR of 500 ppm compared to the starting complexes. The Cp-amido vanadium(IV) dimer **15** appears at +137 ppm, a downfield shift of 800 ppm compared to the Cp-amido vanadium(V) chloride **6**.

There are two possible isomers for **15**, as shown in Figure 2. From the work of Vroegop *et al.* on imido bridged titanium dimers it is known that isomer A is preferred when the bridging imido ligand has a *t*-Bu substituent,¹³ and following this example we propose this structure for **15**.

2.2.6 Structure determination of **10**

The methyl complex **10** was recrystallized from pentane to yield dark red crystals suitable for X-ray structure determination. The structure (Figure 3) shows the η^5, η^1 -bonding of the Cp-amido ligand. The V-Cg bond length (1.9835(15) Å; Cg = center of gravity of the Cp moiety) and V-N(amido) bond length (1.854(2) Å) are normal for vanadium(V).^{6a,14} The planar geometry of the N(amido) and the linear geometry of the N(imido) reflects the π -donation of the nitrogen atom lone pairs. The V-N(imido) unit is more linear than that of other V(V)-(N*t*-Bu) complexes (V-N-C = 175.61(18)° for **10**, reported V-N-C = 161 - 172°),^{6a,15} what could indicate a stronger π -donation than in reported complexes. However, the V-N(imido) bond length is slightly longer than in other complexes (V-N = 1.656(2) Å for **10**, reported V-N = 1.59 - 1.64 Å).^{6a,14} The V-Me distance (2.103(3) Å) is somewhat longer than that of Li[(*t*-Bu₃SiN)₂VMe₂] (2.04 - 2.06 Å),¹⁶ the only other V(V)-methyl complex that is structurally characterized. Proton H8 of the *i*-Pr group is pointing towards the metal center (V1...H8 = 2.84 Å), which is probably the reason for the observed downfield shift of this proton in the ¹H NMR spectrum.

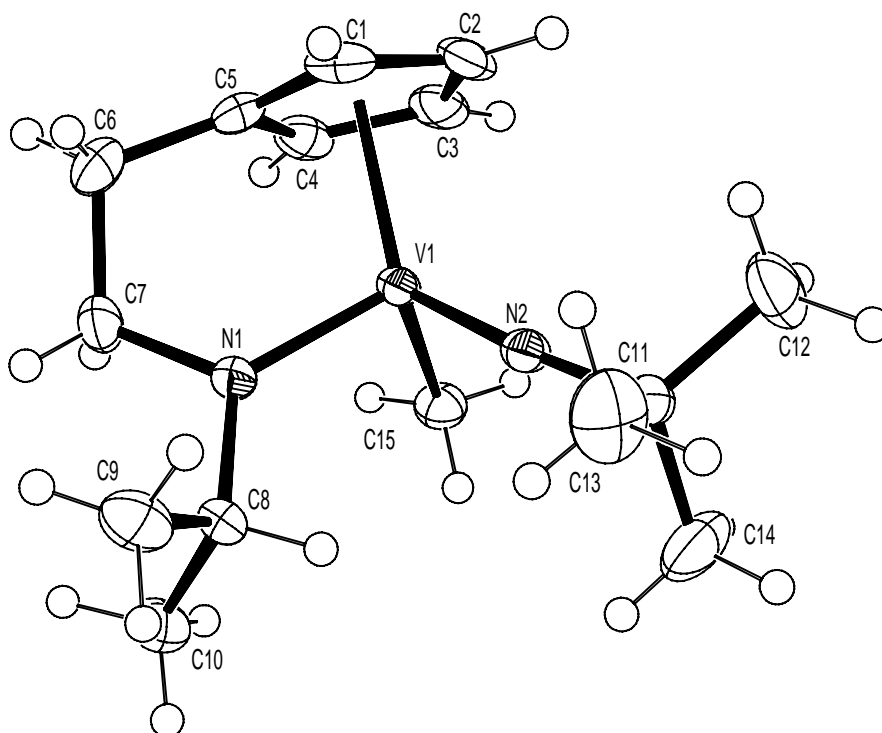


Figure 3: Crystal structure of **10**.

Table 1: Selected bond distances and angles in **10**.

V-N(1)	1.854(2)	Cg-V-N(1)	110.12(7)
V-N(2)	1.656(2)	Cg-V-N(2)	130.45(7)
V-C(15)	2.103(3)	Cg-V-C(15)	111.72(9)
V-Cg	1.9835(15)	N(1)-V-N(2)	105.78(10)
		C(15)-V-N(1)	96.10(11)
		C(15)-V-N(2)	96.87(12)
		V-N(2)-C(11)	175.61(18)

2.2.7 Complexes without a bridge between the Cp and amido functionality

In order to investigate the influence of the bridge between the Cp and amido functionality on the reactivity of the Cp-amido complexes (as will be described in Chapter 4), vanadium(V) complexes with a Cp and amido ligand without a link between them were synthesized for comparison. Preuss *et al.* synthesized the imido vanadium(V) complexes $(t\text{-BuN})\text{V}(\eta^5\text{-C}_5\text{H}_5)(\text{NRR}')\text{Cl}$ ($\text{R} = t\text{-Bu}$, $\text{R}' = \text{H}$; $\text{R} = \text{R}' = i\text{-Pr}$; Scheme 2).⁶ We extended this chemistry by

introducing an aromatic substituent on the imido functionality, so that a comparison with the (Cp-amido)VX(N*p*-Tol) complexes is possible.

The two routes reported by Preuss *et al.* are shown in Scheme 2.⁶ The best method is to introduce the amido ligand on (*t*-BuN)VCpCl₂, as this is the most selective. However, we observed that this route is not available for complexes with an aromatic substituent on the imido ligand, since (*p*-TolN)VCpCl₂ does not react with HN*i*-Pr₂. Therefore we used the second route described by Preuss *et al.*, where the Cp ligand is introduced after introduction of the amido ligand.

Reaction of (RN)VCl₃ (**4**: R = *t*-Bu; **16**: R = *p*-Tol) with two equivalents of HN*i*-Pr₂ yielded (RN)V(N*i*-Pr₂)Cl₂ (**17**: R = *t*-Bu; **18**: R = *p*-Tol) by HCl elimination. In a subsequent reaction with CpNa, the complexes (RN)VCp(N*i*-Pr₂)Cl (**19**: R = *t*-Bu; **20**: R = *p*-Tol) were formed. The ¹H and ¹³C NMR resonances of the Cp and amido ligands in the *p*-Tol imido vanadium(V) complexes **18** and **20** are very similar to those of the reported *t*-Bu imido complexes **17** and **19**.⁶ Table 2 shows the ⁵¹V NMR characteristics of the complexes **4**, **16** - **20**. From it we can conclude that the electron density on the vanadium center increases when a Cp or an amido ligand is introduced. Furthermore, the electron donating capacity of the *t*-Bu substituent on the imido ligand is better than that of the *p*-Tol substituent, although this effect becomes less pronounced when the overall electron density on the metal center increases.

Table 2: ⁵¹V NMR data of Cp vanadium(V) amido complexes.

Complex	chemical shift (ppm)	reference
(<i>t</i> -BuN)VCl ₃ (4)	3	11
(<i>t</i> -BuN)V(N <i>i</i> -Pr ₂)Cl ₂ (17)	-173	6a
(<i>t</i> -BuN)VCp(N <i>i</i> -Pr ₂)Cl (19)	-665	6a
(<i>p</i> -TolN)VCl ₃ (16)	305	10
(<i>p</i> -TolN)V(N <i>i</i> -Pr ₂)Cl ₂ (18)	-67	this work
(<i>p</i> -TolN)VCp(N <i>i</i> -Pr ₂)Cl (20)	-591	this work

The Cp vanadium(V) chloro complexes **19** and **20** react with CpNa, and when their synthesis was attempted with an excess of CpNa the bis-Cp

complexes (RN)VCp₂(N*i*-Pr₂) (**21**: R = *t*-Bu; **22**: R = *p*-Tol) were isolated. Preuss *et al.* synthesized the bis-Cp complexes (*t*-BuN)VCp₂X (X = NH*t*-Bu, O*t*-Bu),^{6b,17} and showed that these complexes contain one η¹-bonded Cp ligand and one that is η⁵-bonded (determined by ¹H NMR spectroscopy at -140°C). Low temperature ¹H NMR measurements on **21** and **22** were limited by the minimum temperature of the used NMR probe (-100°C). Nevertheless, since these NMR spectra resemble the -100°C ¹H NMR spectrum of (*t*-BuN)VCp₂(O*t*-Bu), we assume a similar bonding type of the Cp ligands in **21** and **22** (Figure 4).

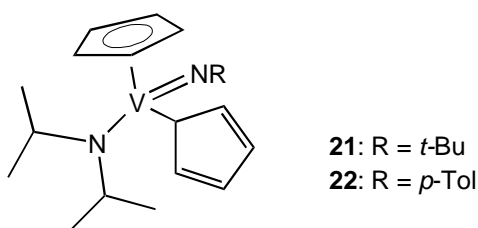


Figure 4: Proposed structure of **21** and **22**.

Reaction of the Cp vanadium(V) chloro complexes **19** or **20** with MeLi yielded the corresponding methyl complexes, (RN)VCp(N*i*-Pr₂)Me (**23**: R = *t*-Bu; **24**: R = *p*-Tol). In both methyl complexes the resonances for the imido, amido and Cp ligand in ¹H and ¹³C NMR do not shift significantly compared to the corresponding chlorides. The ¹H NMR resonance for the V-CH₃ (δ 0.8 ppm, Δ*v*_{1/2} 15Hz) has the same chemical shift as the (Cp-amido)VCH₃(NR) complexes **9**, **10**, **13** and **14**, but is more broadened. The ⁵¹V NMR resonances (δ -600 ppm, Δ*v*_{1/2} 350Hz) are comparable to the other methyl complexes.

2.3 Conclusions

Vanadium(V) imido complexes with Cp-amido ligands are best synthesized by amine elimination from (*t*-BuN)V(NMe₂)₂Cl. From this reaction (Cp-amido)VCl(N*t*-Bu) complexes were isolated in good yields when a ligand is used with an ethylene bridge between the Cp and amido functionality. However,

the route is not versatile and Cp-amido vanadium(V) complexes with a propylene bridge between the Cp and amido functionality could only be obtained by salt metathesis. Reaction of (Cp-amido)VCl(N*t*-Bu) complexes with aniline yielded Cp-amido vanadium(V) imido complexes with an aromatic substituent on the imido functionality. These complexes are not available using the amine elimination route, since the starting complex (*p*-TolN)V(NMe₂)₂Cl could not be obtained.

Stable Cp-amido vanadium(V) alkyl complexes were only obtained for alkyl ligands that do not contain a β-H atom. The crystal structure of (C₅H₄CH₂CH₂N*i*-Pr)VMe(N*t*-Bu) shows that the Cp-amido ligand binds to the vanadium center in a η⁵,η¹-fashion, with strong π-donation from the nitrogen atom, making the ligand an 8-electron donor.

For the synthesis of Cp vanadium(V) amido complexes in which there is no link between the Cp and amido ligand, two routes have been described in literature. Introduction of the Cp ligand by salt metathesis and subsequent introduction of the amido ligand by HCl elimination is preferred, since it is selective in forming (*t*-BuN)VCp(N*i*-Pr₂)Cl. Introduction of the Cp- ligand after the amido ligand is introduced is less selective, and formation of bis-Cp complexes has been observed. Unfortunately, only this last route yields Cp vanadium(V) amido complexes with a *p*-Tol imido substituent.

2.4 Experimental

General considerations

All experiments were performed under nitrogen atmosphere using standard glove-box and Schlenk line techniques. Deuterated solvents (Aldrich) were dried over Na/K alloy and vacuum transferred before use (C₆D₆, C₇D₈, THF-d₈). Pentane, hexane, ether, THF and toluene were distilled from Na or Na/K alloy before use. The following compounds were prepared according to literature procedures: C₅H₅(CH₂)_nNHR (n = 2, R = Me, *i*-Pr; n = 3, R = *i*-Pr),¹⁸ (*t*-BuN)VCl₃ (**4**),¹¹ (*p*-TolN)VCl₃ (**16**),¹⁰ (*t*-BuN)V(N*i*-Pr₂)Cl₂ (**17**)^{6a} and (*t*-BuN)VCp(N*i*-Pr₂)Cl (**19**).^{6a} Me₃CCH₂Li, Me₃SiCH₂Li and PhMe₂CCH₂Li were prepared by refluxing the corresponding chlorides with 3 equivalents of lithium metal overnight, followed by recrystallization from hexane. HNMe₂, 40% in H₂O (Merck), BuLi, 2.5 M in hexane (Acros), MeLi (Aldrich), *p*-TolNH₂ (Aldrich), and HN*i*-Pr₂ (Acros) were used as received. NMR spectra were run on Varian Gemini 200, VXR-300 and VXR-

500 spectrometers. ^1H and ^{13}C NMR chemical shifts are reported in ppm relative to TMS, using residual solvent resonances as internal reference. ^{51}V NMR chemical shifts are reported in ppm relative to VOCl_3 , which is used as an external reference. Coupling constants (J) and line widths at half height ($\Delta\nu_{1/2}$) are reported in Hz. IR spectra were recorded on a Mattson Galaxy 4020FT-IR spectrophotometer. Elemental analyses were performed by the Microanalytical Department of the University of Groningen. Every value is the average of at least two independent determinations.

Synthesis of (*t*-BuN)V(NMe₂)₃ (**1**)

Two 1L three neck flasks were connected with a rubber tube. One flask was charged with 150 g of NaOH pellets, and equipped with a dropping funnel (without a pressure equilizer) containing 20 mL of a 40% solution of HNMe₂ in H₂O (0.16 mol); the other flask was charged with 400 mL of toluene which was cooled to -30°C. The system was put under a reduced pressure (~0.1 bar) and the amine solution was added to the NaOH pellets at such a rate that the pressure did not exceed 0.8 bar. When all amine solution was added and the pressure had dropped back to ~0.1 bar, the two flasks were filled with N₂ gas and disconnected. Slowly 50 mL 2.5 mL BuLi in hexane (0.13 mol) was added to the cooled toluene solution, which was stirred for half an hour at -30°C. An orange solution of 9.9 g of **4** (43 mmol) in 80 mL of toluene was added in five minutes at -30°C. The solution turned brown upon addition and was stirred overnight at room temperature, after which all volatiles were removed *in vacuo*. The resulting red oil was stripped from residual toluene by addition of 2 x 50 mL of hexane and 2 x 50 mL of pentane and subsequent removal *in vacuo*. Extraction of the red oil with 2 x 100 mL of pentane, followed by removal of the solvent *in vacuo* yielded 9.18 g of a red oil. Crude yield: 36 mmol (83%). ^1H NMR showed small amounts of impurities in the region of 0 - 4 ppm. This material is of sufficient purity to use in the subsequent synthesis of **2**, but can be further purified by vacuum transfer if desired.

^1H NMR (200 MHz, C₆D₆, 25°C): δ 3.43 (s, 18H, NCH₃), 1.38 (s, 9H, *t*-Bu). ^{13}C { ^1H } NMR (50.3 MHz, C₆D₆, 25°C): δ 50.0 (br, NCH₃), 31.8 (CH₃ of *t*-Bu), C_q of *t*-Bu not observed. ^{51}V NMR (78.9 MHz, C₆D₆, 25°C): δ -267 (t, J_{V-N} = 84). IR (*neat*): 594 (w), 621 (w), 665 (w), 687 (w), 806 (w), 955 (s), 1047 (s), 1119 (s), 1159 (s), 1211 (s), 1236 (s), 1354 (s), 1412 (s), 1445 (s), 2764 (s), 2807 (s), 2845 (s), 2890 (s), 2918 (s), 2967 (s) cm⁻¹.

Synthesis of (*t*-BuN)VCl(NMe₂)₂ (**2**)

In 40 mL of pentane 1.56 g (6.1 mmol) of **1** and 0.70 g (3.1 mmol) of **4** were dissolved at ambient temperature and stirred for two hours. The solution was filtered, concentrated to half the volume and cooled to -20°C, yielding 1.82 g (7.4 mmol, 81%) of **2** as red crystals.

^1H NMR (200 MHz, C₆D₆, 25°C): δ 3.41 (s, 12H, NCH₃), 1.31 (s, 9H, *t*-Bu). ^{13}C { ^1H } NMR (50.3 MHz, C₆D₆, 25°C): δ 50.9 (NCH₃), 30.6 (CH₃ of *t*-Bu), C_q of *t*-Bu not observed. ^{51}V NMR (78.9 MHz, C₆D₆, 25°C): δ -281 (t, J_{V-N} = 91). IR (*nujol*): 951 (s), 1030 (w), 1045 (w), 1157 (w),

1211 (w), 1233 (s), 1358 (w), 1412 (w) cm^{-1} . *Anal. Calcd (%) for $\text{C}_8\text{H}_{21}\text{N}_3\text{VCl}$* : C: 39.11, H: 8.62, N: 17.10, V: 20.74, Cl: 14.43; Found: C: 38.99, H: 8.57, N: 16.79, V: 20.62, Cl: 14.09.

Synthesis of (*t*-BuN)VCl₂(NMe₂) (**3**)

In 100 mL of pentane 2.46 g (10.8 mmol) of **4** was dissolved and 0.55 g (10.8 mmol) of LiNMe₂ was added. The color of the solution quickly changed from orange to brown, and the solution was stirred for one hour. After filtration the brown solution was concentrated to half the volume and cooled to -25°C, which yielded 1.20 g (5.08 mmol, 47%) of **3** as red crystals.

¹H NMR (200 MHz, C₆D₆, 25°C): δ 3.65 (br, 3H, NCH₃), 3.43 (br, 3H, NCH₃), 1.20 (s, 9H, *t*-Bu). ¹³C {¹H} NMR (50.3 MHz, C₆D₆, 25°C): δ 47.3 (NCH₃), 29.3 (CH₃ of *t*-Bu), C_q of *t*-Bu not observed. ⁵¹V NMR (78.9 MHz, C₆D₆, 25°C): δ -153 ($\Delta\nu_{1/2}$ = 320). IR (nujol): 939 (w), 1163 (w), 1213 (s), 1227 (s) cm^{-1} . *Anal. Calcd (%) for $\text{C}_6\text{H}_{15}\text{N}_2\text{VCl}_2$* : C: 30.40, H: 6.38, N: 11.73, V: 21.49, Cl: 29.91; Found: C: 30.38, H: 6.22, N: 11.73, V: 21.33, Cl: 29.61.

Synthesis of (C₅H₄CH₂CH₂NMe)VCl(N*t*-Bu) (**5**)

To a solution of 0.95 g (3.9 mmol) of **2** in 20 mL of pentane 0.49 g (4.0 mmol) of C₅H₅(CH₂)₂N(H)Me was added. The brown solution was refluxed for 18 hours, after which the color had changed to red. All volatiles were removed *in vacuo* and the resulting solid was extracted twice with 10 mL of pentane. The pentane solution was concentrated and cooled to -20 °C, yielding 0.80 g (2.9 mmol, 74%) of **5** as red crystals.

¹H NMR (500 MHz, C₆D₆, 25°C): δ 6.11 (m, 1H, Cp), 5.88 (m, 2H, Cp), 5.11 (m, 1H, Cp), 4.60 (m, 1H, NCHH), 4.01 (s, 3H, NCH₃), 3.20 (m, 1H, NCHH), 2.46 (m, 1H, CpCHH), 1.98 (m, 1H, CpCHH), 1.19 (s, 9H, *t*-Bu). ¹³C {¹H} NMR (125.7 MHz, C₆D₆, 25°C): δ 137.5 (C_{ipso} of Cp), 116.2, 111.7, 100.6, 99.6 (4 CH of Cp), 81.6 (NCH₃), 61.6 (NCH₂), 30.9 (CH₃ of *t*-Bu), 28.3 (CpCH₂). ⁵¹V NMR (131.4 MHz, C₆D₆, 25°C): δ -679 ($\Delta\nu_{1/2}$ = 350). *Anal. Calcd (%) for $\text{C}_{12}\text{H}_{20}\text{N}_2\text{VCl}$* : C: 51.72, H: 7.23, N: 10.05, found: C: 51.28, H: 7.37, N: 9.99.

Synthesis of (C₅H₄CH₂CH₂N*i*-Pr)VCl(N*t*-Bu) (**6**)

To a solution of 3.26 g (13 mmol) of **2** in 100 mL of pentane 2.00 g (13 mmol) of C₅H₅(CH₂)₂N(H)*i*-Pr was added. The brown solution was refluxed for 18 hours, after which the color had changed to red. All volatiles were removed *in vacuo* and the resulting solid was extracted twice with 50 mL of pentane. The pentane solution was concentrated and cooled to -20 °C, yielding 3.31 g (10.8 mmol, 83%) of **6** as red crystals.

¹H NMR (300 MHz, C₆D₆, 25°C): δ 6.10 (m, 1H, Cp), 5.97 (m, 2H, Cp and CH of *i*-Pr), 5.87 (m, 1H, Cp), 5.13 (m, 1H, Cp), 4.66 (m, 1H, NCHH), 3.25 (dd, J_{H-H} = 6 / 13, 1H, NCHH), 2.47 (m, 1H, CpCHH), 1.76 (m, 1H, CpCHH), 1.19 (s, 9H, *t*-Bu), 1.01 (d, J_{H-H} = 7, 3H, CH₃ of *i*-Pr), 0.98 (d, J_{H-H} = 7, 3H, CH₃ of *i*-Pr). ¹³C {¹H} NMR (75.4 MHz, C₆D₆, 25°C): δ 139.6 (C_{ipso} of Cp), 115.1, 114.6, 100.5, 99.5 (4 CH of Cp), 72.3 (CH of *i*-Pr), 70.5 (NCH₂), 30.0 (CpCH₂), 31.2

Synthesis of vanadium(V) complexes containing amido functionalized cyclopentadienyl ligands

(CH₃ of *t*-Bu), 21.2, 20.5 (2 CH₃ of *i*-Pr), C_q of *t*-Bu not observed. ⁵¹V NMR (131.4 MHz, C₆D₆, 25°C): δ -674 (Δv_{1/2} = 360). IR: 652 (w), 810 (s), 837 (w), 876 (w), 1146 (w), 1169 (w), 1209 (s), 1225 (s), 1356 (s) cm⁻¹. Anal. Calcd (%) for C₁₄H₂₄N₂VCl: C: 54.82, H: 7.89, N: 9.13, V: 16.61, Cl: 11.56, found: C: 54.64, H: 7.92, N: 8.96, V: 16.45, Cl: 11.46.

Synthesis of (C₅H₄CH₂CH₂CH₂N*i*-Pr)VCl(N*t*-Bu) (**7**)

To a solution of 0.27 g (1.5 mmol) C₅H₅(CH₂)₃N(H)*i*-Pr in 5 mL THF was added 0.15 g (1.6 mmol) Me₃SiCH₂Li. The solution was stirred for half an hour and then added to a solution of 0.34 g (1.5 mmol) of **4** in 20 mL of THF, cooled to 0°C. The solution was brought to room temperature and stirred for an additional hour. All volatiles were removed *in vacuo*, and the brown solid was extracted twice with 10 mL of pentane. After removal of the solvent 0.18 g (0.56 mmol, 37%) of **7** is obtained as a red oil. ¹H NMR shows small amounts of impurities in the range of 0 - 2 ppm.

¹H NMR (500 MHz, C₆D₆, 25°C): δ 6.26 (sept, J_{H-H} = 7, 1H, CH of *i*-Pr), 6.04 (m, 1H, Cp), 5.92 (m, 1H, Cp), 5.76 (m, 1H, Cp), 4.96 (m, 1H, Cp), 3.22 (dd, J_{H-H} = 16 / 8, 1H, NCHH), 2.87 (dd, J_{H-H} = 15 / 8, 1H, NCHH), 2.30 (m, 1H, CpCHH), 2.16 (m, 1H, CpCHH), 1.89 (m, 1H, CH₂CHH), 1.44 (m, 1H, CH₂CHH), 1.28 (d, J_{H-H} = 7, 3H, CH₃ of *i*-Pr), 1.18 (s, 9H, *t*-Bu), 0.96 (d, J_{H-H} = 7, 3H, CH₃ of *i*-Pr). ¹³C {¹H} NMR (125.7 MHz, C₆D₆, 25°C): δ 117.7 (C_{ipso} of Cp), 114.4, 102.2, 97.2, 94.8 (4 CH of Cp), 72.2 (CH of *i*-Pr), 48.9 (NCH₂), 28.1 (CpCH₂), 25.6 (CH₃ of *t*-Bu), 22.0 (CH₂CH₂CH₂), 16.5, 15.6 (2 CH₃ of *i*-Pr), C_q of *t*-Bu not observed. ⁵¹V NMR (131.4 MHz, C₆D₆, 25°C): δ -708 (Δv_{1/2} = 380).

Synthesis of (C₅H₄CH₂CH₂N*i*-Pr)VCl(N*p*-Tol) (**8**)

In 20 mL of toluene 0.45 g (1.5 mmol) of **6** and 0.17 g (1.6 mmol) of *p*-toluidine were dissolved. The brown solution was refluxed for 30 hours, during which it was regularly degassed to remove the formed *t*-BuNH₂, after which all volatiles were removed *in vacuo*. The resulting dark solid was stripped of residual toluene by addition of 2 x 10 mL of ether and subsequent removal *in vacuo*. Extraction of the resulting dark solid with 2 x 20 mL of ether gave a dark red solution, which after cooling to -25°C yielded 0.40 g (1.18 mmol, 78%) of **8** as dark red crystals.

¹H NMR (500 MHz, C₆D₆, 25°C): δ 7.15 (overlap with solvent, CH of *p*-Tol), 6.81 (d, J_{H-H} = 8, 2H, CH of *p*-Tol), 6.20 (m, 1H, Cp), 5.96 (m, 1H, Cp), 5.61 (m, 1H, Cp), 5.54 (sept, J_{H-H} = 7, 1H, CH of *i*-Pr), 5.15 (m, 1H, Cp), 4.70 (m, 1H, NCHH), 3.33 (ddd, J_{H-H} = 14 / 7 / 3, 1H, NCHH), 2.49 (ddd, J_{H-H} = 13 / 7 / 2, 1H, CpCHH), 2.05 (s, 3H, CH₃ of *p*-Tol), 1.86 (m, 1H, CpCHH), 1.13 (d, J_{H-H} = 7, 3H, CH₃ of *i*-Pr), 0.97 (d, J_{H-H} = 7, 3H, CH₃ of *i*-Pr). ¹³C {¹H} NMR (125.7 MHz, C₆D₆, 25°C): δ 139.1 (C_{ipso} of Cp), 135.4 (C_{ipso} of *p*-Tol), 129.1, 125.5 (2 CH of *p*-Tol), 115.4, 113.9, 103.9, 100.7 (4 CH of Cp), 72.1 (NCH₂), 71.1 (CH of *i*-Pr), 29.5 (CpCH₂), 22.2 (CH₃ of *i*-Pr), 21.2 (CH₃ of *p*-Tol), 21.1 (CH₃ of *i*-Pr), C_q of *p*-Tol not observed. ⁵¹V NMR (131.4 MHz, C₆D₆, 25°C): δ

-579 ($\Delta\nu_{1/2} = 500$). *Anal. Calcd (%) for $C_{17}H_{22}N_2VCl$* : C: 59.92, H: 6.51, N: 8.22, V: 14.95, Cl: 10.40, found: C: 59.85, H: 6.51, N: 8.16, V: 14.86, Cl: 10.46.

Synthesis of $(C_5H_4CH_2CH_2NMe)VMe(Nt-Bu)$ (**9**)

To a solution of 1.18 g (4.2 mmol) of **5** in 30 mL of Et_2O and 5 mL of toluene was added 2.8 mL of 1.53 M MeLi in Et_2O (4.3 mmol). The solution was stirred for half an hour, after which all volatile compounds were removed *in vacuo*. The resulting red oil was stripped of residual toluene by addition of 2 x 5 mL of pentane and subsequent removal *in vacuo*. Extraction with 2 x 20 mL of pentane and removal of the solvent *in vacuo* yielded 0.89 g of **9** as a red oil. 1H NMR showed small amounts of impurities in the region of 0 - 4 ppm. Crude yield: 3.4 mmol (81%).

1H NMR (500 MHz, C_6D_5Br , 25°C): δ 5.94 (br, 1H, Cp), 5.63 (br, 1H, Cp), 5.53 (br, 1H, Cp), 5.34 (br, 1H, Cp), 4.15 (m, 1H, NCHH), 3.79 (s, 3H, NCH₃), 3.47 (m, 1H, NCHH), 2.57 (m, 1H, CpCHH), 2.40 (m, 1H, CpCHH), 1.23 (s, 9H, *t*-Bu), 0.63 (br, $\Delta\nu_{1/2} = 12$, 3H, VCH₃). ^{13}C { 1H } NMR (125.7 MHz, C_6D_5Br , 25°C): δ 133.9 (C_{ipso} of Cp), 114.7, 106.1, 102.3, 98.3 (4 CH of Cp), 78.6 (NCH₃), 58.9 (NCH₂), 32.2 (CH₃ of *t*-Bu), 29.1 (CpCH₂) C_q of *p*-Tol and VCH₃ not observed. ^{51}V NMR (131.4 MHz, C_6D_5Br , 25°C): δ -679 ($\Delta\nu_{1/2} = 700$).

Synthesis of $(C_5H_4CH_2CH_2Ni-Pr)VMe(Nt-Bu)$ (**10**)

To a solution of 1.14 g (3.7 mmol) of **6** in 20 mL of pentane was added 4.5 mL of 0.88 M MeLi in Et_2O (4.0 mmol). The solution was stirred for an hour, after which all volatile compounds were removed *in vacuo*. The resulting brown solid was extracted twice with 30 mL of pentane and concentrated to ~10 mL. Cooling to -60°C yielded 0.50 g (1.8 mmol, 49%) of analytically pure **10** as a red brown crystals. Recrystallization from pentane produced crystals of **10**, suitable for X-ray diffraction.

1H NMR (300 MHz, C_6D_6 , 25°C): δ 5.83 (m, 1H, Cp), 5.50 (m, 1H, Cp), 5.41 (m, 2H, Cp), 5.29 (sept, $J_{H-H} = 7$, 1H, CH of *i*-Pr), 4.13 (m, 1H, NCHH), 3.30 (m, 1H, NCHH), 2.50 (ddd, $J_{H-H} = 3 / 7 / 13$, 1H, CpCHH), 2.07 (m, 1H, CpCHH), 1.25 (s, 9H, *t*-Bu), 1.15 (d, $J_{H-H} = 7$, 3H, CH₃ of *i*-Pr), 0.95 (d, $J_{H-H} = 7$, 3H, CH₃ of *i*-Pr), 0.69 (br, $\Delta\nu_{1/2} = 8$, 3H, VCH₃). ^{13}C { 1H } NMR (125.7 MHz, C_7D_8 , -70°C): δ 132.9 (C_{ipso} of Cp), 112.7, 107.5, 100.6, 94.1 (4 CH of Cp), 70.4 (C_q of *t*-Bu), 67.1 (CH of *i*-Pr), 66.5 (NCH₂), 29.4 (CpCH₂), 31.2 (CH₃ of *t*-Bu), 21.8, 20.7 (2 CH₃ of *i*-Pr), 17.7 (br, $\Delta\nu_{1/2} = 75$, VCH₃). ^{13}C NMR (125.7 MHz, C_6D_6 , 25°C): δ 132.3 (s, C_q of Cp), 113.0, 107.9, 100.9, 97.5 (d, $J_{C-H} = 170, 172, 173, 173$, 4 CH of Cp), 67.5 (d, 142, CH of *i*-Pr), 66.8 (t, 142, NCH₂), 31.6 (q, 126, CH₃ of *t*-Bu), 29.9 (t, 129, CpCH₂), 22.2 (q, 125, CH₃ of *i*-Pr), 21.1 (q, 125, CH₃ of *i*-Pr), 17 (very broad, VCH₃). C_q of *t*-Bu not observed. ^{51}V NMR (131.4 MHz, C_6D_6 , 25°C): δ -665 ($\Delta\nu_{1/2} = 320$). IR: 656 (w), 667 (w), 689 (w), 814 (s), 851 (w), 868 (w), 957 (w), 990 (w), 1018 (w), 1036 (w), 1044 (w), 1071 (w), 1115 (w), 1148 (w), 1173 (w), 1213 (w), 1248 (s), 1333 (w), 1358 (s) cm^{-1} . *Anal. Calcd (%) for $C_{15}H_{27}N_2V$* : C: 62.92, H: 9.50, N: 9.78, V: 17.79; found: C: 62.66, H: 9.49, N: 9.80, V: 17.68.

Synthesis of $(C_5H_4CH_2CH_2Ni-Pr)V(CH_2CMe_3)(Nt-Bu)$ (**11**)

To a solution of 0.34 g (1.1 mmol) of **6** in 20 mL of pentane was added 0.10 g (1.2 mmol) of $LiCH_2CMe_3$. The solution is stirred for half an hour, after which all volatiles were removed *in vacuo*. The red residue is extracted with 30 mL of pentane. After removal of the solvent 0.33 g of **11** is obtained as a red oil. 1H NMR shows small amounts of impurities in the range of 0 - 2 ppm. Crude yield: 0.96 mmol (87%).

1H NMR (300 MHz, C_6D_6 , 25°C): δ 5.73 (m, 1H, Cp), 5.64 (sept, $J_{H-H} = 7$, 1H, CH of *i*-Pr), 5.44 (m, 1H, Cp), 5.31 (m, 2H, Cp), 4.29 (m, 1H, NCHH), 3.18 (m, 1H, NCHH), 2.46 (dd, $J_{H-H} = 6 / 13$, 1H, CpCHH), 1.93 (m, 1H, CpCHH), 1.56 (m, 2H, VCH₂), 1.36 (s, 9H, *t*-Bu), 1.27 (s, 9H, *t*-Bu), 1.06 (d, $J_{H-H} = 7$, 3H, CH₃ of *i*-Pr), 0.93 (d, $J_{H-H} = 7$, 3H, CH₃ of *i*-Pr). ^{13}C { 1H } NMR (125.7 MHz, C_7D_8 , -70°C): δ 134.0 (C_{ipso} of Cp), 112.1, 109.8, 99.0, 97.5 (4 CH of Cp), 70.9 ($\Delta v_{1/2} = 22$, C_{quart} of *t*-Bu), 69.1 (CH of *i*-Pr), 65.3 (NCH₂), 62.0 ($\Delta v_{1/2} = 67$, VCH₂), 34.3, 31.6 (CH₃ of 2 *t*-Bu), 30.2 (CpCH₂), 22.8, 20.3 (2 CH₃ of *i*-Pr). ^{51}V NMR (131.4 MHz, C_6D_6 , 25°C): δ -579 ($\Delta v_{1/2} = 330$). IR (neat): 654 (w), 689 (w), 812 (s), 851 (w), 864 (w), 953 (w), 978 (w), 1007 (w), 1036 (w), 1045 (w), 1080 (w), 1105 (w), 1146 (w), 1173 (w), 1209 (w), 1238 (s), 1310 (w), 1331 (w), 1354 (s), 1375 (w), 1397 (w), 1454 (s), 2864 (s), 2893 (s), 2940 (s), 2967 (s), 3106 (w) cm^{-1} .

Synthesis of $(C_5H_4CH_2CH_2Ni-Pr)V(CH_2CMe_2Ph)(Nt-Bu)$ (**12**)

To a solution of 0.42 g (1.4 mmol) of **6** in 20 mL of pentane was added 0.26 g (1.5 mmol) of $LiCH_2CMe_2Ph$. The solution is stirred for half an hour, after which all volatiles were removed *in vacuo*. The red residue is extracted with 30 mL of pentane. After removal of the solvent 0.59 g of **12** is obtained as a red oil. 1H NMR shows impurities in the range of 0 - 7 ppm, with $PhCMe_3$ being the main impurity (~5%). Crude yield: 1.4 mmol (100%).

1H NMR (300 MHz, C_6D_6 , 25°C): δ 7.43 (m, 2H, Ph), 7.13 (m, 2H, Ph), 7.00 (m, 1H, Ph), 5.48 (br, 1H, Cp), 5.43 (sept, $J_{H-H} = 7$, 1H, CH of *i*-Pr), 5.20 (br, 1H, Cp), 5.15 (br, 1H, Cp), 4.91 (m, 1H, Cp), 4.03 (m, 1H, NCHH), 3.00 (m, 1H, NCHH), 2.26 (dd, $J_{H-H} = 6 / 12$, 1H, CpCHH), 1.77 (m, 3H, CpCHH and VCH₂), 1.54 (s, 3H, C(CH₃)₂), 1.44 (s, 3H, C(CH₃)₂), 1.04 (s, 9H, *t*-Bu), 0.89 (d, $J_{H-H} = 6$, 3H, CH₃ of *i*-Pr), 0.70 (d, $J_{H-H} = 6$, 3H, CH₃ of *i*-Pr). ^{13}C { 1H } NMR (125.7 MHz, C_7D_8 , -70°C): δ 152.1 (C_{ipso} of Ph), 133.8 (C_{ipso} of Cp), 125.9, 124.5, 107.7 (3 CH of Ph), 111.4, 108.9, 99.7, 97.1 (4 CH of Cp), 71.0 (C_{quart} of *t*-Bu), 68.8 (CH of *i*-Pr), 65.5 (NCH₂), 59.9 ($\Delta v_{1/2} = 100$, VCH₂), 30.0 (CpCH₂), 34.1 (CH₃ of *t*-Bu), 33.8, 31.5 (2 C(CH₃)₂), 22.6, 20.0 (2 CH₃ of *i*-Pr). ^{51}V NMR (131.4 MHz, C_6D_6 , 25°C): δ -596 ($\Delta v_{1/2} = 370$). IR (neat): 654 (w), 667 (w), 700 (s), 764 (s), 814 (s), 851 (w), 868 (w), 953 (w), 978 (w), 1009 (w), 1034 (w), 1044 (w), 1074 (w), 1107 (w), 1125 (w), 1144 (w), 1173 (w), 1188 (w), 1211 (w), 1233 (s), 1333 (w), 1358 (s), 1375 (w), 1447 (s), 1495 (s), 1601 (w), 2863 (s), 2926 (s), 2971 (s), 3023 (w), 3057 (w), 3086 (w) cm^{-1} .

Synthesis of $(C_5H_4CH_2CH_2Ni-Pr)VMe(Np-Tol)$ (**13**)

To a solution of 0.54 g (1.6 mmol) of **8** in 15 mL of Et₂O and 5 mL of toluene was added 1.1 mL of 1.53 M MeLi in Et₂O (1.7 mmol). The solution was stirred for half an hour, after which all volatile compounds were removed *in vacuo*. The resulting brown oil was stripped of residual toluene by addition of 2 x 5 mL of pentane and subsequent removal *in vacuo*. Extraction with 2 x 10 mL of pentane and removal of the solvent *in vacuo* yielded 0.51 g of **13** as a red oil. ¹H NMR showed small amounts of impurities in the region of 0 - 3 ppm. Crude yield: 1.6 mmol (100%).

¹H NMR (500 MHz, C₆D₆, 25°C): δ 7.20 (d, J_{H-H} = 8, 2H, CH of *p*-Tol), 6.89 (d, J_{H-H} = 8, 2H, CH of *p*-Tol), 5.89 (m, 1H, Cp), 5.50 (m, 1H, Cp), 5.43 (m, 1H, Cp), 5.28 (m, 1H, Cp), 4.89 (sept, J_{H-H} = 7, 1H, CH of *i*-Pr), 4.16 (m, 1H, NCHH), 3.38 (m, 1H, NCHH), 2.47 (m, 1H, CpCHH), 2.14 (overlap, CpCHH), 2.11 (s, 3H, CH₃ of *p*-Tol), 1.25 (d, J_{H-H} = 7, 3H, CH₃ of *i*-Pr), 1.09 (d, J_{H-H} = 7, 3H, CH₃ of *i*-Pr), 0.92 (br, Δv_{1/2} = 7, 3H, VCH₃). ¹³C NMR (125.7 MHz, C₆D₆, 25°C): δ 133.3, 133.0 (s, C_{ipso} of Cp and C_{ipso} of *p*-Tol), 129.1, 125.4 (d, J_{C-H} = 156, 159, 2 CH of *p*-Tol), 113.9, 108.2, 102.4, 100.6 (d, J_{C-H} = 173, 173, 174, 174, 4 CH of Cp), 69.3 (t, J_{C-H} = 136, NCH₂), 66.8 (d, J_{C-H} = 138, CH of *i*-Pr), 29.4 (t, J_{C-H} = 129, CpCH₂), 23.3, 22.3, 21.2 (2 CH₃ of *i*-Pr and CH₃ of *p*-Tol), C_q of *p*-Tol and VCH₃ not observed. ⁵¹V NMR (131.4 MHz, C₆D₆, 25°C): δ -571 (Δv_{1/2} = 440).

Synthesis of (C₅H₄CH₂CH₂CH₂N*i*-Pr)VMe(N*t*-Bu) (**14**)

A solution of 0.09 g (0.28 mmol) of **7** in 10 mL of pentane was cooled to 0°C, after which 0.35 mL 0.88 M MeLi (0.31 mmol) in ether was added. The brown solution was stirred for an hour at room temperature, after which all volatiles were removed *in vacuo*. The sticky residue was extracted with 10 mL of pentane. Evaporation of the solvent yielded 0.07 g of **14** as a red oil. ¹H NMR showed small amounts of impurities in the region of 0 - 3 ppm. Crude yield: 0.23 mmol (82%).

¹H NMR (500 MHz, C₆D₆, 25°C): δ 5.91 (sept, J_{H-H} = 7, 1H, CH of *i*-Pr), 5.61 (m, 1H, Cp), 5.52 (m, 1H, Cp), 5.20 (m, 2H, Cp), 2.86 (m, 1H, NCHH), 2.69 (m, 1H, NCHH), 2.20 (m, 2H, CpCH₂), 1.56 (m, 1H, CH₂CHH), 1.44 (m, 1H, CH₂CHH), 1.18 (s, 9H, *t*-Bu), 1.12 (d, J_{H-H} = 7, 3H, CH₃ of *i*-Pr), 1.06 (d, J_{H-H} = 7, 3H, CH₃ of *i*-Pr), 0.68 (br, Δv_{1/2} = 18, 3H, VCH₃). ¹³C {¹H} NMR (125.7 MHz, C₆D₆, 25°C): δ 115.4 (C_{ipso} of Cp), 109.0, 99.6, 95.3, 94.0 (4 CH of Cp), 67.8 (CH of *i*-Pr), 45.9 (NCH₂), 29.6 (CpCH₂), 26.3 (CH₃ of *t*-Bu), 22.5 (CH₂CH₂CH₂), 17.3, 15.5 (2 CH₃ of *i*-Pr), C_q of *t*-Bu and VCH₃ not observed. ⁵¹V NMR (131.4 MHz, C₆D₆, 25°C): δ -701 (Δv_{1/2} = 450).

Synthesis of [(C₅H₄CH₂CH₂CH₂N*i*-Pr)V(μ-N*t*-Bu)]₂ (**15**)

To a solution of 0.27 g (0.88 mmol) of **6** in 20 mL of Et₂O was added 1.6 mL of 0.56 M EtMgCl in Et₂O (0.90 mmol). The solution immediately turned brown and was stirred for half an hour, during which it turned dark purple. All volatile compounds were removed *in vacuo* and the resulting dark solid was extracted with 2 x 30 mL of pentane. Concentrating and cooling the

solution to -25°C yielded 0.084 g of **15** as dark crystals. $^1\text{H NMR}$ showed impurities in the region of 0 - 7 ppm. Crude yield: 0.15 mmol (34%).

$^1\text{H NMR}$ (500 MHz, C_6D_6 , 25°C): δ 6.50 (br, 4H, Cp), 3.72 (t, $J_{\text{H-H}} = 6$, 4H, NCH_2), 3.56 (br, 4H, Cp), 2.76 (sept, $J_{\text{H-H}} = 6$, 2H, CH of *i*-Pr), 2.63 (t, $J_{\text{H-H}} = 6$, 4H, CpCH_2), 1.84 (s, 18H, CH_3 of *t*-Bu), 0.65 (d, $J_{\text{H-H}} = 6$, 12H, CH_3 of *i*-Pr). $^{13}\text{C NMR}$ (125.7 MHz, C_6D_6 , 25°C): δ 138.6 (s, C_{ipso} of Cp), 102.9, 100.5 (d, $J_{\text{C-H}} = 171, 172$, 2 CH of Cp), 64.7 (t, $J_{\text{C-H}} = 133$, NCH_2), 57.7 (d, $J_{\text{C-H}} = 137$, CH of *i*-Pr), 35.9 (q, $J_{\text{C-H}} = 125$, CH_3 of *t*-Bu), 30.7 (t, $J_{\text{C-H}} = 127$, CpCH_2), 21.2 (q, $J_{\text{C-H}} = 124$, CH_3 of *i*-Pr), C_q of *t*-Bu not observed. $^{51}\text{V NMR}$ (131.4 MHz, C_6D_6 , 25°C): δ 137 ($\Delta\nu_{1/2} = 820$).

Synthesis of (*p*-TolN)V(*Ni*-Pr₂)Cl₂ (**18**)

To a suspension of 2.46 g (9.37 mmol) of **16** in 50 mL of ether 2.85 mL (28.1 mmol) of HNi-Pr_2 was added in five minutes. The suspension was stirred for 18 hours at room temperature, after which all volatiles were removed *in vacuo*. Extraction of the dark residue with 2 x 25 mL of ether, followed by concentration of the red solution and cooling to -25°C yielded 2.09 g (6.39 mmol, 68%) of **18** as red crystals.

$^1\text{H NMR}$ (500 MHz, C_6D_6 , 25°C): δ 7.26 (d, $J_{\text{H-H}} = 8$, 2H, CH of *p*-Tol), 6.58 (d, $J_{\text{H-H}} = 9$, 2H, CH of *p*-Tol), 5.89 (sept, $J_{\text{H-H}} = 6$, 1H, CH of *i*-Pr), 3.01 (br, 1H, CH of *i*-Pr), 1.88 (s, 3H, CH_3 of *p*-Tol), 1.31 (d, $J_{\text{H-H}} = 6$, 6H, CH_3 of *i*-Pr), 0.87 (d, $J_{\text{H-H}} = 6$, 6H, CH_3 of *i*-Pr). $^{13}\text{C NMR}$ (125.7 MHz, C_6D_6 , 25°C): δ 138.6 (s, C_{ipso} of *p*-Tol), 129.2, 126.3 (d, $J_{\text{C-H}} = 160, 163$, 2 CH of *p*-Tol), 61.2, 55.7 (d, $J_{\text{C-H}} = 138, 130$, 2 CH of *i*-Pr), 28.5 (q, $J_{\text{C-H}} = 128$, CH_3 of *i*-Pr), 21.2 (q, $J_{\text{C-H}} = 127$, CH_3 of *p*-Tol), 18.8 (q, $J_{\text{C-H}} = 127$, CH_3 of *i*-Pr), C_q of *p*-Tol not observed. $^{51}\text{V NMR}$ (131.4 MHz, C_6D_6 , 25°C): δ -67 (t, $J_{\text{V-N}} = 96$). *Anal. Calcd (%) for $\text{C}_{13}\text{H}_{21}\text{N}_2\text{VCl}_2$* : C: 47.73, H: 6.47, N: 8.56; found: C: 47.27, H: 6.42, N: 8.24.

Synthesis of (*p*-TolN)VCp(*Ni*-Pr₂)Cl (**20**)

Onto 0.536 g (1.64 mmol) of **18** and 0.146 g (1.66 mmol) of CpNa, 30 mL of toluene was condensed at liquid nitrogen temperature. The mixture was thawed out and stirred for three hours at -40°C and for one night at room temperature, after which all volatiles were removed *in vacuo*. The resulting dark solid was stripped of residual toluene by addition of 2 x 5 mL of pentane and subsequent removal *in vacuo*. Extraction with 10 mL of pentane, concentration of the red solution and cooling to -25°C yielded 0.47 g (1.26 mmol, 77%) of **20** as red crystals.

$^1\text{H NMR}$ (500 MHz, C_6D_6 , 25°C): δ 7.19 (d, $J_{\text{H-H}} = 8$, 2H, CH of *p*-Tol), 6.78 (d, $J_{\text{H-H}} = 8$, 2H, CH of *p*-Tol), 5.83 (s, 5H, Cp), 4.96 (sept, $J_{\text{H-H}} = 7$, 1H, CH of *i*-Pr), 3.33 (sept, $J_{\text{H-H}} = 6$, 1H, CH of *i*-Pr), 2.03 (s, 3H, CH_3 of *p*-Tol), 1.85 (d, $J_{\text{H-H}} = 7$, 3H, CH_3 of *i*-Pr), 1.25 (d, $J_{\text{H-H}} = 7$, 3H, CH_3 of *i*-Pr), 1.04 (d, $J_{\text{H-H}} = 7$, 3H, CH_3 of *i*-Pr), 0.74 (d, $J_{\text{H-H}} = 6$, 3H, CH_3 of *i*-Pr). $^{13}\text{C} \{^1\text{H}\} \text{NMR}$ (125.7 MHz, C_6D_6 , 25°C): δ 136.0 (C_{ipso} of *p*-Tol), 129.2, 125.1 (2 CH of *p*-Tol), 108.6 (Cp), 65.0, 58.5 (2 CH of *i*-Pr), 31.1, 27.4 (2 CH_3 of *i*-Pr), 21.2 (CH_3 of *p*-Tol), 19.4, 17.6 (2 CH_3 of *i*-Pr), C_q

of *p*-Tol not observed. ^{51}V NMR (131.4 MHz, C_6D_6 , 25°C): δ -591 ($\Delta\nu_{1/2} = 400$). *Anal. Calcd (%) for $\text{C}_{18}\text{H}_{26}\text{N}_2\text{VC}$* : C: 60.59, H: 7.35, N: 7.85, Cl: 9.94; found: C: 60.45, H: 7.44, N: 7.87, Cl: 10.14.

Synthesis of (*t*-BuN)VCp₂(*Ni*-Pr₂) (**21**)

To a mixture of 2.07 g (7.0 mmol) of **17** and 1.3 g (15 mmol) of CpNa 50 mL of cold THF (-30°C) was added and the resulting solution was stirred for one night at room temperature. After removal of all volatiles *in vacuo*, the dark residue was stripped of residual THF by addition of 2 x 10 mL of pentane and subsequent removal *in vacuo*. Extraction with 4 x 50 mL of pentane, followed by concentration of the red solution and cooling to -25°C yielded 2.12 g (6.57 mmol, 93%) of **21** as red crystals.

^1H NMR (500 MHz, THF- d_8 , 50°C): δ 6.01 (br, 5H, Cp), 5.24 (br, 5H, Cp), 4.86 (sept, $J_{\text{H-H}} = 6$, 1H, CH of *i*-Pr), 3.60 (sept, $J_{\text{H-H}} = 6$, 1H, CH of *i*-Pr), 1.89 (br, 3H, CH_3 of *i*-Pr), 1.46 (s, 9H, *t*-Bu), 1.37 (br, 3H, CH_3 of *i*-Pr), 1.12 (d, $J_{\text{H-H}} = 7$, 6H, 2 CH_3 of *i*-Pr). ^{13}C $\{^1\text{H}\}$ NMR (125.7 MHz, THF- d_8 , 50°C): δ 116.8, 109.1 (2 Cp), 65.8, 56.7 (2 CH of *i*-Pr), 33.7 (CH_3 of *i*-Pr), 33.4 (CH_3 of *t*-Bu), 28.5, 22.2, 22.1 (3 CH of *i*-Pr), C_q of *t*-Bu not observed. ^{51}V NMR (131.4 MHz, C_6D_6 , 25°C): δ -623 ($\Delta\nu_{1/2} = 300$). *Anal. Calcd (%) for $\text{C}_{20}\text{H}_{33}\text{N}_2\text{V}$* : C: 68.16, H: 9.44, N: 7.95, V: 14.57; found: C: 67.89, H: 9.67, N: 7.93, V: 14.30.

Synthesis of (*p*-TolN)VCp₂(*Ni*-Pr₂) (**22**)

A suspension of 2.0 g (6.1 mmol) of **18** and 1.1 g (13 mmol) of CpNa in 40 mL of toluene was stirred for 18 hours at room temperature, after which all volatiles were removed *in vacuo*. Residual toluene was removed by addition of 2 x 5 mL of pentane and subsequent removal *in vacuo*. Extraction with 12 x 50 mL of pentane and cooling of the red solution to -25°C yielded 0.96 g (2.48 mmol, 41%) of **22** as red crystals.

^1H NMR (500 MHz, THF- d_8 , 50°C): δ 7.18 (d, $J_{\text{H-H}} = 8$, 2H, CH of *p*-Tol), 7.05 (d, $J_{\text{H-H}} = 8$, 2H, CH of *p*-Tol), 6.05 (s, 5H, Cp), 5.22 (s, 5H, Cp), 4.91 (sept, $J_{\text{H-H}} = 6$, 1H, CH of *i*-Pr), 3.66 (sept, $J_{\text{H-H}} = 7$, 1H, CH of *i*-Pr), 2.32 (s, 3H, CH_3 of *p*-Tol), 1.89 (d, $J_{\text{H-H}} = 6$, 3H, CH_3 of *i*-Pr), 1.37 (d, $J_{\text{H-H}} = 6$, 3H, CH_3 of *i*-Pr), 1.16 (m, 6H, 2 CH_3 of *i*-Pr). ^{13}C $\{^1\text{H}\}$ NMR (125.7 MHz, THF- d_8 , 50°C): δ 136.7 (C_{ipso} of *p*-Tol), 130.7, 126.5 (2 CH of *p*-Tol), 117.0, 110.4 (2 Cp), 65.4, 58.7 (2 CH of *i*-Pr), 33.3, 28.3, 26.7, 22.2, 22.0 (4 CH_3 of *i*-Pr and CH_3 of *p*-Tol), C_q of *p*-Tol not observed. ^{51}V NMR (131.4 MHz, C_6D_6 , 25°C): δ -546 ($\Delta\nu_{1/2} = 330$). *Anal. Calcd (%) for $\text{C}_{23}\text{H}_{31}\text{N}_2\text{V}$* : C: 71.48, H: 8.09, N: 7.25, V: 13.18; found: C: 70.80, H: 7.86, N: 7.13, V: 12.93.

Synthesis of (*t*-BuN)VCp(*Ni*-Pr₂)Me (**23**)

A solution of 0.57 g (1.77 mmol) of **19** in 25 mL of ether was cooled to -50°C , after which 1.2 mL 1.53 M MeLi (1.84 mmol) in ether was added. After stirring for 20 minutes at -10°C the color of the solution had changed from red to yellow. All volatiles were removed *in vacuo* and the resulting solid was stripped of residual ether by addition of 2 x 5 mL of cold pentane and

subsequent removal *in vacuo* at -10°C. Extraction with 30 mL of cold pentane and slow removal of the solvent *in vacuo* at -10°C yielded 0.47 g (1.55 mmol, 88%) of **23** as a yellow oil, which crystallized at -35°C. ¹H NMR of the yellow crystals showed no impurities.

¹H NMR (500 MHz, C₆D₅CD₃, -50°C): δ 5.58 (s, 5H, Cp), 4.29 (m, 1H, CH of *i*-Pr), 3.09 (br, 1H, CH of *i*-Pr), 1.76 (d, J_{H-H} = 6, 3H, CH₃ of *i*-Pr), 1.38 (d, J_{H-H} = 6, 3H, CH₃ of *i*-Pr), 1.23 (s, 9H, *t*-Bu), 0.83 (d, J_{H-H} = 6, 3H, CH₃ of *i*-Pr), 0.80 (d, J_{H-H} = 6, 3H, CH₃ of *i*-Pr), 0.62 (s, 3H, VCH₃). ¹³C {¹H} NMR (125.7 MHz, C₆D₅CD₃, -50°C): δ 104.6 (Cp), 62.0, 52.6 (2 CH of *i*-Pr), 32.2 (CH₃ of *i*-Pr), 31.5 (CH₃ of *t*-Bu), 27.1, 20.1, 19.1 (3 CH₃ of *i*-Pr), C_q of *t*-Bu and VCH₃ not observed. ⁵¹V NMR (131.4 MHz, C₆D₅CD₃, 25°C): δ -673 (t, J_{N-V} = 89).

Synthesis of (*p*-TolN)VCp(N*i*-Pr₂)Me (**24**)

A solution of 0.42 g (1.18 mmol) of **20** in 30 mL of ether was cooled to -40°C, after which 0.77 mL 1.53 M MeLi (1.18 mmol) in ether was added. After stirring for 20 minutes at -10°C the color of the solution has changed from red to orange. All volatiles were removed *in vacuo* and the resulting solid was stripped of residual ether by addition of 2 x 5 mL of cold pentane and subsequent removal *in vacuo* at -10°C. Extraction with 30 mL of cold pentane and slow removal of the solvent *in vacuo* at -10°C yielded 0.204 g (0.61 mmol, 51%) of **24** as yellow crystals.

¹H NMR (500 MHz, C₆D₆, 25°C): δ 7.16 (overlap with solvent, CH of *p*-Tol), 6.86 (d, J_{H-H} = 8, 2H, CH of *p*-Tol), 5.59 (s, 5H, Cp), 4.36 (sept, J_{H-H} = 7, 1H, CH of *i*-Pr), 3.21 (br, 1H, CH of *i*-Pr), 2.10 (s, 3H, CH₃ of *p*-Tol), 1.78 (d, J_{H-H} = 6, 3H, CH₃ of *i*-Pr), 1.42 (d, J_{H-H} = 6, 3H, CH₃ of *i*-Pr), 0.85 (d, J_{H-H} = 7, 3H, CH₃ of *i*-Pr), 0.82 (d, J_{H-H} = 7, 3H, CH₃ of *i*-Pr), 0.79 (br, Δv_{1/2} = 16, 3H, VCH₃). ¹³C {¹H} NMR (125.7 MHz, C₆D₆, 25°C): δ 131.6 (C_{ipso} of *p*-Tol), 127.0, 122.8 (2 CH of *p*-Tol), 103.9 (Cp), 59.6, 52.8 (2 CH of *i*-Pr), 30.0, 24.9 (2 CH₃ of *i*-Pr), 19.0 (CH₃ of *p*-Tol), 18.4, 16.9 (2 CH₃ of *i*-Pr), C_q of *p*-Tol and VCH₃ not observed. ⁵¹V NMR (131.4 MHz, C₆D₆, 25°C): δ -600 (Δv_{1/2} = 320). *Anal. Calcd (%) for C₁₉H₂₉N₂V*: C: 67.84, H: 8.69, N: 8.33, V: 15.14, found: C: 67.65, H: 9.03, N: 8.27, V: 15.09.

2.5 References

- (1) Hughes, A.K.; Meetsma, A.; Teuben, J.H., *Organometallics*, **1993**, *12*, 1936.
- (2) Sinnema, P.-J.; van der Veen, L.; Spek, A.L.; Veldman, N.; Teuben, J.H., *Organometallics*, **1997**, *16*, 4245.
- (3) Okuda, J., *Chem. Ber.*, **1990**, *123*, 1649.
- (4) (a) Shapiro, P.J.; Bunel, E.; Schaefer, W.P.; Bercaw, J.E., *Organometallics*, **1990**, *9*, 867. (b) Brintzinger, H.H.; Fischer, D.; Mülhaupt, R.; Rieger, B.; Waymouth, R.M., *Angew. Chem. Int. Ed. Eng.*, **1995**, *34*, 1143. (c) Liang, Y.; Yap, G.P.A.; Rheingold, A.L.; Theopold, K.H., *Organometallics*, **1996**, *15*, 5284.

- (5) (a) Antonelli, D.M.; Green, M.L.H.; Mountford, P., *J. Organomet. Chem.*, **1992**, 438, C4.
(b) Herrmann, W.A.; Baratta, W., *J. Organomet. Chem.*, **1996**, 506, 357. (c) Blake Jr., R.E.; Antonelli, D.M.; Henling, L.M.; Schaefer, W.P.; Hardcastle, K.I.; Bercaw, J.E., *Organometallics*, **1998**, 17, 718.
- (6) (a) Preuss, F.; Steidel, M.; Vogel, M.; Overhoff, G.; Hornung, G.; Towae, W.; Frank, W.; Reiss, G.; Müller-Becker, S., *Z. Anorg. Allg. Chem.*, **1997**, 623, 1220. (b) Preuss, F.; Becker, H.; Wieland, T., *Z. Naturforsch.*, **1990**, 45b, 191.
- (7) Fröhlich, H-O.; Kacholdt, H., *Z. Chem.*, **1975**, 15, 233.
- (8) Priebisch, W.; Rehder, D., *Inorg. Chem.*, **1985**, 24, 3058.
- (9) Chan, M.C.W.; Cole, J.M.; Gibson, V.C.; Howard, J.A.K., *Chem. Comm.*, **1997**, 2345.
- (10) Maatta, E.A., *Inorg. Chem.*, **1984**, 23, 2560.
- (11) Preuss, F.; Fuchslocher, E.; Leber, E.; Towae, W., *Z. Naturforsch.*, **1989**, 44b, 271.
- (12) (a) Buijink, J.K.F., *Ph.D. Thesis*, Groningen, the Netherlands, **1995**. (b) Preuss, F.; Becker, H.; Kaub, J.; Sheldrick, W.S., *Z. Naturforsch.*, **1988**, 43b, 1195.
- (13) Jekel-Vroegop, C. T., *Ph.D. Thesis*, Groningen, the Netherlands, **1984**.
- (14) (a) Song, J-I.; Gambarotta, S., *Chem. Eur. J.*, **1996**, 2, 1258. (b) Cummins, C.C.; Schrock, R.R.; Davis, W.M., *Inorg. Chem.*, **1994**, 33, 1448.
- (15) (a) Preuss, F.; Wieland, T.; Günther, B., *Z. Anorg. Allg. Chem.*, **1992**, 609, 45. (b) Preuss, F.; Noichl, H.; Kaub, J., *Z. Naturforsch.*, **1986**, 41b, 1085. (c) Preuss, F.; Fuchslocher, E.; Sheldrick, W.S., *Z. Naturforsch.*, **1985**, 40b, 1040.
- (16) de With, J.; Horton, A.D.; Orpen, A.G., *Organometallics*, **1990**, 9, 2207.
- (17) Preuss, F.; Becker, H.; Häusler, H-J., *Z. Naturforsch.*, **1987**, 42b, 881.
- (18) Sinnema, P-J.; Liekelema, K.; Staal, O.K.B.; Hessen, B.; Teuben, J.H., *J. Mol. Catal. A*, **1998**, 128, 143.

Chapter 3

Generation of cationic vanadium(V) complexes

3.1 Introduction

Cationic alkyl species are presumed to be the active species in the catalytic olefin polymerization (see Chapter 1).¹ MAO (MethylAluminOxane) is often used as a cocatalyst for the generation of these cationic species, but since MAO is an ill-defined system,² and a large excess of the cocatalyst is needed, the reaction mixtures are difficult to study. Well-defined cationic complexes can be generated by alkyl abstraction from a metal alkyl compound with a strong Lewis acid such as $B(C_6F_5)_3$ or $[Ph_3C][B(C_6F_5)_4]$, or by protonation with a Brønsted acid, for instance $[PhNHMe_2][B(C_6F_5)_4]$ (see Chapter 1).³ Most of this work has been performed on group 4 metal complexes, and the number of cationic vanadium catalysts generated with these cocatalysts is limited to only a few examples.⁴

This chapter describes the generation and characterization of cationic Cp-amido vanadium(V) complexes from neutral vanadium methyl complexes described (see Chapter 2). Alkyl abstraction by $B(C_6F_5)_3$ generated the expected $[(Cp\text{-amido})V(NR)][MeB(C_6F_5)_3]$ complexes, which exists as a mixture of the solvent separated and contact ion pair in solution. The ratio between these two species depends on the solvent. Alkyl abstraction by $[Ph_3C][B(C_6F_5)_4]$ generated $[(Cp\text{-amido})V(NR)][B(C_6F_5)_4]$, which is only present as the solvent separated ion pair in solution. The attempted generation of $[(Cp\text{-amido})V(NR)][B(C_6F_5)_4]$ by protonation with $[PhNHMe_2][B(C_6F_5)_4]$ resulted in activation of the substituent on the amido functionality of the Cp-amido ligand.

The cationic complexes described in this chapter are unsuitable for olefin polymerization, since they lack a V-C(alkyl) bond. However, this allows for a study of the reactivity of the V-N(amido) and V-N(imido) bonds towards unsaturated substrates. In the cationic complex $[(CpCH_2CH_2Ni\text{-}Pr)V(Nt-$

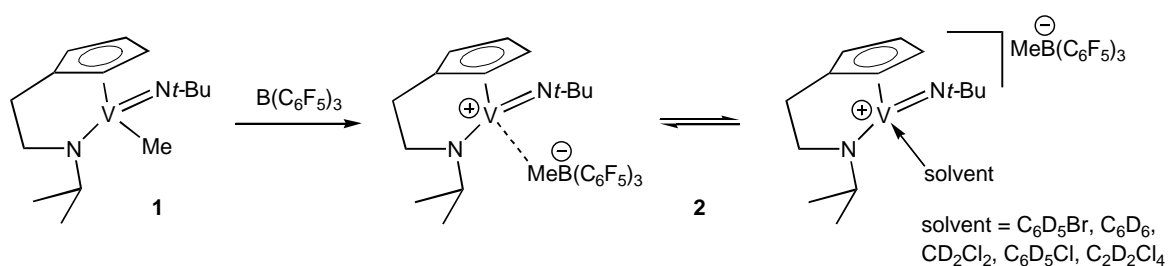
Bu)]][MeB(C₆F₅)₃], insertion of 2,3-dimethyl-butadiene and 2-butyne into the V-N(amido) bond was observed, generating aza-metallacyclic complexes. No reactivity of the V-N(imido) bond was observed.

Isolation of the cationic complexes described in this chapter as crystalline solids proved difficult. Therefore, many of the complexes were generated *in situ* and studied by different NMR techniques.

3.2 Results and Discussion

3.2.1 Methyl abstraction from (η^5, η^1 -C₅H₄CH₂CH₂N*i*-Pr)VMe(N*t*-Bu)

A frequently employed method to generate cationic complexes is alkyl (methyl or benzyl) abstraction by the Lewis acid B(C₆F₅)₃. The anion [RB(C₆F₅)₃][−] (R = Me, CH₂Ph) thus formed can remain coordinated to the metal center or dissociate, depending on the circumstances (see Chapter 1, section 1.3). Methyl abstraction from (η^5, η^1 -C₅H₄CH₂CH₂N*i*-Pr)VMe(N*t*-Bu) (**1**) by B(C₆F₅)₃ in pentane formed [(η^5, η^1 -C₅H₄CH₂CH₂N*i*-Pr)V(N*t*-Bu)]⁺[MeB(C₆F₅)₃][−] (**2**, Scheme 1) as an analytically pure orange precipitate, in an 81% isolated yield.



Scheme 1

The ¹⁹F NMR chemical shift difference between the *p*-F and *m*-F resonances of the C₆F₅ groups of the anion ($\Delta\delta_{m-p}$) is very sensitive to anion coordination.⁵ In C₆D₅Br solution **2** is predominantly present as the solvent separated ion pair, as indicated by a $\Delta\delta_{m-p}$ of 2.4 ppm (contact ion pair: $\Delta\delta_{m-p} > 3$ ppm). Small resonances in the ¹⁹F NMR spectrum of **2** ($\Delta\delta_{m-p} = 4.3$ ppm)

indicate that the contact ion pair is also present in C_6D_5Br , although in a small amount ($< 10\%$, Scheme 1).

There is a significant difference in the 1H NMR methyl resonance between **1** and **2**. For the methyl complex **1** this resonance appears at 0.7 ppm ($\Delta\nu_{1/2}$ 7 Hz), for **2** it appears at 1.13 ppm ($\Delta\nu_{1/2}$ 25 Hz) in C_6D_5Br , and an additional small resonance at -0.2 ppm can be assigned to the contact ion pair. This is confirmed by NMR measurements of **2** in the apolar solvent C_6D_6 , where the ^{19}F NMR indicates that **2** is predominantly present as the contact ion pair ($\Delta\delta_{m-p} = 4.4$ ppm), and the methyl resonance appears at -0.2 ppm ($\Delta\nu_{1/2}$ 24 Hz) in the 1H NMR spectrum. In chlorinated solvents (CD_2Cl_2 , C_6D_5Cl and $C_2D_2Cl_4$) 1H NMR spectra show a mixture of solvent separated and contact ion pair. From the ^{19}F NMR spectra the ratios of the two species is determined (ratio solvent separated: contact ion pair; CD_2Cl_2 4:1; C_6D_5Cl 2:1; $C_2D_2Cl_4$ 1:2).

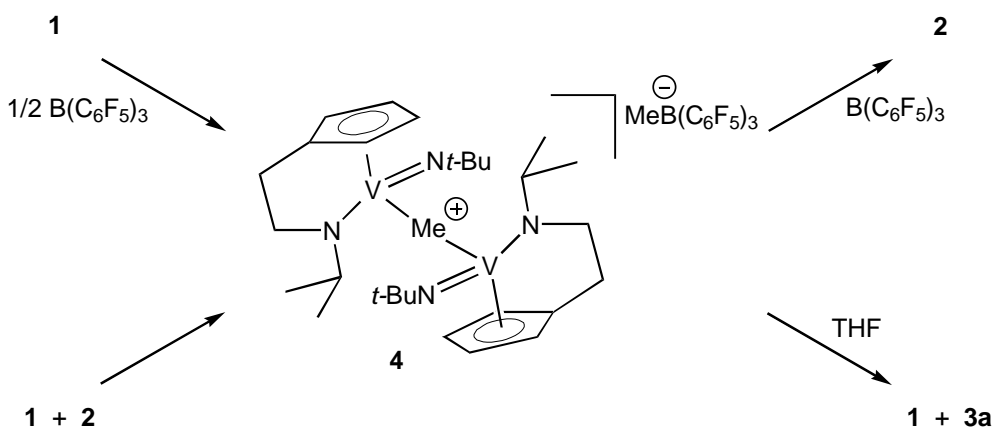
Methyl abstraction from **1** by the Lewis acidic trityl reagent $[Ph_3C][B(C_6F_5)_4]$ in C_6D_5Br generated Ph_3CMe and $[(\eta^5, \eta^1-C_5H_4CH_2CH_2Ni-Pr)V(Nt-Bu)][B(C_6F_5)_4]$ (**2'**), which has an identical 1H NMR spectrum as the solvated cation **2** in C_6D_5Br . In the ^{19}F NMR spectrum the $[B(C_6F_5)_4]^-$ anion is observed.

Although solvent coordination to **2** has not been observed directly by spectroscopic methods, it is a reasonable assumption.⁶ Theoretical calculations, that will be presented in Chapter 4, predict a very low inversion barrier (< 2 $kJ\cdot mol^{-1}$) for the pyramidal vanadium metal center in the unsolvated cation $[(Cp-amido)V(Nt-Bu)]^+$. However, in the 1H and ^{13}C NMR spectra the cationic complex **2** is observed as an asymmetric complex, indicating that inversion of the metal center does not occur (on NMR time scale), probably because of solvent stabilization.

Addition of Lewis bases to a C_6D_5Br solution of **2** cleanly generated the corresponding adducts $[(\eta^5, \eta^1-C_5H_4CH_2CH_2Ni-Pr)V(L)(Nt-Bu)][MeB(C_6F_5)_3]$ (**3a**: $L = THF$; **3b**: $L = PMe_3$; **3c**: $L = PhNMe_2$). In the 1H and ^{13}C NMR spectra, resonances of the Lewis bases shift slightly upon coordination. In the ^{31}P NMR spectrum of **3b** a broad plateau-shaped resonance is observed for the coordinated PMe_3 ligand, because of unresolved coupling with the quadrupolar

vanadium nucleus. Complex **3a** showed no exchange (on the NMR time scale) with an excess (~3 eq.) of THF. The Lewis base adducts **3** are insoluble in C_6D_6 .

Reaction of **1** with 0.5 equivalent of $B(C_6F_5)_3$ in C_6D_5Br did not generate an equimolar mixture of **1** and **2**, but a new complex, which was identified as the methyl bridged bimetallic Cp-amido vanadium(V) complex $[(\eta^5, \eta^1-C_5H_4CH_2CH_2Nt\text{-}Pr)V(Nt\text{-}Bu)]_2(\mu\text{-}Me)[MeB(C_6F_5)_3]$ (**4**, Scheme 2). Since **4** has two asymmetric vanadium centers it can consist of two diastereomers, as previously observed in methyl bridged bimetallic *ansa*-zirconocenes.⁷ Resonances of the Cp-amido and imido ligand of **4** in the 1H and ^{13}C NMR are comparable to those of **1** and **2**; only in the ^{13}C NMR spectrum are some of the resonances for the two diastereomers resolved. Unlike the 1H NMR resonances for the methyl group of the neutral Cp-amido methyl complexes, which are all broadened due to unresolved coupling with the quadrupolar vanadium nucleus ($\Delta\nu_{1/2}$ 7 - 18 Hz), the resonance of the bridging methyl group in **4** is relatively sharp ($\Delta\nu_{1/2}$ 2 Hz).

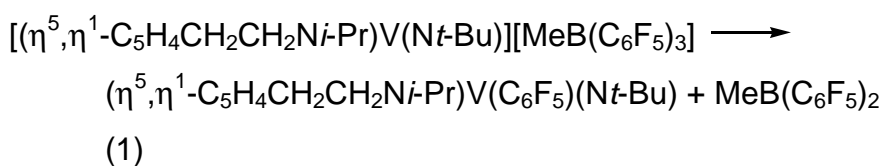


Scheme 2

The bimetallic complex **4** could also be generated by mixing equimolar amounts of **1** and **2**, and reacted with additional $B(C_6F_5)_3$ to form **2**. Addition of THF to a solution of **4** resulted in the formation of an equimolar mixture of the neutral methyl complex **1** and the cationic THF adduct **3a** (Scheme 2).

3.2.2 Thermolysis of $[(\eta^5, \eta^1\text{-C}_5\text{H}_4\text{CH}_2\text{CH}_2\text{N}i\text{-Pr})\text{V}(\text{N}t\text{-Bu})][\text{MeB}(\text{C}_6\text{F}_5)_3]$

Although the cationic complex **2** was stable as a solid at room temperature for several months, decomposition was observed in solution. In $\text{C}_6\text{D}_5\text{Br}$ an unidentified solid was formed (two days at room temperature); in C_6D_6 slow and clean decomposition to a new complex was observed when a sealed NMR tube was kept at room temperature for about one year (at 60°C the decomposition was faster, but unidentified side products were formed as well). From the ^1H and ^{13}C NMR spectra it can be concluded that the $\eta^5, \eta^1\text{-C}_5\text{H}_4\text{CH}_2\text{CH}_2\text{N}i\text{-Pr}$ structure is retained in the decomposition product. The ^{19}F NMR spectrum showed the formation of $\text{MeB}(\text{C}_6\text{F}_5)_2$,^{3d} and a new complex which is probably $(\eta^5, \eta^1\text{-C}_5\text{H}_4\text{CH}_2\text{CH}_2\text{N}i\text{-Pr})\text{V}(\text{C}_6\text{F}_5)(\text{N}t\text{-Bu})$ (**5**, Equation 1).



The transfer of a C_6F_5 group from a borate anion to a cationic metal center has been observed before,^{3d} and is indicated by a downfield shift of the $\sigma\text{-F}$ resonance of the newly formed $\text{M-C}_6\text{F}_5$ group in the ^{19}F NMR. For example, the cationic zirconium complex $\{[1,2\text{-(Me}_3\text{Si)C}_5\text{H}_3\}_2\text{ZrMe}\}[\text{MeB}(\text{C}_6\text{F}_5)_3]$ decomposes in one day at room temperature to generate $\text{MeB}(\text{C}_6\text{F}_5)_2$ and $\{1,2\text{-(Me}_3\text{Si)C}_5\text{H}_3\}_2\text{Zr}(\text{Me})(\text{C}_6\text{F}_5)$, which displays two $\sigma\text{-F}$ resonances at -109 and -110 ppm.^{3d} In the vanadium complex **5** rapid rotation of the C_6F_5 ligand occurs and only one $\sigma\text{-F}$ resonance is found (-109 ppm).

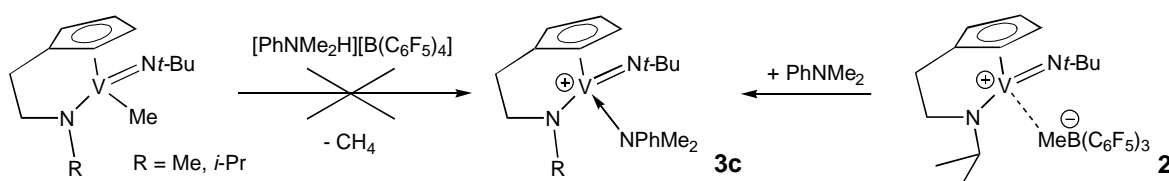
3.2.3 Methyl abstraction from other vanadium(V) methyl complexes

Methyl abstractions from other vanadium(V) methyl complexes containing the Cp-amido ligand or unbridged Cp and amido ligands (see Chapter 2) were performed *in situ* in $\text{C}_6\text{D}_5\text{Br}$ using $\text{B}(\text{C}_6\text{F}_5)_3$. The cationic

complexes $[(\eta^5, \eta^1\text{-C}_5\text{H}_4\text{CH}_2\text{CH}_2\text{NMe})\text{V}(\text{N}t\text{-Bu})][\text{MeB}(\text{C}_6\text{F}_5)_3]$ (**6**), $[(\eta^5, \eta^1\text{-C}_5\text{H}_4\text{CH}_2\text{CH}_2\text{N}i\text{-Pr})\text{V}(\text{N}p\text{-Tol})][\text{MeB}(\text{C}_6\text{F}_5)_3]$ (**7**), $[(t\text{-BuN})\text{VCp}(\text{N}i\text{-Pr}_2)][\text{MeB}(\text{C}_6\text{F}_5)_3]$ (**8**) and $[(p\text{-TolN})\text{VCp}(\text{N}i\text{-Pr}_2)][\text{MeB}(\text{C}_6\text{F}_5)_3]$ (**9**) were identified by ^1H , ^{13}C , ^{51}V and ^{19}F NMR. In all four complexes the ^{19}F NMR spectrum shows that a mixture of the solvent separated and the contact ion pair is present in solution; no significant differences in the ratio between the two species was observed. Just as for the cationic Cp-amido vanadium(V) complex **2** described above, the solvent separated ion pair is the predominant species in $\text{C}_6\text{D}_5\text{Br}$ (> 90%).

3.2.4 Cationic complexes through protonation

As mentioned in the introduction of this chapter, another way to generate cationic complexes is by protonation with a Brønsted acid. A reagent frequently used for this reaction is $[\text{PhNMe}_2\text{H}][\text{B}(\text{C}_6\text{F}_5)_4]$, which upon reaction with a metal alkyl species liberates the alkyl group as the alkane and generates the conjugate base PhNMe_2 . Thus, protonation of the Cp-amido vanadium methyl complex **1** with $[\text{PhNMe}_2\text{H}][\text{B}(\text{C}_6\text{F}_5)_4]$ was expected to generate methane and $[(\eta^5, \eta^1\text{-C}_5\text{H}_4\text{CH}_2\text{CH}_2\text{N}i\text{-Pr})\text{V}(\text{NPhMe}_2)(\text{N}t\text{-Bu})][\text{B}(\text{C}_6\text{F}_5)_4]$ (Scheme 3). The cationic part of this complex was generated previously by reaction of the cationic complex **2** with PhNMe_2 (complex **3c**, section 3.2.1).



Scheme 3

In the protonation of $(\eta^5, \eta^1\text{-C}_5\text{H}_4\text{CH}_2\text{CH}_2\text{NR})\text{VMe}(\text{N}t\text{-Bu})$ ($\text{R} = \text{Me}, i\text{-Pr}$; in $\text{C}_6\text{D}_5\text{Br}$ or THF-d_8) gas evolution was observed, but the expected aniline adducts were not formed. Instead, the substituent on the amido functionality of the Cp-amido ligand was activated. In the ^1H NMR spectra of the protonation

products, the former NMe group appears as two doublets ($J_{\text{H-H}} = 9 \text{ Hz}$, integral $2 \times 1\text{H}$), and the former *Ni*-Pr group as two singlets (integral $2 \times 3\text{H}$), indicating that the amido substituents have been deprotonated. In the ^{13}C NMR spectra the NC resonances appear at 65 ppm (t, 163 Hz) and 78 ppm (s) respectively. These resonances compare well to those of the tantalum complex $\text{Cp}^*\text{Ta}(\text{H}_2\text{CNMe})\text{Me}_2$ (NC: 65 ppm, t, 155 Hz), formed by thermal decomposition of the amido complex $\text{Cp}^*\text{Ta}(\text{NMe}_2)\text{Me}_3$.⁸ Based on the ^1H and ^{13}C NMR spectra, the tantalum complex is described as a metallacyclic structure (Figure 1A). In contrast, deprotonation of one of the *i*-Pr groups of the hafnium di-aza-butadiene complex $\text{Cp}^*\text{Hf}(\sigma^2, \pi-(i\text{-Pr})_2\text{-DAB})\text{Cl}$, yields an imine adduct (Figure 1B),⁹ of which the NC resonance (157 ppm, s) compares better to free the imine $\text{MeN}=\text{CH}_2$ (NC: 155 ppm, no $J_{\text{C-H}}$ reported).¹⁰

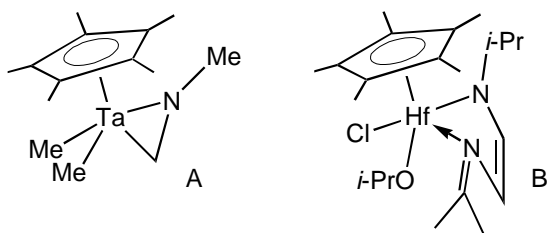
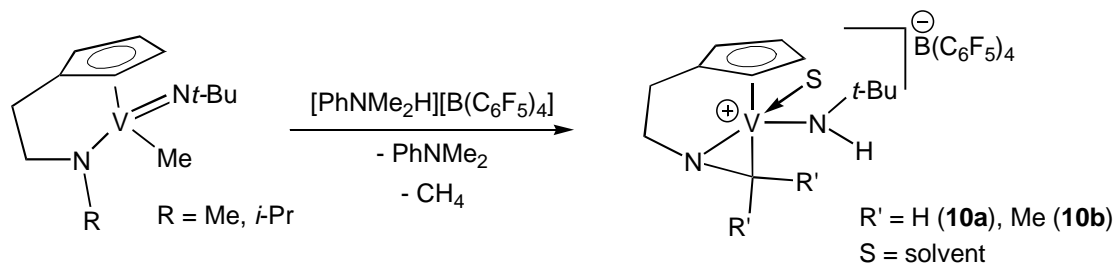


Figure 1: Other imine species

After the protonation of the vanadium complexes with $[\text{PhNMe}_2\text{H}][\text{B}(\text{C}_6\text{F}_5)_4]$ a new resonance appears (integral 1H) with a solvent dependent chemical shift (5.5 ppm in THF-d_8 , 3.7 in $\text{C}_6\text{D}_5\text{Br}$). The (unresolved) coupling pattern that is observed for this resonance does not arise from coupling with other protons, as was shown in a $2\text{D-}^1\text{H}, ^1\text{H}$ COSY NMR experiment. Instead, it probably arises from coupling with a nitrogen atom, therefore this resonance is ascribed to a N-H group. No resonances are observed for the V-Me group.

We propose that protonation of the imido ligand has taken place, after which the amido substituent is deprotonated by the V-Me group to generate methane and a vanadium complex of the type $[(\text{C}_5\text{H}_4\text{CH}_2\text{CH}_2\text{NCR}_2)\text{V}(\text{NH}t-$

Bu)]][B(C₆F₅)₄] (**10a**: R = H; **10b**: R = Me, Scheme 4). Based on the ¹³C NMR data complexes **10** are described as metallacyclic compounds.



Scheme 4

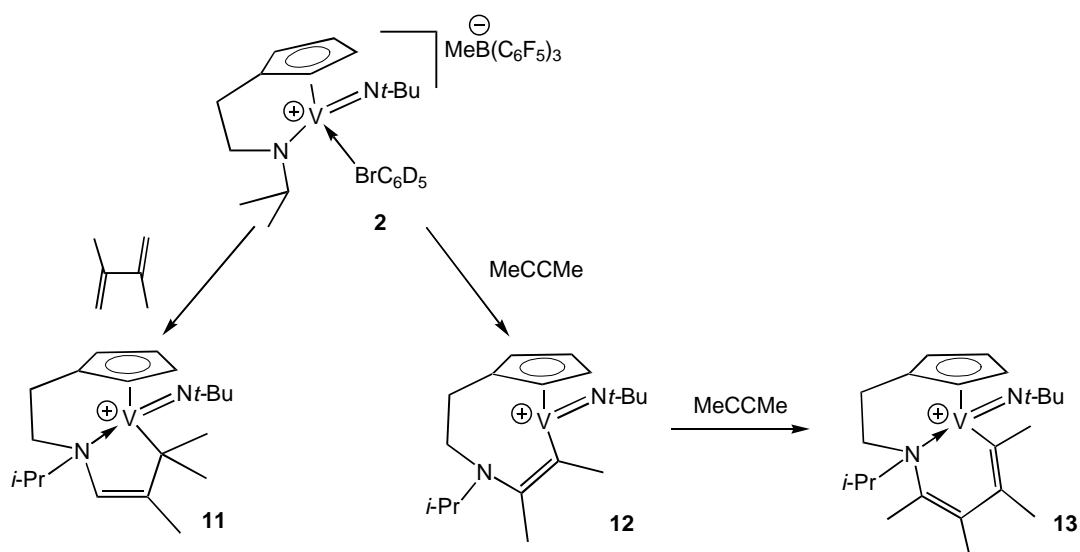
When complex **10b** was generated in C₆D₅Br, the formed PhNMe₂ did not coordinate to the vanadium center, and could be washed out by precipitating the cationic complex in pentane. When **10b** was generated in THF-d₈ and subsequently precipitated in pentane, the PhNMe₂ was also washed out. However, the ¹H NMR spectrum of this precipitated complex in C₆D₅Br was slightly different from the spectrum of **10b** in C₆D₅Br, probably because of coordination of THF-d₈ to the cationic vanadium center (no resonances of coordinated THF-d₈ could be observed in the ¹H or ¹³C NMR spectra). Although no further experiments were performed to prove this, we believe that complexes **10** are stabilized in solution by solvent coordination, and that the aniline that is formed in the generation of **10** is too sterically hindered to coordinate to the vanadium center. This could also explain the results obtained in the generation of the sterically less hindered species **10a** in C₆D₅Br, where a mixture of compounds is formed, which are probably the solvated species and the aniline adduct.

3.2.5 Reactivity of [(C₅H₄CH₂CH₂N*i*-Pr)V(N*t*-Bu)]⁺ towards unsaturated substrates

The cationic complexes described in this chapter lack a metal-alkyl bond, and it is therefore unlikely that they will catalyze the polymerization of olefins.

However, they do give the opportunity to study the interaction of a cationic d^0 metal center with different substrates, and to study the relative reactivity of the V-N(amido) and V-N(imido) bonds in these complexes. The cationic Cp-amido complex **2** reacted with simple olefins like ethene and propene to form the corresponding olefin adducts. These d^0 metal olefin adducts will be extensively described in Chapter 4.

The reactivity of 2,3-dimethyl-butadiene or 2-butyne with **2**, described here, is very different from that of mono-olefins. The NMR data suggest that these substrates insert into the V-N(amido) bond to generate the complexes $[\{\eta^5, \eta^1, \eta^1\text{-C}_5\text{H}_4\text{CH}_2\text{CH}_2\text{N}(i\text{-Pr})\text{CH}=\text{C}(\text{Me})\text{CMe}_2\}\text{V}(\text{N}t\text{-Bu})][\text{MeB}(\text{C}_6\text{F}_5)_3]$ (**11**), $[\{\eta^5, \eta^1\text{-C}_5\text{H}_4\text{CH}_2\text{CH}_2\text{N}(i\text{-Pr})(\text{CMe})_2\}\text{V}(\text{N}t\text{-Bu})][\text{MeB}(\text{C}_6\text{F}_5)_3]$ (**12**) and $[\{\eta^5, \eta^1, \eta^1\text{-C}_5\text{H}_4\text{CH}_2\text{CH}_2\text{N}(i\text{-Pr})(\text{CMe})_4\}\text{V}(\text{N}t\text{-Bu})][\text{MeB}(\text{C}_6\text{F}_5)_3]$ (**13**, Scheme 5).



Scheme 5

The involvement of the V-N(amido) bond in the insertions is clearly indicated by the strong upfield shift of the CH resonance of the *i*-Pr substituent in the ¹H NMR spectrum. In all previously described (Cp-amido)V(NR)X complexes this proton points towards the metal center (Chapter 2, section 2.2.6) and experiences an anisotropic effect of the metal, resulting in a downfield shift in the ¹H NMR. After the insertion into the V-N(amido) bond, the

sp^3 hybridization of the nitrogen atom in the newly formed amine functionality moves the *i*-Pr group away from the metal, thereby eliminating the anisotropic effect. This is indicated in the ^1H NMR spectrum by an upfield shift of the methine proton (**2**: δ 5.7 ppm; **11**: δ 3.3 ppm; **12**: δ 2.2 ppm; **13**: δ 2.8 ppm; ligand precursor $\text{C}_5\text{H}_5(\text{CH}_2)_2\text{NH}i\text{-Pr}$: δ 2.6 ppm).

In the ^1H and ^{13}C NMR spectra of **12** and **13**, insertion of 2-butyne leads to respectively two and four new resonances for CH_3 groups. In the ^{13}C NMR spectra the carbon atom bonded directly to the vanadium is probably too broad to observe, and respectively one and three new quaternary carbons are found. In the ^1H and ^{13}C NMR spectra of **11**, three new CH_3 and one new CH group are observed, indicating that the diene did not insert into the V-N(amido) bond in the expected 1,2 or 1,4 fashion. The resonance of the CH group shows a large downfield shift (^1H : 7.55 ppm; ^{13}C : 183 ppm), and in the ^1H NMR NOE interactions with both methyls of the *Ni*-Pr group and with the NCH_2 moiety of the ethylene bridge are observed (Figure 2). This clearly indicates that the reaction has taken place with the V-N(amido) bond, and not with the V-N(imido) bond. The *Nt*-Bu group only has NOE interactions with two of the Cp protons.

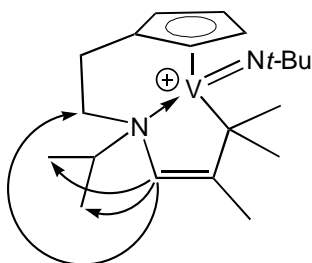
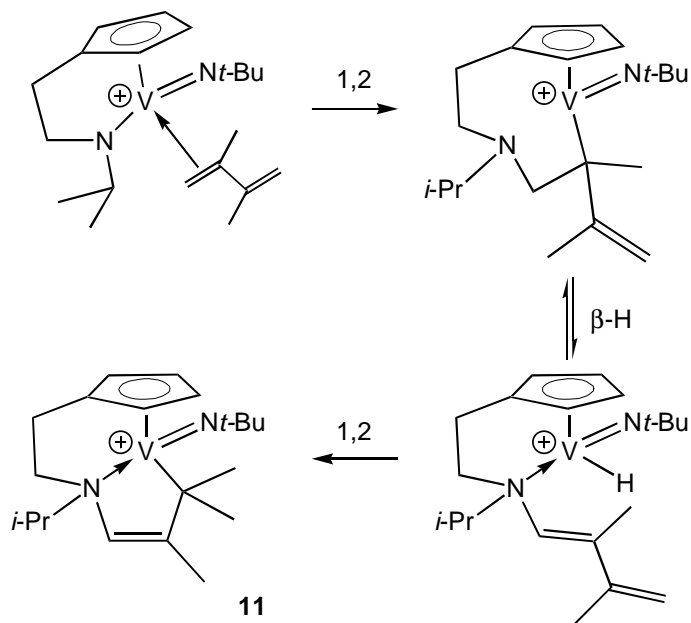


Figure 2: Selected NOE interactions in **11**

In the ^{51}V NMR spectra, complexes **11** and **13** appear at a comparable chemical shift (**11**: -492 ppm; **13**: -441 ppm), while **12** appears at -186 ppm. We propose that this large chemical shift difference is caused by amine decoordination in **12**, probably because of ring strain in the small four-membered ring.

**Scheme 6**

Complexes **12** and **13** are formed by insertion of 2-butyne in the V-N(amido) bond and subsequent insertion of a second molecule of 2-butyne in the newly formed V-C bond. Formation of **11** is less straight forward. A possible mechanism for the formation of **11** is shown in Scheme 6; a 1,2 insertion of one of the double bonds of the diene into the V-N(amido) bond takes place, followed by β -H elimination and subsequent insertion of the other double bond of the diene in the newly formed vanadium-hydride. The formation of **11** is not clean, and impurities may arise from a 2,1-insertion of one of the double bonds, or decomposition of one of the intermediates. Complex **11** is thermally stable in solution at room temperature for one week, unlike complexes **12** and **13** which decompose even at 0°C.

Insertion of an unsaturated substrate into a metal-amido bond is not uncommon,¹¹ but has so far only been observed for polar substrates (for instance CO₂, SO₂), or for alkynes with strongly electron-withdrawing substituents (for instance CO₂Me). It is possible that coordination of the non-polar diene and alkyne substrates to the cationic vanadium center polarizes the

unsaturated carbon-carbon bond, thus making it susceptible for nucleophilic attack by the amido ligand.

In contrast to the high reactivity of the V-N(amido) bond, the V-N(imido) bond appears to be inert. Metal imido complexes are known to react with non-activated substrates with unsaturated carbon-carbon bonds (for instance 2-butyne, ethene) by a [2+2] cycloaddition, to form aza-metallacyclic products.¹² The cationic vanadium complex **2** can react with dimethyl-butadiene either by a [2+2] cycloaddition over the V-N(imido) bond or insertion into the V-N(amido) bond. The geometry of the complex only allows a subsequent β -H elimination to take place if the nitrogen atom decoordinates from the metal center (Scheme 6). Since this is only possible when the diene has reacted with the V-N(amido) bond, it can explain why no reaction of dimethyl-butadiene with the V-N(imido) bond is observed. Reaction of 2-butyne with the mixed amido imido vanadium complex $(RN)_2V(NHR)(OEt_2)$ ($R = t\text{-Bu}_3\text{Si}$) takes place exclusively with the imido ligand,^{12a} and, as other examples,^{12b} it is irreversible. It is therefore unclear why no reaction of 2-butyne with the V-N(imido) bond of **2** is observed.

3.3 Conclusions

Cationic vanadium(V) Cp-amido complexes could be obtained by methyl abstraction by the Lewis acid $B(C_6F_5)_3$ from the neutral metal methyl complexes, described in Chapter 2. In solution the complexes exist as a mixture of the solvent separated and the contact ion pair, and both species are observed in all used solvents. There appears to be no ligand influence in the ratio between solvent separated and contact ion pair, instead, this ratio is determined by the coordinating properties of the solvent. In chlorinated solvents (CD_2Cl_2 , C_6D_5Cl , $C_2D_2Cl_4$) approximately the same amount of solvent separated and contact ion pair is observed. However, in C_6D_5Br , which has a similar dielectric constant as C_6D_5Cl , the major species is the solvent separated complex. Apparently, the bromine atom of bromobenzene is more Lewis basic than the chlorine atom of chlorobenzene.

Attempts to generate [(Cp-amido)V(N*t*-Bu)]⁺ complexes by protonation with [PhNMe₂H][B(C₆F₅)₄] led to the unexpected protonation of the imido ligand, and a subsequent deprotonation of the substituent on the amido functionality by the V-Me group. Such a deprotonation has not been observed in the neutral methyl precursors.

In the cationic complex [(C₅H₄CH₂CH₂N*i*-Pr)V(N*t*-Bu)][MeB(C₆F₅)₃], the imido functionality appeared to be inert towards C-C unsaturated substrates. Instead, insertion into the V-N(amido) bond was observed for 2,3-dimethylbutadiene and 2-butyne. This is the first example known to us where insertion of an olefin or an apolar alkyne into a metal-amido bond was observed. It is possible that the C-C unsaturated bond is polarized by coordination to the cationic metal center, making it susceptible for a nucleophilic attack by the amido ligand.

3.4 Experimental

General considerations

All experiments were performed under nitrogen atmosphere using standard glove-box, Schlenk and vacuum line techniques. Deuterated solvents (Aldrich) were dried over Na/K alloy and vacuum transferred before use (C₆D₆, THF-d₈), or degassed and stored on mol. sieves under nitrogen (C₆D₅Br, C₆D₅Cl, CD₂Cl₂, C₂D₂Cl₄). Pentane and THF were distilled from Na/K alloy before use. PMe₃ was prepared according to literature procedures, using MeMgI in stead of MeMgBr.¹³ B(C₆F₅)₃¹⁴ was prepared according to literature procedures. [Ph₃C][B(C₆F₅)₄] and [PhNHMe₂][B(C₆F₅)₄] were kindly provided by Dr. H.J.G. Luttikhedde from Åbo Akademi University, Finland. (η⁵,η¹-C₅H₄CH₂CH₂N*i*-Pr)VMe(N*t*-Bu) (**1**), (η⁵,η¹-C₅H₄CH₂CH₂NMe)VMe(N*t*-Bu), (η⁵,η¹-C₅H₄CH₂CH₂N*i*-Pr)VMe(N*p*-Tol), (*t*-BuN)VCp(N*i*-Pr₂)Me and (*p*-TolN)VCp(N*i*-Pr₂)Me are described in the previous chapter. 2,3-dimethyl-1,3-butadiene (Aldrich) was degassed, dried over MgSO₄ and distilled before use. 2-butyne was degassed and stored under nitrogen. NMR spectra were run on Varian Gemini 200, VXR-300 and VXR-500 spectrometers. ¹H and ¹³C NMR chemical shifts are reported in ppm relative to TMS, using residual solvent resonances as internal reference. ¹⁹F NMR chemical shifts are reported in ppm relative to CFCl₃, which is used as an external reference. ¹⁹F NMR shifts are only reported for **2** and **2'**, and are the same for all other complexes. ⁵¹V NMR chemical shifts are reported in ppm relative to VOCl₃, which is used as an external reference. Coupling constants (J) and line widths at half height (Δ*v*_½) are reported in Hz. Elemental analyses were performed by the Microanalytical Department of the University of Groningen. Every value is the average of at least two independent determinations.

Synthesis of [(C₅H₄CH₂CH₂N*i*-Pr)V(N*t*-Bu)][MeB(C₆F₅)₃] (**2**)

In 2 mL of pentane 43 mg (0.15 mmol) of **1** was dissolved and slowly added to a stirred solution of 100 mg (0.19 mmol) of B(C₆F₅)₃ in 10 mL of pentane, and the resulting suspension was stirred for 5 more minutes. After 10 minutes an orange precipitate had settled and the solution was decanted. The orange powder was washed three times with 5 mL of pentane and dried *in vacuo*. This yielded 97 mg (0.12 mmol = 81%) of analytically pure **2** as an orange powder.

¹H NMR (500 MHz, C₆D₆, 25°C): δ 5.86 (br, 1H, Cp), 5.80 (sept, J_{H-H} = 6, 1H, CH of *i*-Pr), 5.59 (br, 1H, Cp), 5.46 (br, 1H, Cp), 4.74 (m, 1H, NCHH), 4.52 (br, 1H, Cp), 2.98 (dd, J_{H-H} = 7 / 13, 1H, NCHH), 2.28 (dd, J_{H-H} = 7 / 13, 1H, CpCHH), 1.44 (m, 1H, CpCHH), 0.84 (s, 9H, *t*-Bu), 0.63 (d, J_{H-H} = 6, 3H, CH₃ of *i*-Pr), 0.47 (d, J_{H-H} = 6, 3H, CH₃ of *i*-Pr), -0.20 (br, Δν_{1/2} = 24, 3H, BCH₃). ¹³C {¹H} NMR (125.7 MHz, C₆D₆, 25°C): δ 148.9 (d, J_{C-F} = 242, C₆F₅), 142.9 (C_{ipso} of Cp), 139.3 (d, J_{C-F} = 240, C₆F₅), 137.6 (d, J_{C-F} = 245, C₆F₅), 112.6, 112.3, 102.1, 100.9 (4 CH of Cp), 75.5 (CH of *i*-Pr), 72.8 (NCH₂), 29.3 (CpCH₂), 30.5 (CH₃ of *t*-Bu), 21.3, 20.2 (2 CH₃ of *i*-Pr), C_q of *t*-Bu and B-Me not observed. ⁵¹V NMR (131.4 MHz, C₆D₆, 25°C): δ -514 (Δν_{1/2} = 1600). ¹⁹F NMR (188.2 MHz, C₆D₆, 25°C): δ -133.6, -134.9* (*o*-F), -162.2*, -166.2 (*p*-F), -166.8*, -168.7 (*m*-F). Resonances marked with an asterisk are from the contact ion pair (>90%).

¹H NMR (200 MHz, C₆D₅Br, 25°C): δ 6.06 (br, 1H, Cp), 5.73 (sept, J_{H-H} = 6, 1H, CH of *i*-Pr), 5.52 (br, 1H, Cp), 5.37 (br, 1H, Cp), 5.13 (br, 1H, Cp), 4.70 (m, 1H, NCHH), 3.56 (dd, J_{H-H} = 7 / 13, 1H, NCHH), 2.70 (dd, J_{H-H} = 6 / 13, 1H, CpCHH), 2.09 (m, 1H, CpCHH), 1.13 (br, Δν_{1/2} = 25, 3H, BCH₃), 1.01 (s, 9H, *t*-Bu), 0.99 (shoulder, *i*-Pr), 0.76 (d, J_{H-H} = 6, 3H, *i*-Pr). ¹³C {¹H} NMR (125.7 MHz, C₆D₅Br, 25°C): δ 148.9 (d, J_{C-F} = 239, C₆F₅), 143.2 (C_{ipso} of Cp), 138.0 (d, J_{C-F} = 241, C₆F₅), 136.0 (d, J_{C-F} = 248, C₆F₅), 112.8, 110.8, 103.4, 103.0 (4 CH of Cp), 75.8 (CH of *i*-Pr), 73.9 (NCH₂), 29.2 (CpCH₂), 30.7 (CH₃ of *t*-Bu), 22.3, 20.7 (2 CH₃ of *i*-Pr), 11.5 (br, Δν_{1/2} ~ 100 Hz, BCH₃), C_q of *t*-Bu not observed. ⁵¹V NMR (131.4 MHz, C₆D₅Br, 25°C): δ -544 (Δν_{1/2} = 1300). ¹⁹F NMR (188.2 MHz, C₆D₅Br, 25°C): δ -133.4, -134.5* (*o*-F), -162.0*, -165.7 (*p*-F), -166.3*, -168.1 (*m*-F). Resonances marked with an asterisk are from the contact ion pair (<10%).

¹⁹F NMR (188.2 MHz, CD₂Cl₂, 25°C): δ -135.3*, -135.8 (*o*-F), -163.3*, -165.7 (*p*-F), -167.5*, -168.5 (*m*-F). Resonances marked with an asterisk are of the contact ion pair (20%). ¹⁹F NMR (188.2 MHz, C₆D₅Cl, 25°C): δ -134.4 (overlap of solvent separated and contact ion pair) (*o*-F), -161.9*, -164.9 (*p*-F), -166.2*, -167.4 (*m*-F). Resonances marked with an asterisk are of the contact ion pair (33%). ¹⁹F NMR (188.2 MHz, C₂D₂Cl₄, 25°C): δ -134.9, -135.3* (*o*-F), -162.4*, -165.8 (*p*-F), -166.8*, -168.4 (*m*-F). Resonances marked with an asterisk are of the contact ion pair (66%). *Anal. calcd (%) for C₃₃H₂₇BF₁₅N₂V*: C: 49.65, H: 3.41, N: 3.51, V: 6.38, found: C: 49.78, H: 3.28, N: 3.40, V: 6.31.

Generation of [(C₅H₄CH₂CH₂N*i*-Pr)V(N*t*-Bu)][B(C₆F₅)₄] (**2'**)

A solution of 10.5 mg (37 μmol) of **1** in 0.1 mL of $\text{C}_6\text{D}_5\text{Br}$ was added to a suspension of 39 mg (42 μmol) of $[\text{Ph}_3\text{C}][\text{B}(\text{C}_6\text{F}_5)_4]$ in 0.4 mL of $\text{C}_6\text{D}_5\text{Br}$. ^1H NMR showed clean conversion to **2'** and Ph_3CMe .

^1H NMR (300 MHz, $\text{C}_6\text{D}_5\text{Br}$, 25 $^\circ\text{C}$): Ph_3CMe δ 7.08 (m, 15H, Ph), 2.02 (s, 3H, Me); chemical shifts for **2'** identical to those of **2** in $\text{C}_6\text{D}_5\text{Br}$. ^{19}F NMR (188.2 MHz, $\text{C}_6\text{D}_5\text{Br}$, 25 $^\circ\text{C}$): δ -133.5 (o-F), -163.9 (p-F), -167.7 (m-F).

Generation of $[(\text{C}_5\text{H}_4\text{CH}_2\text{CH}_2\text{N}i\text{-Pr})\text{V}(\text{THF})(\text{N}t\text{-Bu})][\text{MeB}(\text{C}_6\text{F}_5)_3]$ (**3a**)

A solution of 20 mg (0.07 mmol) of **1** in 0.1 mL of $\text{C}_6\text{D}_5\text{Br}$ was added to a solution of 10 mg (0.08 mmol) of $\text{B}(\text{C}_6\text{F}_5)_3$ in 0.4 mL of $\text{C}_6\text{D}_5\text{Br}$ and 6 μl (0.07 mmol) of THF was added subsequently by microsyringe. NMR showed clean conversion to **3a**.

^1H NMR (500 MHz, $\text{C}_6\text{D}_5\text{Br}$, 25 $^\circ\text{C}$): δ 6.12 (m, 1H, Cp), 5.89 (m, 1H, Cp), 5.64 (sept, $J_{\text{H-H}} = 7$, 1H, CH of *i*-Pr), 5.37 (m, 1H, Cp), 5.02 (m, 1H, Cp), 4.93 (m, 1H, NCHH), 3.48 (m, 1H, NCHH), 3.42 (m, 2H, α -H of THF), 3.32 (m, 2H, α -H of THF), 2.75 (m, 1H, CpCHH), 2.01 (m, 1H, CpCHH), 1.52 (m, 4H, β -H of THF), 1.02 (s, 9H, *t*-Bu), 0.93 (d, $J_{\text{H-H}} = 7$, 3H, CH_3 of *i*-Pr), 0.73 (d, $J_{\text{H-H}} = 7$, 3H, CH_3 of *i*-Pr). ^{13}C $\{^1\text{H}\}$ NMR (125.7 MHz, $\text{C}_6\text{D}_5\text{Br}$, 25 $^\circ\text{C}$): δ 143.2 (C_{ipso} of Cp), 112.4, 111.8 (2 CH of Cp), 102.7 (br, 2 CH of Cp), 80.8 (α -C of THF), 75.0 (CH of *i*-Pr), 73.2 (NCH₂), 31.6 (CH_3 of *t*-Bu), 30.1 (CpCH₂), 26.5 (β -C of THF), 22.2, 22.0 (2 CH_3 of *i*-Pr), C_q of *t*-Bu not observed. ^{51}V NMR (131.4 MHz, $\text{C}_6\text{D}_5\text{Br}$, 25 $^\circ\text{C}$): δ -567 ($\Delta\nu_{1/2} = 940$).

Generation of $[(\text{C}_5\text{H}_4\text{CH}_2\text{CH}_2\text{N}i\text{-Pr})\text{V}(\text{PMe}_3)(\text{N}t\text{-Bu})][\text{MeB}(\text{C}_6\text{F}_5)_3]$ (**3b**)

A solution of 20 mg (0.07 mmol) of **1** in 0.1 mL of $\text{C}_6\text{D}_5\text{Br}$ was added to a solution of 10 mg (0.08 mmol) of $\text{B}(\text{C}_6\text{F}_5)_3$ in 0.4 mL of $\text{C}_6\text{D}_5\text{Br}$. This solution was transferred into an NMR tube equipped with a Teflon Young valve. The tube was connected to a high vacuum line, frozen in liquid nitrogen and evacuated. Subsequently, one equivalent of PMe_3 was condensed into the NMR tube, which was then closed and thawed out. NMR showed clean conversion to **3b**.

^1H NMR (500 MHz, $\text{C}_6\text{D}_5\text{Br}$, 25 $^\circ\text{C}$): δ 5.58 (br, 1H, Cp), 5.52 (br, 1H, Cp), 5.50 (br, 1H, Cp), 5.33 (sept, $J_{\text{H-H}} = 7$, 1H, CH of *i*-Pr), 5.01 (br, 1H, Cp), 4.11 (m, 1H, NCHH), 3.36 (m, 1H, NCHH), 2.42 (m, 1H, CpCHH), 2.09 (m, 1H, CpCHH), 0.98 (d, $J_{\text{P-H}} = 10$, 9H, $\text{P}(\text{CH}_3)_3$), 0.91 (s, 9H, *t*-Bu), 0.93 (d, $J_{\text{H-H}} = 7$, 3H, CH_3 of *i*-Pr), 0.62 (d, $J_{\text{H-H}} = 7$, 3H, CH_3 of *i*-Pr). ^{13}C $\{^1\text{H}\}$ NMR (125.7 MHz, $\text{C}_6\text{D}_5\text{Br}$, 25 $^\circ\text{C}$): δ 137.2 (C_{ipso} of Cp), 108.6, 106.2, 104.7, 100.3 (4 CH of Cp), 73.1 (CH of *i*-Pr), 70.7 (NCH₂), 31.8 (CH_3 of *t*-Bu), 29.1 (CpCH₂), 23.5, 21.4 (2 CH_3 of *i*-Pr), 17.3 (d, $J_{\text{P-C}} = 28$, $\text{P}(\text{CH}_3)_3$), C_q of *t*-Bu not observed. ^{51}V NMR (131.4 MHz, $\text{C}_6\text{D}_5\text{Br}$, 25 $^\circ\text{C}$): δ -832 (d, $J_{\text{P-V}} = 280$). ^{31}P NMR (202 MHz, $\text{C}_6\text{D}_5\text{Br}$, 25 $^\circ\text{C}$): δ 7 (plateau, $\Delta\nu_{\text{top}} = 2225$).

Generation of $[(\text{C}_5\text{H}_4\text{CH}_2\text{CH}_2\text{N}i\text{-Pr})\text{V}(\text{NPhMe}_2)(\text{N}t\text{-Bu})][\text{MeB}(\text{C}_6\text{F}_5)_3]$ (**3c**)

Complex **3c** was generated similarly to **3a**, using PhNMe_2 in stead of THF. ^1H NMR showed clean conversion to **3c** and additional resonances for the excess of PhNMe_2 (~ 3 eq.)

$^1\text{H NMR}$ (500 MHz, $\text{C}_6\text{D}_5\text{Br}$, 25°C): δ 7.22 (partial overlap, *o*-CH of Ph), 7.04 (t, $J_{\text{H-H}} = 7$, 2H, *m*-CH of Ph), 5.88 (m, 2H, Cp and CH of *i*-Pr), 4.96 (m, 2H, Cp and NCHH), 4.65 (m, 1H, Cp), 3.93 (m, 1H, Cp), 3.38 (m, 1H, NCHH), 2.82 (s, 3H, NCH₃), 2.59 (s, 3H, NCH₃), 2.50 (m, 1H, CpCHH), 1.84 (m, 1H, CpCHH), 1.08 (s, 9H, *t*-Bu), 0.96 (d, $J_{\text{H-H}} = 7$, 3H, CH₃ of *i*-Pr), 0.87 (d, $J_{\text{H-H}} = 7$, 3H, CH₃ of *i*-Pr), *p*-CH of Ph not observed. $^{51}\text{V NMR}$ (131.4 MHz, $\text{C}_6\text{D}_5\text{Br}$, 25°C): δ -551 ($\Delta\nu_{1/2} = 830$).

Generation of $[(\text{C}_5\text{H}_4\text{CH}_2\text{CH}_2\text{N}i\text{-Pr})\text{V}(\text{N}t\text{-Bu})_2(\mu\text{-Me})][\text{MeB}(\text{C}_6\text{F}_5)_3]$ (**4**)

A solution of 5 mg (17 μmol) of **1** in 0.1 mL of $\text{C}_6\text{D}_5\text{Br}$ was added to a solution of 5 mg (9.7 μmol) of $\text{B}(\text{C}_6\text{F}_5)_3$ in 0.4 mL of $\text{C}_6\text{D}_5\text{Br}$. NMR showed formation of **4** (additional small resonances probably arose from **2** since a small excess of borane was used). The resonances marked with an asterisk are well-resolved resonances for the two diastereomers that appeared with almost equal chemical shift.

$^1\text{H NMR}$ (500 MHz, $\text{C}_6\text{D}_5\text{Br}$, 25°C): δ 5.80 (m, 2H, Cp), 5.53 (sept, $J_{\text{H-H}} = 7$, 1H, *i*-Pr), 5.39 (m, 1H, Cp), 5.32 (m, 1H, Cp), 4.61 (m, 1H, NCHH), 3.43 (m, 1H, NCHH), 2.66 (m, 1H, CpCHH), 2.06 (m, 1H, CpCHH), 1.09 (s, 9H, *t*-Bu), 1.02 (m, 3H, *i*-Pr), 0.79 (m, 3H, *i*-Pr), -0.57, -0.58 (2 x s, $\Delta\nu_{1/2} = 2$, total 3H, $\mu\text{-CH}_3$). $^{13}\text{C}\{^1\text{H}\}$ NMR (125.7 MHz, $\text{C}_6\text{D}_5\text{Br}$, 25°C): δ 140.2* (C_{ipso} of Cp), 111.9*, 109.9, 102.6*, 101.1 (4 CH of Cp), 73.2* (CH of *i*-Pr), 71.6 (NCH₂), 30.1 (CpCH₂), 31.7 (CH₃ of *t*-Bu), 22.2*, 21.8* (2 CH₃ of *i*-Pr), C_q of *t*-Bu and $\mu\text{-Me}$ not observed. $^{51}\text{V NMR}$ (131.4 MHz, $\text{C}_6\text{D}_5\text{Br}$, 25°C): δ -628 ($\Delta\nu_{1/2} = 1184$).

Generation of $(\text{C}_5\text{H}_4\text{CH}_2\text{CH}_2\text{N}i\text{-Pr})\text{V}(\text{C}_6\text{F}_5)(\text{N}t\text{-Bu})$ (**5**)

Approximately 20 mg (0.07 mmol) of **2** was dissolved in 0.5 mL of C_6D_6 and kept at room temperature for one year in a sealed NMR tube. NMR showed the clean conversion to **5** and $\text{MeB}(\text{C}_6\text{F}_5)_2$.

$^1\text{H NMR}$ (500 MHz, C_6D_6 , 25°C): $\text{MeB}(\text{C}_6\text{F}_5)_2$: δ 1.34 (m, CH₃); **5**: δ 5.64 (m, 1H, Cp), 5.62 (m, 1H, *i*-Pr), 5.60 (m, 1H, Cp), 5.46 (m, 1H, Cp), 5.29 (m, 1H, Cp), 4.77 (m, 1H, NCHH), 3.29 (m, 1H, NCHH), 2.48 (m, 1H, CpCHH), 1.96 (m, 1H, CpCHH), 1.18 (s, 9H, *t*-Bu), 1.01 (d, $J_{\text{H-H}} = 7$, 3H, *i*-Pr), 0.88 (d, $J_{\text{H-H}} = 7$, 3H, *i*-Pr). $^{13}\text{C}\{^1\text{H}\}$ NMR (125.7 MHz, C_6D_6 , 25°C , due to overlap in the region of 135 to 150 ppm resonances for the C_6F_5 moieties of $\text{MeB}(\text{C}_6\text{F}_5)_2$ and **5** could not be assigned): $\text{MeB}(\text{C}_6\text{F}_5)_2$: δ 1.34 (s, CH₃); **5** δ 131.0 (C_{ipso} of Cp), 105.4, 103.5, 96.3, 93.9 (4 CH of Cp), 66.4 (CH of Pr), 63.6 (NCH₂), 24.3 (CpCH₂), 26.4 (CH₃ of *t*-Bu), 17.0, 16.6 (2 CH₃ of *i*-Pr), C_q of *t*-Bu not observed. $^{51}\text{V NMR}$ (131.4 MHz, C_6D_6 , 25°C): δ -827 ($\Delta\nu_{1/2} = 390$). $^{19}\text{F NMR}$ (470.3 MHz, C_6D_6 , 25°C): $\text{MeB}(\text{C}_6\text{F}_5)_2$: δ -131.6 (*o*-F), -148.7 (*p*-F), -163.2 (*m*-F).

Generation of $[(\text{C}_5\text{H}_4\text{CH}_2\text{CH}_2\text{NMe})\text{V}(\text{N}t\text{-Bu})][\text{MeB}(\text{C}_6\text{F}_5)_3]$ (**6**)

A solution of 17 mg (67 μmol) of $(\text{C}_5\text{H}_4\text{CH}_2\text{CH}_2\text{NMe})\text{VMe}(\text{N}t\text{-Bu})$ in 0.1 mL of $\text{C}_6\text{D}_5\text{Br}$ was added to a solution of 40 mg (78 μmol) of $\text{B}(\text{C}_6\text{F}_5)_3$ in 0.4 mL of $\text{C}_6\text{D}_5\text{Br}$. NMR showed the

complete conversion to **6**, without observed side products. ^{19}F NMR showed a small amount of contact ion pair (<10%).

^1H NMR (500 MHz, $\text{C}_6\text{D}_5\text{Br}$, -30°C): δ 6.04 (br, 1H, Cp), 5.44 (br, 1H, Cp), 5.33 (br, 1H, Cp), 5.08 (br, 1H, Cp), 4.44 (m, 1H, NCHH), 3.87 (s, 3H, NCH_3), 3.61 (m, 1H, NCHH), 2.48 (m, 1H, CpCHH), 2.28 (m, 1H, CpCHH), 0.92 (s, 9H, *t*-Bu). ^{13}C $\{^1\text{H}\}$ NMR (125.7 MHz, $\text{C}_6\text{D}_5\text{Br}$, -30°C): δ 143.0 (C_{ipso} of Cp), 114.7, 108.1, 104.8, 104.1 (4 CH of Cp), 84.9 (NCH_3), 79.2 (C_q of *t*-Bu), 64.5 (NCH_2), 30.9 (CH_3 of *t*-Bu), 28.3 (CpCH₂). ^{51}V NMR (131.4 MHz, $\text{C}_6\text{D}_5\text{Br}$, -30°C): δ -565 ($\Delta\nu_{1/2} = 7000$).

Generation of $[(\text{C}_5\text{H}_4\text{CH}_2\text{CH}_2\text{N}i\text{-Pr})\text{V}(\text{N}p\text{-Tol})][\text{MeB}(\text{C}_6\text{F}_5)_3]$ (**7**)

Complex **7** was generated similarly to **6**, starting from $(\text{C}_5\text{H}_4\text{CH}_2\text{CH}_2\text{N}i\text{-Pr})\text{VMe}(\text{N}p\text{-Tol})$. NMR showed the complete conversion to **7**, without observed side products. ^{19}F NMR showed a small amount of contact ion pair (<10%).

^1H NMR (500 MHz, $\text{C}_6\text{D}_5\text{Br}$, -30°C): δ 6.83 (br, 4H, CH of *p*-Tol), 5.85 (br, 1H, Cp), 5.74 (br, 1H, Cp), 5.45 (br, 2H, Cp and CH of *i*-Pr), 5.05 (m, 1H, Cp), 4.69 (m, 1H, NCHH), 3.63 (m, 1H, NCHH), 2.72 (m, 1H, CpCHH), 2.16 (s, 4H, CH_3 of *p*-Tol and shoulder of CpCHH), 1.09 (d, $J_{\text{H-H}} = 7$, 3H, CH_3 of *i*-Pr), 0.71 (d, $J_{\text{H-H}} = 7$, 3H, CH_3 of *i*-Pr). ^{13}C $\{^1\text{H}\}$ NMR (125.7 MHz, $\text{C}_6\text{D}_5\text{Br}$, -30°C): δ 160.7, 143.5, 142.3 (2 C_q of *p*-Tol and C_{ipso} of Cp), 137.9 (CH of *p*-Tol), 113.4, 110.8, 106.2, 105.5 (4 CH of Cp), 75.2 (NCH_2), 73.6 (CH of *i*-Pr), 29.3 (CpCH₂), 23.1 (CH_3 of *i*-Pr), 22.1 (CH_3 of *p*-Tol), 21.6 (CH_3 of *i*-Pr), 1 CH of *p*-Tol not observed (probably due to overlap with solvent resonances). ^{51}V NMR (131.4 MHz, $\text{C}_6\text{D}_5\text{Br}$, -30°C): δ -430 ($\Delta\nu_{1/2} = 10500$).

Generation of $[(t\text{-BuN})\text{VCp}(\text{N}i\text{-Pr}_2)][\text{MeB}(\text{C}_6\text{F}_5)_3]$ (**8**)

Complex **8** was generated similarly to **6**, starting from $(t\text{-BuN})\text{VCp}(\text{Ni-Pr}_2)\text{Me}$. NMR showed the complete conversion to **8**, without observed side products. ^{19}F NMR showed a small amount of contact ion pair (<10%).

^1H NMR (500 MHz, $\text{C}_6\text{D}_5\text{Br}$, -30°C): δ 5.60 (s, 5H, Cp), 5.00 (sept, $J_{\text{H-H}} = 6$, 1H, CH of *i*-Pr), 3.31 (sept, $J_{\text{H-H}} = 6$, 1H, CH of *i*-Pr), 1.41 (d, $J_{\text{H-H}} = 6$, 3H, CH_3 of *i*-Pr), 1.03 (s, 9H, *t*-Bu), 0.98 (d, $J_{\text{H-H}} = 7$, 3H, CH_3 of *i*-Pr), 0.78 (d, $J_{\text{H-H}} = 6$, 3H, CH_3 of *i*-Pr), 0.75 (d, $J_{\text{H-H}} = 7$, 3H, CH_3 of *i*-Pr). ^{13}C $\{^1\text{H}\}$ NMR (125.7 MHz, $\text{C}_6\text{D}_5\text{Br}$, -30°C): δ 109.7 (Cp), 81.0 (C_q of *t*-Bu), 71.6, 61.3 (2 CH of *i*-Pr), 33.1 (CH_3 of *i*-Pr), 31.7 (CH_3 of *t*-Bu), 27.6, 21.0, 20.8 (3 CH_3 of *i*-Pr). ^{51}V NMR (131.4 MHz, $\text{C}_6\text{D}_5\text{Br}$, 25°C): δ -492 ($\Delta\nu_{1/2} = 1400$).

Generation of $[(p\text{-TolN})\text{VCp}(\text{N}i\text{-Pr}_2)][\text{MeB}(\text{C}_6\text{F}_5)_3]$ (**9**)

Complex **9** was generated similarly to **6**, starting from $(p\text{-TolN})\text{VCp}(\text{Ni-Pr}_2)\text{Me}$. NMR showed the complete conversion to **9**, without observed side products. ^{19}F NMR showed a small amount of contact ion pair (<10%).

$^1\text{H NMR}$ (500 MHz, $\text{C}_6\text{D}_5\text{Br}$, -30°C): δ 6.91 (s, 4H, CH of *p*-Tol), 5.65 (s, 5H, Cp), 5.04 (sept, $J_{\text{H-H}} = 6$, 1H, CH of *i*-Pr), 3.36 (sept, $J_{\text{H-H}} = 6$, 1H, CH of *i*-Pr), 2.18 (s, 3H, CH_3 of *p*-Tol), 1.40 (d, $J_{\text{H-H}} = 6$, 3H, CH_3 of *i*-Pr), 1.05 (d, $J_{\text{H-H}} = 7$, 3H, CH_3 of *i*-Pr), 0.84 (d, $J_{\text{H-H}} = 6$, 3H, CH_3 of *i*-Pr), 0.78 (d, $J_{\text{H-H}} = 7$, 3H, CH_3 of *i*-Pr). $^{13}\text{C}\{^1\text{H}\}$ NMR (125.7 MHz, $\text{C}_6\text{D}_5\text{Br}$, -30°C): δ 161.3, 140.6 (2 C_{ipso} of *p*-Tol), 130.4, 126.2 (2 CH of *p*-Tol), 110.7 (Cp), 70.9, 62.7 (2 CH of *i*-Pr), 33.0, 27.3 (2 CH_3 of *i*-Pr), 22.2 (CH_3 of *p*-Tol), 20.9, 20.8 (2 CH_3 of *i*-Pr). $^{51}\text{V NMR}$ (131.4 MHz, $\text{C}_6\text{D}_5\text{Br}$, 25°C): δ -397 ($\Delta\nu_{1/2} = 2500$).

Generation of $[(\text{C}_5\text{H}_4\text{CH}_2\text{CH}_2\text{N}=\text{CMe}_2)\text{V}(\text{NH}t\text{-Bu})][\text{MeB}(\text{C}_6\text{F}_5)_3]$ (**10b**)

A solution of 30 mg (105 μmol) of **1** in 0.5 mL of THF- d_8 was added to 84 mg (105 μmol) of $[\text{PhNMe}_2][\text{B}(\text{C}_6\text{F}_5)_4]$. Gas evolution was observed immediately and the color of the solution changed from brown to red-brown while the $[\text{PhNMe}_2\text{H}][\text{B}(\text{C}_6\text{F}_5)_4]$ dissolved (~ 30 seconds). NMR showed clean conversion to **10b** and free PhNMe_2 .

$^1\text{H NMR}$ (300 MHz, THF- d_8 , 25°C): free PhNMe_2 : δ 7.11 (t, $J_{\text{H-H}} = 7$, 2H, *m*-CH of Ph), 6.68 (d, $J_{\text{H-H}} = 8$, 2H, *o*-CH of Ph), 6.59 (t, $J_{\text{H-H}} = 7$, 1H, *p*-CH of Ph), 2.89 (s, 6H, CH_3); **10b** δ 6.20 (m, 2H, Cp), 5.88 (m, 1H, Cp), 5.69 (m, 1H, Cp), 5.50 (br, 1H, NH), 4.04 (m, 2H, NCH_2), 2.78 (m, 1H, CpCHH), 2.69 (m, 1H, CpCHH), 1.99 (s, 3H, $=\text{CCH}_3$), 1.91 (s, 3H, $=\text{CCH}_3$), 1.38 (s, 9H, *t*-Bu). $^1\text{H NMR}$ (300 MHz, $\text{C}_6\text{D}_5\text{Br}$, 25°C): δ 5.47 (br, 1H, Cp), 5.37 (br, 1H, Cp), 5.27 (br, 1H, Cp), 5.17 (br, 1H, Cp), 3.71 (br, NH), 3.59 (m, 1H, NCHH), 3.44 (m, 1H, NCHH), 2.21 (m, 2H, CpCH $_2$), 1.72 (s, 3H, $=\text{CCH}_3$), 1.42 (s, 3H, $=\text{CCH}_3$), 0.98 (s, 9H, *t*-Bu). $^{13}\text{C NMR}$ (125.7 MHz, THF- d_8 , -50°C): free PhNMe_2 : δ 151.8 (s, C_{ipso} of Ph), 130.7 (dd, $J_{\text{C-H}} = 156 / 8$, CH of Ph), 114.5 (d, $J_{\text{C-H}} = 158$, CH of Ph), 42.0 (q, $J_{\text{C-H}} = 136$, $\text{N}(\text{CH}_3)_2$); **10b** δ 140.0 (s, C_{ipso} of Cp), 119.0, 107.6, 102.8, 98.7 (d, $J_{\text{C-H}} = 173, 176, 175, 173$, 4 CH of Cp), 79.1 (br, $\Delta\nu_{1/2} = 21$, C_q of *t*-Bu), 78.2 (s, $=\text{C}(\text{CH}_3)_2$), 60.0 (t, $J_{\text{C-H}} = 140$, NCH_2), 34.7 (q, $J_{\text{C-H}} = 127$, $=\text{C}(\text{CH}_3)_2$), 32.3 (q, $J_{\text{C-H}} = 127$, CH_3 of *t*-Bu), 31.4 (t, $J_{\text{C-H}} = 129$, CpCH $_2$), 25.6 (q, $J_{\text{C-H}} = 125$, $=\text{C}(\text{CH}_3)_2$). $^{51}\text{V NMR}$ (131.4 MHz, THF- d_8 , 25°C): δ -354 ($\Delta\nu_{1/2} = 1900$).

Generation of $[(\text{C}_5\text{H}_4\text{CH}_2\text{CH}_2\text{N}=\text{CH}_2)\text{V}(\text{NH}t\text{-Bu})][\text{MeB}(\text{C}_6\text{F}_5)_3]$ (**10a**)

Complex **10a** was generated similarly to **10b**, starting from $(\eta^5, \eta^1\text{-C}_5\text{H}_4\text{CH}_2\text{CH}_2\text{NMe})\text{VMe}(\text{N}t\text{-Bu})$. NMR showed clean conversion to **10a** and PhNMe_2 .

$^1\text{H NMR}$ (500 MHz, THF- d_8 , 25°C): δ 6.47 (br, 1H, Cp), 6.29 (br, 1H, Cp), 6.18 (br, 1H, NH), 5.88 (br, 1H, Cp), 5.75 (br, 1H, Cp), 4.08 (m, 1H, NCHH), 3.62 (m, 1H, NCHH), 3.20 (d, $J_{\text{H-H}} = 9$, 1H, $=\text{CHH}$), 2.65 (m, 3H, CpCH $_2$ and $=\text{CHH}$), 1.33 (s, 9H, *t*-Bu). $^{13}\text{C NMR}$ (125.7 MHz, THF- d_8 , -90°C): δ 139.6 (C_{ipso} of Cp), 118.1, 106.8, 105.0, 98.7 (4 CH of Cp), 79.0 (br, $\Delta\nu_{1/2} = 39$, C_q of *t*-Bu), 65.2 (t, $J_{\text{C-H}} = 142$, NCH_2), 64.4 (t, $J_{\text{C-H}} = 163$, $=\text{CH}_2$), 32.0 (CH_3 of *t*-Bu), 29.0 (CpCH $_2$). $^{51}\text{V NMR}$ (131.4 MHz, THF- d_8 , 25°C): δ -563 ($\Delta\nu_{1/2} = 470$).

Generation of $[(\text{C}_5\text{H}_4\text{CH}_2\text{CH}_2\text{N}(i\text{-Pr})\text{CH}=\text{CMeCMe}_2)\text{V}(\text{N}t\text{-Bu})][\text{MeB}(\text{C}_6\text{F}_5)_3]$ (**11**)

To a solution of 45 mg (56 μmol) of **2** in $\text{C}_6\text{D}_5\text{Br}$, 8 μl (70 μmol) of 2,3-dimethyl-butadiene was added by microsyringe, after which the color of the solution changed from brown to red-brown. ^1H NMR showed complete conversion to **11**, additional resonances for the excess of the diene and small impurities in the region of 0 - 7 ppm.

^1H NMR (500 MHz, $\text{C}_6\text{D}_5\text{Br}$, -30°C): 7.55 (s, 1H, =CH), 5.60 (br, 1H, Cp), 5.32 (br, 1H, Cp), 5.13 (br, 1H, Cp), 5.02 (br, 1H, Cp), 3.33 (m, 1H, CH of *i*-Pr), 3.2 - 2.7 (m, 4H, NCH_2 and CpCH_2), 1.64 (s, 3H, CCH_3), 1.51 (s, 3H, CCH_3), 1.64 (s, 3H, CCH_3), 1.00 (br, CH_3 of *i*-Pr with shoulder of CCH_3), 0.86 (s, 9H, CH_3 of *t*-Bu), 0.82 (br, 3H, CH_3 of *i*-Pr). ^{13}C $\{^1\text{H}\}$ NMR (125.7 MHz, $\text{C}_6\text{D}_5\text{Br}$, -30°C): 182.9 (=CH), 157.3 (=CCH₃), 143.9 (C_q of Cp), 114.0, 107.6, 101.9, 96.5 (4 CH of Cp), 77.8 (C_q of *t*-Bu), 72.7 (NCH_2), 62.2 (CH of *i*-Pr), 36.6 (CpCH_2), 30.8 (CH_3 of *t*-Bu), 27.3, 26.9, 25.6 (=CCH₃ and $\text{VC}(\text{CH}_3)_2$), 24.5, 23.1 (2 CH_3 of *i*-Pr). ^{51}V NMR (131.4 MHz, $\text{C}_6\text{D}_5\text{Br}$, 25°C): -492 ($\Delta\nu_{1/2} = 1000$).

Generation of [$\{\text{C}_5\text{H}_4\text{CH}_2\text{CH}_2\text{N}(\textit{i}\text{-Pr})(\text{CMe})_2\}\text{V}(\text{Nt-Bu})\][\text{MeB}(\text{C}_6\text{F}_5)_3]$ (**12**)

A solution of 10 mg (35 μmol) of **1** in 0.1 mL of $\text{C}_6\text{D}_5\text{Br}$ was added to a solution of 23 mg (45 μmol) of $\text{B}(\text{C}_6\text{F}_5)_3$ in 0.4 mL of $\text{C}_6\text{D}_5\text{Br}$. This solution was transferred into an NMR tube equipped with a Teflon Young valve. The tube was connected to a high vacuum line, frozen in liquid nitrogen and evacuated. Subsequently, 1.2 equivalents of 2-butyne were condensed into the NMR tube, which was then closed, thawed out and kept at 0°C for 10 minutes. ^1H NMR showed complete conversion to **12**, small amounts of **13**, 2-butyne and impurities in the region of 0 - 7 ppm.

^1H NMR (500 MHz, $\text{C}_6\text{D}_5\text{Br}$, -30°C): 6.53 (br, Cp), 5.71 (br, Cp), 5.27 (br, Cp), 4.99 (br, Cp), 2.86 (m, NCHH), 2.65 (m, NCHH), 2.37 (m, CpCHH), 2.21 (m, CH of *i*-Pr), 2.00 (m, CpCHH), 1.84 (s, CCH_3), 1.16 (s, CCH_3), 1.03 (s, CH_3 of *t*-Bu), 0.63 (br, CH_3 of *i*-Pr), 0.23 (br, CH_3 of *i*-Pr). ^{13}C $\{^1\text{H}\}$ NMR (125.7 MHz, $\text{C}_6\text{D}_5\text{Br}$, -30°C): 132.9 (C_q of Cp), 122.3 (CCH_3), 120.6, 110.2, 104.0, 95.1 (4 CH of Cp), 78.9 (C_q of *t*-Bu), 58.7, 56.6 (CH of *i*-Pr and NCH_2), 31.5 (CH_3 of *t*-Bu), 26.3, 24.2, 23.0, 21.3, 5.0 (2 CH_3 of *i*-Pr, 2 CCH_3 and CpCH_2). ^{51}V NMR (131.4 MHz, $\text{C}_6\text{D}_5\text{Br}$, -30°C): -181 ($\Delta\nu_{1/2} = 8900$).

Generation of [$\{\text{C}_5\text{H}_4\text{CH}_2\text{CH}_2\text{N}(\textit{i}\text{-Pr})(\text{CMe})_4\}\text{V}(\text{Nt-Bu})\][\text{MeB}(\text{C}_6\text{F}_5)_3]$ (**13**)

The NMR tube in which **12** was generated was connected to a high vacuum line, frozen in liquid nitrogen and evacuated. Subsequently, 2 equivalents of 2-butyne were condensed into the NMR tube, which was then closed, thawed out and kept at room temperature for 30 minutes. NMR showed complete conversion to **13**, 2-butyne and small amounts of impurities in the region of 0 - 7 ppm.

^1H NMR (500 MHz, $\text{C}_6\text{D}_5\text{Br}$, -30°C): 5.56 (br, Cp), 5.1 (br, Cp), 5.27 (br, Cp), 5.09 (br, Cp), 2.83 (CH of *i*-Pr and NCHH), 2.37 (m, NCHH), 2.16 (m, CpCHH), 1.96 (m, CpCHH), 2.16 (s, CCH_3), 1.39 (s, CCH_3), 1.35 (s, CCH_3), 1.31 (s, CCH_3), 1.03 (s, CH_3 of *t*-Bu), 0.75 (br, CH_3 of

i-Pr), 0.60 (br, CH₃ of *i*-Pr). ¹³C {¹H} NMR (125.7 MHz, C₆D₅Br, -30°C): 135.1, 133.0, 129.2, 114.0 (C_q of Cp and 3 CCH₃), 113.8, 108.5, 105.4, 97.4 (CH of Cp), 77.5 (br, C_q of *t*-Bu), 66.6 (CH of *i*-Pr), 59.0 (NCH₂), 31.1 (CH₃ of *t*-Bu), 26.0 (CpCH₂), 30.6, 22.1, 20.8, 20.1, 18.9, 18.4 (2 CH₃ of *i*-Pr, 4 CCH₃). ⁵¹V NMR (131.4 MHz, C₆D₅Br, -30°C): -436 (Δv_{1/2} = 8100).

3.5 References

- (1) See for instance: Jordan, J.F., *Adv. Organometall. Chem.*, **1991**, 32, 325.
- (2) Sinn, H., *Macromol. Symp.*, **1995**, 97, 27.
- (3) (a) Jia, L.; Yang, X.; Stern, C.L.; Marks, T.J., *Organometallics*, **1997**, 16, 842. (b) Bochmann, M.; Lancaster, S.J., *J. Organometallic Chem.*, **1992**, 434, C1. (c) Chien, J.C.W.; Tsai, W-M.; Rausch, M.D., *J. Am. Chem. Soc.*, **1991**, 113, 8570. (d) Yang, X.; Stern, C.L.; Marks, T.J., *J. Am. Chem. Soc.*, **1994**, 116, 10015.
- (4) (a) Choukroun, R.; Douziech, B.; Pan, C.; Dahan, F.; Cassoux, P., *Organometallics*, **1995**, 14, 4471. (b) Budzelaar, P.H.M.; van Oort, A.B.; Orpen, A.G., *Eur. J. Inorg. Chem.*, **1998**, 1485. (c) Kim, W-K.; Fevola, M.J.; Liable-Sands, L.M.; Rheingold, A.L.; Theopold, K.H., *Organometallics*, **1998**, 17, 4541.
- (5) Horton, A.D.; de With, J.; van der Linden, A.J.; van de Weg, H., *Organometallics*, **1996**, 15, 2672.
- (6) Reaction of Cp*TiMe₃ with B(C₆F₅)₃ in aromatic solvents yields the arene complexes [Cp*Ti(η⁶-arene)Me₂][MeB(C₆F₅)₃] (ref. 6a), but other arene coordination modes have also been proposed (ref. 6b). Halogenated solvents can coordinate by its halogen atom (ref. 6c), although this is most frequently observed for late transition metal complexes (ref. 6d). (a) Gillis, D.J.; Tudoret, M-J.; Baird, M.C., *J. Am. Chem. Soc.*, **1993**, 115, 2543. (b) Eisch, J.J.; Pombrik, S.I.; Zheng, G-X., *Organometallics*, **1993**, 12, 3856. (c) Plenio, H., *Chem. Rev.*, **1997**, 97, 3363, and ref. 125 herein. (d) Kulawiec, R.J.; Crabtree, R.H., *Coord. Chem. Rev.*, **1990**, 99, 89.
- (7) (a) Bochmann, M.; Lancaster, S.J., *Angew. Chem. Int. Ed. Eng.*, **1994**, 33, 1634. (b) Chen, Y-X.; Stern, C.L.; Yang, S.; Marks, T.J., *J. Am. Chem. Soc.*, **1996**, 118, 12451.
- (8) Mayer, J.M.; Curtis, C.J.; Bercaw, J.E., *J. Am. Chem. Soc.*, **1983**, 105, 2651.
- (9) Bol, J.E.; Hessen, B.; Teuben, J.H.; Smeets, W.J.J.; Spek, A.L., *Organometallics*, **1992**, 11, 1981.
- (10) Guillemin, J-C.; Denis, J-M., *Tetrahedron*, **1988**, 4, 4431.
- (11) Chisholm, M.H.; Rothwell, I.P., *Comp. Coord. Chem.*, **1987**, 2, 161.
- (12) (a) de With, J.; Horton, A.D.; Orpen, A.G., *Organometallics*, **1993**, 12, 1493. (b) Bennet, J.L.; Wolczanski, P.T., *J. Am. Chem. Soc.*, **1994**, 116, 2179.
- (13) Luetkens Jr., M.L.; Sattelberger, A.P.; Murray, H.H.; Basil, J.D.; Fackler Jr., J.P.; Jones, R.A.; Heaton, D.E., *Inorg. Synth.*, **1989**, 26, 7.

- (14) Tjaden, A.B.; Swenson, D.C.; Jordan, R.F.; Petersen, J.L., *Organometallics*, **1995**, *14*, 371.

Chapter 4

Olefin coordination towards cationic d^0 vanadium complexes

4.1 Introduction

Olefin coordination to a metal center consists of two contributions: σ -donation from a π -orbital of the olefin to an empty d-orbital of the metal, and π -back donation from a filled d-orbital on the metal to a π^* -orbital of the olefin (Figure 1).¹

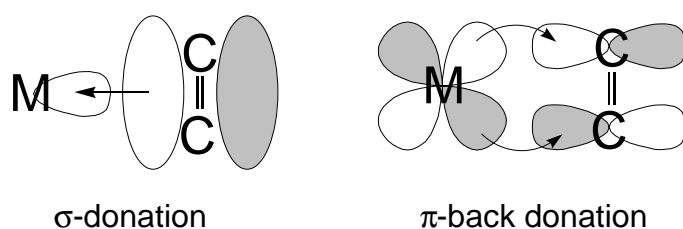


Figure 1: Olefin coordination to a metal center.

Since d^0 metals have no filled d-orbitals, they lack the possibility for π -back donation and olefin coordination is expected to be relatively weak. Nevertheless, olefin coordination to a cationic d^0 metal center has been proposed as one of the steps in the olefin polymerization catalyzed by cationic group 4 metallocene complexes.² Due to its high reactivity, the intermediate olefin adduct has never been observed. In fact, only few olefin adducts of d^0 metal centers have been described in literature, and in most complexes the olefin is held in the proximity of the metal by a covalently bonded tether (Figure 2).³

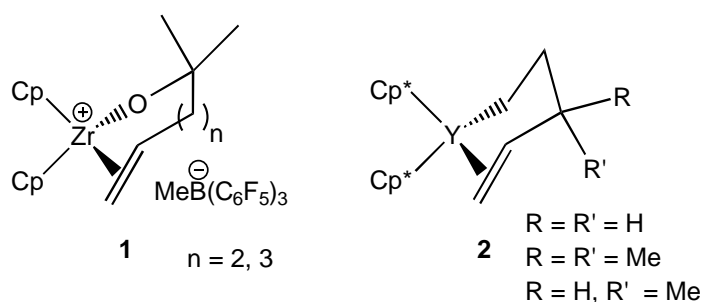
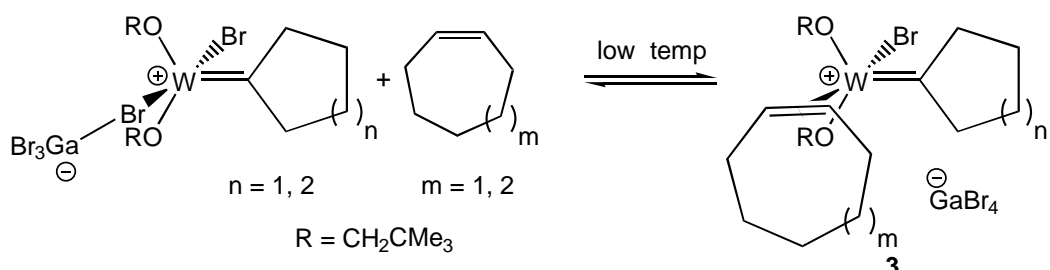


Figure 2: Coordination of a tethered olefin to d^0 metal centers.

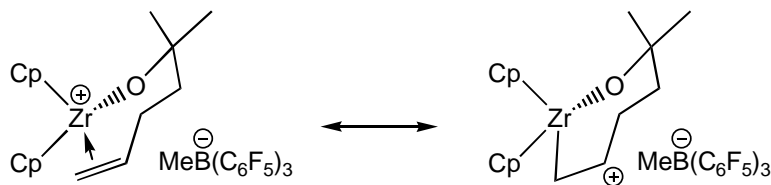
The above described compounds do not form stable adducts with olefins that are not tethered to the metal center. So far, only one d^0 metal complex is reported that coordinates olefins that are not tethered to the metal center. The tungsten alkylidene $[(Me_3CCH_2O)_2W(=C(CH_2)_n)Br][GaBr_4]$ ($n = 1, 2$) reacted with cycloheptene or cyclooctene at low temperatures to generate the olefin adducts **3**, which were identified by 1H and ^{13}C NMR (Scheme 1).⁴ When the compounds were mixed at ambient temperatures, ring opening metathesis polymerization (ROMP) of the cyclic olefin took place.



Scheme 1

The cationic zirconium compound **1** ($n = 2$) is the only isolated and structurally characterized d^0 olefin adduct.^{3a} The olefinic moiety of the alkoxy group coordinates in an asymmetric fashion ($Zr-CH_2 = 2.68(2)$, $Zr-CH = 2.89(2)$ Å). In the ^{13}C NMR spectra of **1** the olefinic carbon atom closest to the metal center shows an upfield shift of 20 ppm compared to the free olefin, while the other olefinic carbon atom shows a downfield shift of 19 ppm. This can be

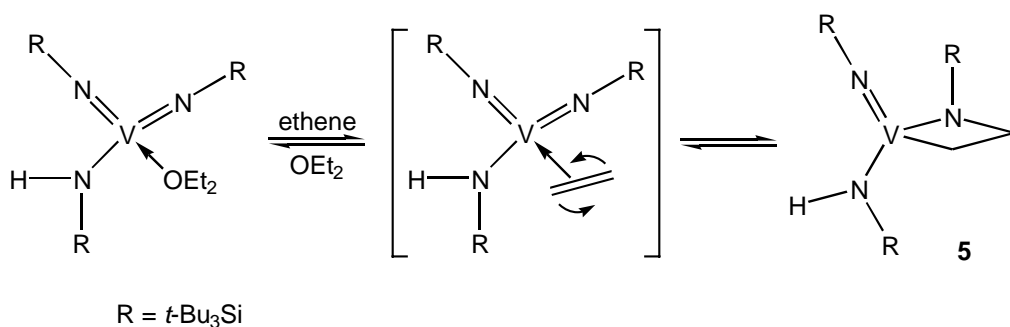
explained by a resonance structure in which the positive charge is on the substituted carbon atom (Scheme 2).



Scheme 2

It is possible that the observed polarization in **1** is influenced by the tether, which can force the olefinic moiety into an asymmetric coordination. Furthermore, the positive charge on the olefinic carbon atom will be stabilized by the substituent on this carbon atom. Nevertheless, in theoretical calculations on ethene coordination to cationic d⁰ metal complexes, the ethene coordination is also asymmetric.⁵ For example, in the model compounds for a ‘constrained geometry’ catalyst, $[(\eta^5, \eta^1\text{-C}_5\text{H}_4\text{SiH}_2\text{NH})\text{M}(\eta^2\text{-ethene})\text{Me}]^+$ (**4**, M = Ti, Zr, Hf), Ti-C distances of 2.39 and 2.44 Å were calculated (no distances reported for M = Zr or Hf). Although the interaction of the ethene with the cationic d⁰ metal centers is expected to be weak, calculations predict a high metal-olefin bond strength (**4**, M = Ti: 20.8 kcal·mol⁻¹; M = Zr: 24.2 kcal·mol⁻¹; M = Hf: 25.7 kcal·mol⁻¹).

An ethene adduct of a d⁰ vanadium(V) imido complex has been proposed as intermediate in the [2+2] cycloaddition of ethene over the vanadium-imido bond. In their work with vanadium(V) imido complexes, Horton *et al.* discovered that ethene reacts with one imido ligand of (*t*-Bu₃SiN)₂V(NHSi*t*-Bu₃)(OEt₂) to form the aza-metallacycle (*t*-Bu₃SiN)V(NHSi*t*-Bu₃)($\eta^1, \eta^1\text{-CH}_2\text{CH}_2\text{NSi}t\text{-Bu}_3$) (**5**, identified by ¹H, ¹³C and ⁵¹V NMR, Scheme 3).⁶ The CH₂CH₂-moiety of **5** is observed in ¹H and ¹³C NMR as a singlet, which is explained by an equilibrium between the aza-metallacycle and an ethene adduct, in which the ethene is rapidly rotating. The intermediate d⁰ vanadium ethene adduct is not observed.



Scheme 3

This chapter describes the reversible coordination of a series of olefins to the cationic d^0 vanadium complexes described in Chapter 3. The effects of substituents on the olefin, amido, and imido ligands, on the coordination of the olefin is discussed, based on the various equilibrium constants of the adduct formation. Theoretical calculations on a model compound were performed to get an insight into the structure of the olefin adducts and the strength of the olefin coordination. For the coordination of cyclopentene to the solvated species of $[(C_5H_4CH_2CH_2N*i*-Pr)V(N*t*-Bu)][MeB(C_6F_5)_3]$, the thermodynamic parameters ΔH^0 and ΔS^0 were determined by variable temperature NMR.

4.2 Results and Discussion

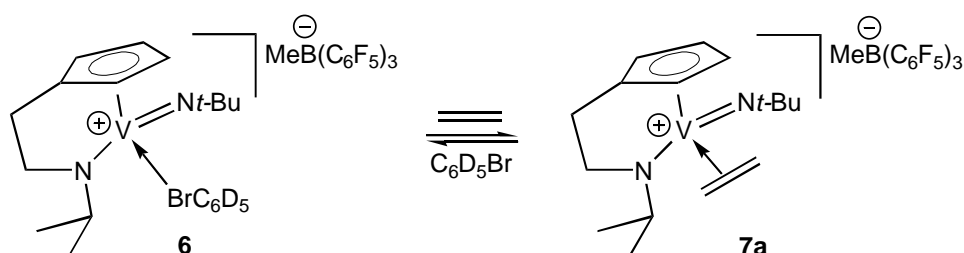
4.2.1 Reactivity of $[(\eta^5, \eta^1-C_5H_4CH_2CH_2N*i*-Pr)V(N*t*-Bu)]^+$ towards olefins

Addition of an excess of ethene to a C_6D_5Br solution of $[(\eta^5, \eta^1-C_5H_4CH_2CH_2N*i*-Pr)V(N*t*-Bu)][MeB(C_6F_5)_3]$ (**6**, present as the solvent separated species, see Chapter 3), led to the generation of the ethene adduct $[(\eta^5, \eta^1-C_5H_4CH_2CH_2N*i*-Pr)V(\eta^2-H_2C=CH_2)(N*t*-Bu)][MeB(C_6F_5)_3]$ (**7a**, Scheme 4). The olefin complexation is fully reversible, and **7a** reverted to the solvated species of **6** upon pumping off the ethene. Therefore we did not attempt to isolate the adduct, but instead identified it by its 1H , ^{13}C and ^{51}V NMR spectra. In addition to the expected resonances for the Cp-amido and *t*-Bu-imido ligand, which have

shifted little compared to **6**, **7a** shows two multiplets in the ^1H NMR spectrum (4.72 and 4.61 ppm, integral of $2 \times 2\text{H}$) and one triplet in the ^{13}C NMR spectrum (103.2 ppm, $J_{\text{C-H}}$ 164 Hz). These characteristics differ considerably from those of the vanadium aza-metallacyclic complex **5** reported by Horton (Scheme 2: ^1H : 3.22 ppm; ^{13}C : 48.3 ppm, $J_{\text{C-H}}$ 149 Hz),⁶ and are much closer to the NMR data for free ethene (^1H : 5.29 ppm; ^{13}C : 123.9 ppm, $J_{\text{C-H}}$ 160 Hz). From this we conclude that **7a** is an ethene adduct, the first one observed for a d^0 metal center.

At room temperature the resonances of coordinated and free ethene are sharp, and only at high temperatures (80 °C) do the resonances of the coordinated ethene start to broaden. This is an indication that the exchange of coordinated ethene with the excess of free ethene is remarkably slow.

A clean sample of **7a** in $\text{C}_6\text{D}_5\text{Br}$ is stable at room temperature for at least one week, however, it appears that small amounts of impurities can cause the ethene to polymerize, even at low temperatures.



Scheme 4

Complex **6** reacted reversibly with propene to form the propene adduct $[(\eta^5, \eta^1\text{-C}_5\text{H}_4\text{CH}_2\text{CH}_2\text{N}i\text{-Pr})\text{V}(\eta^2\text{-H}_2\text{C}=\text{CHMe})(\text{N}t\text{-Bu})][\text{MeB}(\text{C}_6\text{F}_5)_3]$ (**7b**), which is observed in the ^1H , ^{13}C and ^{51}V NMR spectra as a mixture of two diastereomers (ratio ~ 4:5), due to the two possible coordination modes of the propene (Figure 3). Upon coordination, the olefinic carbon atoms of the propene show ^{13}C NMR chemical shift differences comparable to those in the zirconium adduct **1** (Scheme 2, Table 1).^{3a} Therefore we propose that in **7b** the propene

coordinates asymmetrically with the substituted olefinic carbon atom further away from the metal center, comparable to the zirconium adduct **1**.

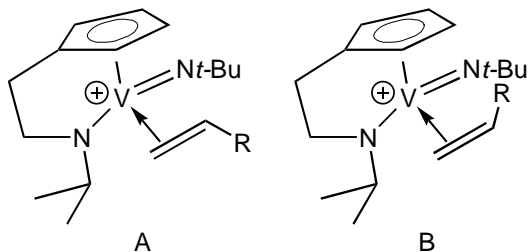


Figure 3: Two diastereomers of the propene adduct **7b**.

As expected, the isobutene adduct $[(\eta^5, \eta^1\text{-C}_5\text{H}_4\text{CH}_2\text{CH}_2\text{Ni-Pr})\text{V}(\eta^2\text{-H}_2\text{C}=\text{CMe}_2)(\text{Nf-Bu})][\text{MeB}(\text{C}_6\text{F}_5)_3]$ (**7c**) appears as a single species in the ^1H , ^{13}C and ^{51}V NMR spectra. The ^{13}C NMR shifts of the olefinic moiety upon coordination (Table 1) are consistent with a polarization of the coordinated olefin as is described for **1**, and we again propose a structure with the substituted olefinic carbon atom further away from the metal than the unsubstituted carbon atom.

Table 1 shows the observed ^{13}C NMR chemical shift differences ($\Delta\delta$) for the olefinic carbon atoms upon olefin coordination. The larger downfield shift of the substituted carbon atom in the isobutene adduct **7c** compared to the propene adduct **7b** leads to the conclusion that the polarization in **7c** is more pronounced than in **7b**. This can be rationalized by two factors: the two methyl groups in the coordinating isobutene cause a larger steric interaction with other ligands on the vanadium metal, and they better stabilize the positive charge on the olefinic carbon atom.

Table 1: ^{13}C NMR chemical shift differences ($\Delta\delta$) for the olefinic moiety upon coordination.

Complex	$\Delta\delta(\text{CH}_2)$	$\Delta\delta(\text{CR})$
1	-20	+19
7a	-21	

7b	-24	+1
7c	-27	+35

Although the polarization of the coordinating olefin is clear when electron donating substituents are placed on one of the olefinic carbon atoms, it becomes unclear when olefins are used with electron withdrawing substituents, or with electron donating substituents on both olefinic carbon atoms. The cyclopentene adduct $[(\eta^5, \eta^1\text{-C}_5\text{H}_4\text{CH}_2\text{CH}_2\text{N}i\text{-Pr})\text{V}(\eta^2\text{-C}_5\text{H}_8)(\text{N}t\text{-Bu})][\text{MeB}(\text{C}_6\text{F}_5)_3]$ (**7d**) and the styrene adduct $[(\eta^5, \eta^1\text{-C}_5\text{H}_4\text{CH}_2\text{CH}_2\text{N}i\text{-Pr})\text{V}(\eta^2\text{-H}_2\text{C}=\text{CHPh})(\text{N}t\text{-Bu})][\text{MeB}(\text{C}_6\text{F}_5)_3]$ (**7e**) can be identified by ¹H, ¹³C and ⁵¹V NMR spectroscopy, and their ¹³C NMR spectra show an upfield shift for both olefinic carbon atoms upon coordination.⁷ It is unclear what causes this.

Just as the propene adduct **7b**, the styrene adduct **7e** is observed as a mixture of two diastereomers (ratio ~ 4:5). However, in **7e** interconversion of the two diastereomers is observed at room temperature. In the ¹H and ¹³C NMR spectra of the **7e** broad resonances are observed at ambient temperatures, which split up into two sets of resonances for the two diastereomers at lower temperatures. By determining the coalescence temperature (T_c) of one set of two resonances, the free energy of activation (ΔG^\ddagger) for the interconversion of the two diastereomers can be calculated from Equation 1.⁸ With $T_c = 283 \pm 2$ K and $\Delta\nu = 37 \pm 1$ Hz, $\Delta G^\ddagger = 58.8 \pm 0.5$ kJ·mol⁻¹.

$$\Delta G^\ddagger = 1.914 \cdot 10^{-2} \times T_c \times [9.972 + \log(T_c/\Delta\nu)] \quad (1)$$

For the olefin adducts **1** ($n = 2$) and **2** ($R = \text{H}$, $R' = \text{Me}$) the interconversion of the two diastereomers has a ΔG^\ddagger of 44.2 kJ·mol⁻¹ (no error reported) and 40.6 ± 0.2 kJ·mol⁻¹ respectively,^{3a,3b} however, it is uncertain if these processes proceed by the same mechanism as the interconversion in **7e**. The diastereomers of the adducts **1** and **2** can only interconvert by dissociation and subsequent recoordination of the olefin, however, the styrene in **7e** does not have to dissociate for interconversion. Instead, the coordinated styrene can change its coordination from the olefinic bond to the phenyl group, after which

the vinylic group can rotate and recoordinate with its other face. The cationic zirconium complex $[\text{Cp}^*\text{ZrMe}_2][\text{MeB}(\text{C}_6\text{F}_5)_3]$ is known to coordinate added styrene by its phenyl group, while no interaction with the vinylic group is observed.

4.2.2 Comparison of the equilibrium constants

The coordination of olefins to $[(\text{C}_5\text{H}_4\text{CH}_2\text{CH}_2\text{N}i\text{-Pr})\text{V}(\text{N}t\text{-Bu})][\text{MeB}(\text{C}_6\text{F}_5)_3]$ (**6**) is reversible, and in the NMR spectra of the adducts **7** the starting compound **6** and an amount of free olefin is always observed. By careful integration of well-resolved resonances in the ^1H NMR spectra, measured from samples with a known concentration, the K_{eq} for the reaction in Equation 2 was determined (Table 2). In these measurements we assume there is no influence from coordination of the $[\text{MeB}(\text{C}_6\text{F}_5)_3]^-$ anion.



Table 2: Coordination of different olefins to **6**.

Olefin ^a	compound	K_{eq}^{b}
ethene	7a	100 ± 10
propene	7b	44 ± 4
isobutene	7c	23 ± 2
cyclopentene	7d	8 ± 1
styrene	7e	10 ± 1

a) No reaction observed with 10 equivalents of 3,3-dimethyl-1-butene (*t*-Bu-ethene), 2,3-dimethyl-2-butene (tetramethyl-ethene). b) K_{eq} (at 25 °C) = $[\mathbf{7}] \times [\text{C}_6\text{D}_5\text{Br}] \times [\mathbf{6}]^{-1} \times [\text{olefin}]^{-1}$.

The interaction of an olefin with a d^0 metal center consists only of σ -donation of the olefin to the metal. Therefore, olefins that are more electron rich are expected to interact more strongly with d^0 metal centers. Although the olefinic moiety of propene is electron richer than that of ethene (because of electron donation of the methyl substituent) the K_{eq} of the formation of **7b** is much lower than that of **7a**. Apparently, the effect of the steric bulk of the

methyl substituent dominates the electronic effect. When the steric bulk is further increased (3,3-dimethyl-1-butene) or when four small substituents are introduced on the olefin (2,3-dimethyl-2-butene) no olefin adducts are observed. Di-substituted olefins (isobutene, cyclopentene) form adducts with complex **6**, but with a low K_{eq} . It appears that the steric hindrance of the 1,1-di-substituted olefin isobutene is less than that of the 1,2-di-substituted olefin cyclopentene. Because of the asymmetric coordination of the isobutene in **7c** (see section 4.2.1) the two methyl substituents are pointing away from the metal, which decreases the steric interactions with other ligands. In the cyclopentene adduct **7d** an asymmetric coordination will not help to decrease the steric interactions of the coordinating olefin.

Placing an electron withdrawing substituent on the olefin (styrene), lowers the K_{eq} , although this probably is a combination of the electron deficiency of the olefin in combination with a large substituent.

In order to investigate the influence of the steric and electronic properties of the vanadium center itself on the olefin coordination, the Cp-amido vanadium complexes $[(\eta^5, \eta^1\text{-C}_5\text{H}_4\text{CH}_2\text{CH}_2\text{NMe})\text{V}(\text{N}t\text{-Bu})][\text{MeB}(\text{C}_6\text{F}_5)_3]$ and $[(\eta^5, \eta^1\text{-C}_5\text{H}_4\text{CH}_2\text{CH}_2\text{N}i\text{Pr})\text{V}(\text{N}p\text{-Tol})][\text{MeB}(\text{C}_6\text{F}_5)_3]$ (see Chapter 3) were reacted with ethene and the K_{eq} was determined. The K_{eq} for the formation of the ethene adducts $[(\eta^5, \eta^1\text{-C}_5\text{H}_4\text{CH}_2\text{CH}_2\text{NR})\text{V}(\eta^2\text{-ethene})(\text{NR})][\text{MeB}(\text{C}_6\text{F}_5)_3]$ (**8**: R = Me, R' = *t*-Bu; **9**: R = *i*-Pr, R' = *p*-Tol) is equal to the K_{eq} for the formation of **7a** (measured for **8**: $K_{\text{eq}} = 99$; **9**: $K_{\text{eq}} = 98$).¹⁰ Apparently, the changes on the metal center influence the coordination of the olefin in the same way as they influence the stabilization by the solvent. These results compare well to the solvent coordination to the complexes $[(\text{Cp-amido})\text{V}(\text{NR})][\text{MeB}(\text{C}_6\text{F}_5)_3]$ as described in Chapter 3, sections 3.2.1 and 3.2.3, where the position of the equilibrium between the contact ion pair and the solvent separated ion pair depended on the coordinating properties of the solvent and not on the electronic or steric properties of the vanadium complex.

4.2.3 Theoretical calculations on the ethene coordination

In order to get more information on the structure of the olefin adducts and the metal-olefin bond strength, theoretical calculations (DFT/B3LYP) on the model compound $[(\eta^5, \eta^1\text{-C}_5\text{H}_4\text{CH}_2\text{CH}_2\text{NH})\text{V}(\eta^2\text{-H}_2\text{C}=\text{CH}_2)(\text{NH})]^+$ (**7calc**) were performed.¹¹ These calculations were performed by Dr. P.H.M. Budzelaar of the University of Nijmegen.

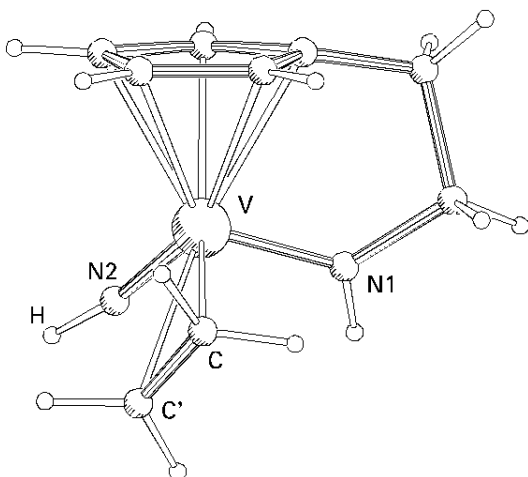


Figure 4: Conformation of **7calc** with the lowest calculated energy.

In Figure 4 the conformation of **7calc** with the lowest calculated energy is shown, in which the ethene is coordinating parallel to the vanadium-imido bond. A second conformation with the ethene coordinating parallel to the vanadium-amido bond has a local energy minimum that is $1.2 \text{ kcal}\cdot\text{mol}^{-1}$ higher in energy. However, the barrier for ethene rotation is low and the energy minima are shallow, so there appears to be no preference for a specific orientation of the ethene. This has also been found for the Cp-amido group 4 model complexes $[(\eta^5, \eta^1\text{-C}_5\text{H}_4\text{SiH}_2\text{NH})\text{M}(\eta^2\text{-ethene})\text{Me}]^+$ (**4**, $\text{M} = \text{Ti}, \text{Zr}, \text{Hf}$).⁵

The ethene coordination in **7calc** is asymmetric ($\text{V-C} = 2.43$; $\text{V-C}' = 2.54 \text{ \AA}$). As observed in calculations on the group 4 complexes **4**, the $\text{C}=\text{C}$ bond distance of the olefin has increased only slightly upon coordination (1.36 \AA vs. 1.33 \AA for free ethene), indicating the lack of backbonding from the metal center. The calculated metal-ethene bond strength in **7calc** ($31 \text{ kcal}\cdot\text{mol}^{-1}$) is

higher than in **4** (M = Ti: 20.8, M = Zr: 24.2, M = Hf: 25.7 kcal·mol⁻¹), which may be caused by the following three factors.

Charge on metal center: Olefin coordination to a cationic metal center becomes stronger when the positive charge on the metal increases.¹² However, both the vanadium and the group 4 model complexes have a formal charge of +1, and in addition, the vanadium center (16 valence electrons) is less electron deficient than the group 4 metal centers (12 valence electrons). This would therefore predict a somewhat lower metal-olefin bond strength for **7calc**.

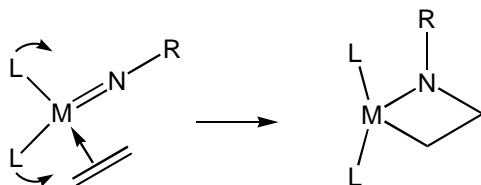
Reorganization energy: When olefin coordination to a metal center requires the metal center to change its structure, this will decrease the total metal-olefin bond strength. The bare cationic complexes [(η^5, η^1 -C₅H₄SiH₂NH)TiMe]⁺ and [(η^5, η^1 -C₅H₄CH₂CH₂NH)V(NH)]⁺ both have a pyramidal structure, with an inversion barrier of less than 3 kcal·mol⁻¹,⁵ therefore the reorganization energy of the olefin coordination will have no significant influence on the calculated metal-olefin bond strength.

Steric interactions: Ziegler *et al.* state that the main steric interaction of ethene in **4** will be with the methyl group.⁵ The smaller steric interaction of the linear imido group in **7calc**, compared to the tetrahedral methyl group in **4**, can cause the stronger metal-olefin bond in **7calc**.

4.2.4 Influence of the bridge between the Cp and amido functionality

In the introduction of this chapter (section 4.1, Scheme 3) the reaction of a neutral vanadium(V) imido complex with ethene is described, which generates a metallacyclic complex (**5**) by a [2+2] cycloaddition of the olefin over the V-N(imido) bond. Much to our surprise no reactivity of the cationic Cp-amido vanadium(V) complex **6** with olefins was observed. Our first assumption was that this is caused by the constrained geometry of the Cp-amido ligand.¹³ A [2+2] cycloaddition of ethene over a vanadium-imido bond would generate an aza-metallacycle with a small N-V-C bite angle. In order to compensate for this small angle the other ligands can open up, as is shown in Scheme 5. We assumed that the bridge between the Cp and amido functionality in the adducts

7 prevented opening of the Cp-V-amido bite angle, so that the aza-metallacycle could not be formed.



Scheme 5

Theoretical calculations predicted that the formation of an aza-metallacyclic product from an ethene adduct takes place without a significant energy barrier, and several structures with almost equal energies were calculated. From this we conclude that there is an equilibrium between the olefin adduct and the aza-metallacycle, which was also reported by Horton *et al.* (Scheme 3).⁶ However, in Horton's case the equilibrium was shifted towards the aza-metallacycle, while we observe only the olefin adduct. To test if the equilibrium can be shifted to the aza-metallacycle, we investigated olefin coordination to Cp-amido vanadium complexes in which there is no bridge between the Cp and amido functionality.

The complexes [(RN)VCp(N*i*-Pr₂)] [MeB(C₆F₅)₃] (R = *t*-Bu, *p*-Tol, see Chapter 3) coordinated ethene to form the adducts [(RN)VCp(η²-ethene)(N*i*-Pr₂)] [MeB(C₆F₅)₃] (**10**: R = *t*-Bu; **11**: R = *p*-Tol). However, in contrast to the coordination of ethene to **6** the ethene is quickly polymerized, even at -30°C and even if the methyl complexes used for the generation of the cation are analytically pure. It was therefore not possible to obtain good ¹H NMR spectra of the ethene adducts **10** and **11**. Nevertheless, resonances around 4.6 ppm are very comparable to the observed resonances for coordinating ethene in the ethene adducts **7a**, **8** and **9**.

We propose that in complexes **10** and **11** insertion of ethene in the vanadium amido bond generates a small amount of a cationic vanadium alkyl species which quickly polymerizes the ethene in the NMR tube. Although this

species is not observed, it is a reasonable assumption based on the reactivity of the Cp-amido complexes towards dimethyl-butadiene and 2-butyne as described in Chapter 3. No attempts have been made to identify the end groups of the polymer.

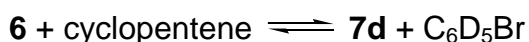
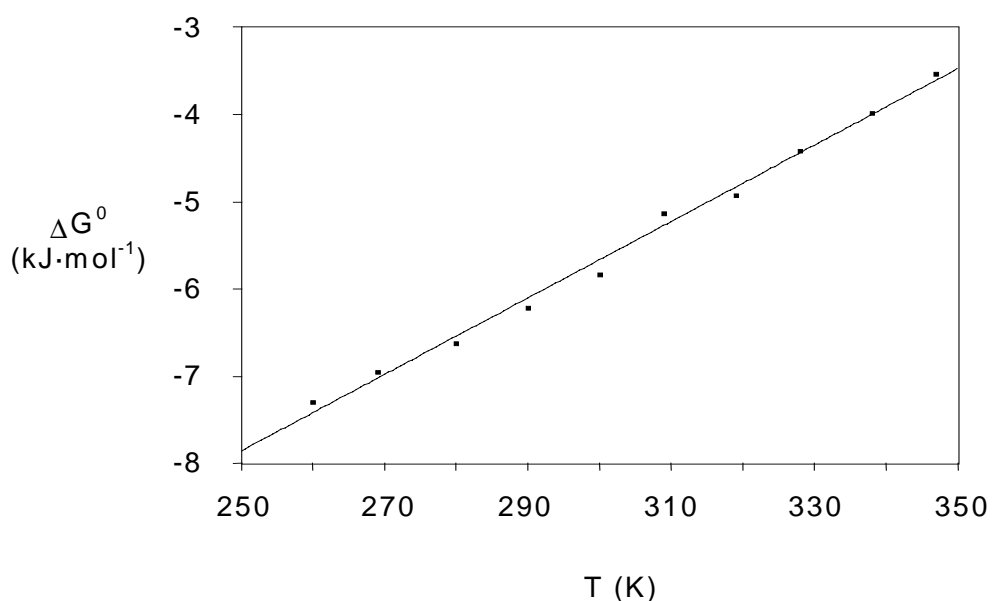
Since the polymerization of ethene is very fast, even at low temperatures, full characterization of the ethene adducts **10** and **11** was not possible. Instead, the cyclopentene adducts [(RN)VCp(η^2 -C₅H₈)(Ni-Pr₂)] [MeB(C₆F₅)₃] (**12**: R = *t*-Bu; **13**: R = *p*-Tol) were fully characterized by ¹H, ¹³C and ⁵¹V NMR spectroscopy. No significant differences between **12**, **13** and **7d** were observed.

4.2.5 Thermodynamic measurements on the olefin coordination to **6**

From ¹H, ¹³C and ⁵¹V NMR measurements it is clear that the equilibrium of coordination of olefins to **6** can be shifted to the olefin adducts by lowering the temperature. After carefully measuring the K_{eq} at different temperatures, the Gibbs free energy (ΔG^0 , in J·mol⁻¹) could be calculated from Equation 3.¹⁴ The parameters ΔH^0 and ΔS^0 could be calculated from Equation 4 after plotting ΔG^0 versus the temperature (T, in K, Figure 5).¹⁵ For these measurements we investigated the coordination of cyclopentene, since the cyclopentene adduct **7d** exists as only one isomer. Furthermore cyclopentene is a liquid at room temperature, so olefin exchange between solution and the gas phase can be neglected and the total amount of olefin in solution can be assumed to be constant. In the measurements we assumed no influence of anion coordination.

$$\Delta G^0 = -R \times T \times \ln K_{eq} \quad (3)$$

$$\Delta G^0 = \Delta H^0 - \Delta S^0 \times T \quad (4)$$



$$\Delta S^0 = -0.04 \pm 0.01 \text{ kJ}\cdot\text{mol}^{-1}\cdot\text{K}^{-1}$$

$$\Delta H^0 = -19 \pm 1 \text{ kJ}\cdot\text{mol}^{-1}$$

Figure 5: Plot of ΔG^0 versus T for the formation of **7d**.

The ΔS^0 value for the formation of **7d** ($-0.04 \pm 0.01 \text{ kJ}\cdot\text{mol}^{-1}\cdot\text{K}^{-1}$) is smaller than the value for the displacement of the $[\text{MeB}(\text{C}_6\text{F}_5)_3]^-$ anion by PMe_3 in the zirconium complex $[\text{Cp}_2\text{ZrMe}][\text{MeB}(\text{C}_6\text{F}_5)_3]$ ($-0.08 \pm 0.01 \text{ kJ}\cdot\text{mol}^{-1}\cdot\text{K}^{-1}$),¹⁶ and the displacement of the $[\text{GaBr}_4]^-$ anion in the tungsten complex **3** ($n = 1$) by cycloheptene ($-0.23 \pm 0.01 \text{ kJ}\cdot\text{mol}^{-1}\cdot\text{K}^{-1}$).⁴ All three ΔS^0 values are small, since there is no change in the number of particles during the reactions. However, in the reported literature examples an anionic particle ($[\text{MeB}(\text{C}_6\text{F}_5)_3]^-$ or $[\text{GaBr}_4]^-$) is replaced by a neutral particle (PMe_3 or cycloheptene). It is possible that the observed differences in the ΔS^0 values reflect the cation-anion interactions that are still present after the anion displacements, and that will further decrease the entropy.

The ΔH^0 of $-19 \pm 1 \text{ kJ}\cdot\text{mol}^{-1}$ shows that cyclopentene coordination to **6** is slightly exothermic, although the value is much lower than the above mentioned displacements ($-41 \text{ kJ}\cdot\text{mol}^{-1}$ for $[\text{Cp}_2\text{ZrMe}][\text{MeB}(\text{C}_6\text{F}_5)_3]/\text{PMe}_3$;¹⁶ $-57 \pm 2 \text{ kJ}\cdot\text{mol}^{-1}$

for **3**, $n = 1$).⁴ From the measurements on the equilibrium constants of the formation of the olefin adducts **7** (Tabel 2) it is clear that the bonding of cyclopentene to the vanadium center is weak, compared to the bonding of ethene. It is therefore expected that the formation of the ethene adduct **7a** is more exothermic than the cyclopentene adduct **7e**, and will be more in the range of the above mentioned displacements.

4.3 Conclusion

The cationic d⁰ vanadium(V) complexes described in Chapter 3 reacted reversibly with a range of olefins to generate the corresponding olefin adducts. This is only the second example of olefin adduct formation with a d⁰ metal complex in which the olefin is free and not also connected to the metal by a covalently bonded tether, and the first example where simple olefins such as ethene and propene coordinate to the d⁰ metal center.

Theoretical calculations predict an unusually high vanadium-ethene bond strength. Measurement of the equilibrium constants of the formation of adducts with several olefins shows that the strength of the interaction of the olefin with the metal center decreases when the steric bulk of the coordinating olefin increases. Although the bonding of the olefin to the vanadium center is only established by σ -donation, even electron donating substituents on the olefin decrease the tendency to form adducts, probably because of increased steric interactions. Steric interactions probably also decrease the tendency of the vanadium center to form adducts with the solvent, which is abundant in much larger quantities than the olefins.

The exchange of coordinated ethene with free ethene, as well as the stabilization of the equilibrium of olefin adduct formation is slow. An associative displacement of a coordinated ligand is difficult, because of the steric crowding around the metal center, while dissociative displacement requires a lot of energy, because of the high vanadium-ligand bond strength.

We have determined the ΔS^0 and ΔH^0 values for the coordination of cyclopentene to the solvated species of [(C₅H₄CH₂CH₂N*i*-Pr)V(N*t*-

Bu)]][MeB(C₆F₅)₃]. The ΔS^0 value of the displacement of a solvent molecule by an olefin is small since there is no change in the number of particles in this reaction. The formation of the cyclopentene adduct is an exothermic process, although the ΔH^0 value for the coordination of cyclopentene to the cationic vanadium Cp-amido complex is smaller than for other reported adduct formations. Since ethene binds stronger to the metal center than cyclopentene, a larger ΔH^0 value is expected for ethene coordination.

4.4 Experimental

General considerations

All reactions were carried out under N₂, using standard glove-box and vacuum line techniques. C₆D₅Br was degassed and stored on mol. sieves under nitrogen. NMR spectra were recorded on a Varian Unity 500 spectrometer, all spectra were recorded in C₆D₅Br at -30°C. ¹H and ¹³C NMR chemical shifts are reported in ppm relative to TMS, using residual solvent resonances as internal reference. ⁵¹V NMR chemical shifts are reported in ppm relative to VOCl₃, which is used as an external reference. Coupling constants (J) and line widths at half height ($\Delta v_{1/2}$) are reported in Hz. The density of C₆D₅Br was measured in the region of 5 to 35°C on an Anton Paar DMA 35n portable density meter. [(η^5, η^1 -C₅H₄CH₂CH₂N*i*-Pr)V(N*t*-Bu)]][MeB(C₆F₅)₃] (**6**), [(η^5, η^1 -C₅H₄CH₂CH₂NMe)V(N*t*-Bu)]][MeB(C₆F₅)₃], [(η^5, η^1 -C₅H₄CH₂CH₂N*i*-Pr)V(N*p*-Tol)]][MeB(C₆F₅)₃], [(*t*-BuN)VCp(N*i*-Pr₂)]][MeB(C₆F₅)₃] and [(*p*-ToIN)VCp(N*i*-Pr₂)]][MeB(C₆F₅)₃] are described in the previous chapter. Ethene (99.9%, Hoekloos), propene (99.9%, Hoekloos) and isobutene (99%, Aldrich) were used as received. Cyclopentene (Acros) and styrene (Aldrich) were stored under nitrogen and used as received. The 1D-¹H NMR spectra of the styrene adduct **7e** and the cyclopentene adducts **7d**, **12** and **13** contained too much of the starting vanadium complex and free olefin to perform an integration of the resonances (product resonances were small compared to other resonances and many resonances overlap). Therefore these NMR spectra were interpreted based on the 2D-¹H, ¹H and 2D-¹H, ¹³C NMR spectra.

Generation of [(η^5, η^1 -C₅H₄CH₂CH₂N*i*-Pr)V(η^2 -ethene)(N*t*-Bu)]][MeB(C₆F₅)₃] (**7a**)

An NMR tube equipped with a Teflon (Young) valve was filled with 0.874 g of a 66 mM solution of **6** in C₆D₅Br. The tube was connected to a high vacuum line, frozen and evacuated. Subsequently, a calibrated volume of ethene was condensed into the NMR tube, so that a pressure of approximately 1 bar was reached after the NMR tube was closed and thawed out. The NMR tube was kept at room temperature for one hour before measuring, to let the equilibrium stabilize. The exact amount of ethene in solution was determined by ¹H NMR.

¹H NMR (500 MHz, C₆D₅Br, 25°C): *free olefin*: δ 5.29 (s); **7a**: δ 5.71 (br, 1H, Cp), 5.61 (br, 1H, Cp), 5.34 (sept, J_{H-H} = 6, 1H, CH of *i*-Pr), 5.27 (br, 1H, Cp), 5.02 (br, 1H, Cp), 4.72 (m, 2H, =CHH), 4.61 (m, 1H, NCHH), 4.33 (m, 2H, =CHH), 3.26 (dd, J_{H-H} = 15 / 7, 1H, NCHH), 2.70 (dd, J_{H-H} = 13 / 7, 1H, CpCHH), 1.91 (m, 1H, CpCHH), 0.94 (s, 9H, *t*-Bu), 0.82, 0.59 (d, J_{H-H} = 6, 7, 3H, 2 CH₃ of *i*-Pr). ¹³C NMR (125.7 MHz, C₆D₆, -30°C): *free olefin*: δ 123.9 (t, J_{C-H} = 160); **7a**: δ 141.9 (C_{ipso} of Cp), 109.6, 109.2, 103.1, 101.3 (d, J_{C-H} = 173, 173, 179 and 181 respectively, 4 CH of Cp), 103.2 (d, J_{C-H} = 164, =CH₂), 76.3 (d, J_{C-H} = 143, CH of *i*-Pr), 73.3 (t, J_{C-H} = 138, NCH₂), 29.5 (t, partial overlap, CpCH₂), 31.1 (q, J_{C-H} = 132, CH₃ of *t*-Bu), 22.6, 20.7 (q, J_{C-H} = 127 and 127 respectively, 2 CH₃ of *i*-Pr), C_q of *t*-Bu not observed. ⁵¹V NMR (131.4 MHz, C₆D₅Br, 25°C): δ -707 (Δv_{1/2} = 750).

Generation of [(η⁵,η¹-C₅H₄CH₂CH₂N*i*-Pr)V(η²-propene)(N*t*-Bu)][MeB(C₆F₅)₃] (**7b**)

The same procedure was used as for **7a**, only now the propene pressure after thawing out the NMR tube was approximately 2 bars. The exact amount of propene in solution was determined by ¹H NMR. Two isomers were formed (A:B ~ 4:5).

¹H NMR (500 MHz, C₆D₅Br, -30°C): *free olefin*: 5.71 δ (m, 1H, =CHCH₃), 5.00 (d, J_{H-H} = 17, 1H, =CHH cis to CH₃), 4.94 (d, J_{H-H} = 10, 1H, =CHH trans to CH₃), 1.58 (d, J_{H-H} = 6, 3H, =CHCH₃); **7b**: δ 6.26^B, 6.01^A (m, =CHCH₃), 5.98, 5.93, 5.55, 5.43, 5.40, 5.34, 5.30, 5.08 (m, Cp), 5.66, 5.42 (CH of *i*-Pr), 4.65, 4.39 (m, NCHH), 4.33^B, 4.01^A (d, J_{H-H} = 17^B, 17^A, =CHH cis to CH₃), 4.15^A, 3.65^B (d, J_{H-H} = 9^A, 8^B, =CHH trans to CH₃), 3.31, 3.16 (m, NCHH), 2.58, 2.54 (m, CpCHH), 1.99, 1.88 (m, CpCHH), 1.32^A, 1.28^B (d, J_{H-H} = 5^A, 5^B, =CHMe), 0.98, 0.95 (s, *t*-Bu), 0.80, 0.72, 0.66, 0.56 (d, J_{H-H} = 6, Me of *i*-Pr). ¹³C NMR (125.7 MHz, C₆D₆, -30°C): *free olefin*: 134.4 (d, J_{C-H} = 155, =CHCH₃), 116.8 (t, J_{C-H} = 153, =CH₂), 20.5 (q, overlap, CH₃); **7b**: δ 142.2, 141.8 (s, 2 C_{ipso} of Cp), 137.7, 135.4 (d, J_{C-H} = 157, 159, 2 =CHCH₃), 111.2, 110.3, 109.6, 109.2, 102.4, 102.3, 101.3, 101.2 (d, J_{C-H} = 182, 177, 175, 173, 174, 174, 177 and 177 respectively, 8 CH of Cp), 92.7, 92.5 (t, J_{C-H} = 160, 159, 2 =CH₂), 77.0, 76.4 (t, 2 NCH₂), 73.4, 72.7 (d, 2 CH of *i*-Pr), 31.2, 30.9 (q, J_{C-H} = 127 and 128 respectively, 2 CH₃ of *t*-Bu), 29.7, 29.5 (2 CpCH₂), 23.4, 22.9, 22.8, 22.6 (4 CH₃ of *i*-Pr), 20.2, 20.1 (2 =CHCH₃), C_q of *t*-Bu not observed. ⁵¹V NMR (131.4 MHz, C₆D₅Br, 25°C): δ -646, -650 (partial overlap).

Generation of [(η⁵,η¹-C₅H₄CH₂CH₂N*i*-Pr)V(η²-isobutene)(N*t*-Bu)][MeB(C₆F₅)₃] (**7c**)

The same procedure was used as for **7a**, only now the isobutene pressure after thawing out the NMR tube was approximately 2 bars. The exact amount of isobutene in solution was determined by ¹H NMR.

¹H NMR (500 MHz, C₆D₅Br, -30°C): *free olefin*: δ 4.70 (s, 2H, =CH₂), 1.59 (s, 6H, =CCH₃); **7c**: δ 5.79 (br, 1H, Cp), 5.60 (m, 2H, CH of *i*-Pr and Cp), 5.26 (br, 1H, Cp), 4.99 (br, 1H, Cp), 4.54 (m, 1H, NCHH), 3.76 (s, 1H, =CHH), 3.69 (s, 1H, =CHH), 3.24 (m, 1H, NCHH), 2.60 (m, 1H, CpCHH), 1.82 (m, 1H, CpCHH), 1.72 (s, 3H, =CCH₃), 0.96 (s, 3H, =CCH₃), 0.94 (s, 9H,

t-Bu), 0.87 (d, $J_{\text{H-H}} = 7$, 3H, CH_3 of *i*-Pr), 0.64 (d, $J_{\text{H-H}} = 7$, 3H, CH_3 of *i*-Pr). ^{13}C NMR (125.7 MHz, $\text{C}_6\text{D}_5\text{Br}$, -30°C): *free olefin*: δ 142.6 (s, $=\text{CCH}_3$), 112.0 (t, $J_{\text{C-H}} = 154$, $=\text{CH}_2$), 25.1 (q, $J_{\text{C-H}} = 125$, $=\text{CCH}_3$); **7c**: δ 177.5 (s, $=\text{CCH}_3$), 142.3 (C_{ipso} of Cp), 112.0, 110.7, 101.0, 101.4 (4 CH of Cp), 84.8 (t, $J_{\text{C-H}} = 156$, $=\text{CH}_2$), 76.5 (CH of *i*-Pr), 72.7 (NCH₂), 30.9 (CH_3 of *t*-Bu), 29.9 (CpCH₂), 29.1, 29.0, 23.9, 19.2 (2 CH_3 of *i*-Pr and 2 $=\text{CCH}_3$), C_q of *t*-Bu not observed. ^{51}V NMR (131.4 MHz, $\text{C}_6\text{D}_5\text{Br}$, 25°C): δ -577 ($\Delta\nu_{1/2} = 860$).

Generation of $[(\eta^5, \eta^1\text{-C}_5\text{H}_4\text{CH}_2\text{CH}_2\text{N}i\text{-Pr})\text{V}(\eta^2\text{-cyclopentene})(\text{N}t\text{-Bu})][\text{MeB}(\text{C}_6\text{F}_5)_3]$ (**7d**)

An NMR tube equipped with a Teflon (Young) valve was filled with 0.687 g of a 111 mM solution of **6** in $\text{C}_6\text{D}_5\text{Br}$. The tube was connected to a high vacuum line, frozen and evacuated. Subsequently, 0.197 mmol of cyclopentene was condensed into the NMR tube, after which the NMR tube was closed and thawed out.

^1H NMR (500 MHz, $\text{C}_6\text{D}_5\text{Br}$, -30°C): *free olefin*: δ 5.65 (s, 2H, $=\text{CH}$), 2.20 (t, $J_{\text{H-H}} = 8$, $=\text{CH-CH}_2$), 1.68 (q, $J_{\text{H-H}} = 8$, $=\text{CH-CH}_2\text{-CH}_2$); **7d**: δ 5.83 (Cp), 5.79, 5.78 (2 $=\text{CH}$), 5.77 (CH of *i*-Pr), 5.65, 5.15, 5.09 (3 Cp), 4.62 (NCHH), 3.40 (NCHH), 2.67 (CpCHH), 2.00 ($=\text{CH-CH}_2$), 1.94 (CpCHH), 1.00 (*t*-Bu), 0.91 (CH_3 of *i*-Pr), 0.79 ($=\text{CH-CH}_2\text{-CH}_2$), 0.70 (CH_3 of *i*-Pr). ^{13}C NMR (125.7 MHz, C_6D_6 , -30°C): *free olefin*: δ 131.3 (d, $J_{\text{C-H}} = 159$, $=\text{CH}$), 33.3 (t, $J_{\text{C-H}} = 128$, $=\text{CH-CH}_2$), 23.7 (t, $J_{\text{C-H}} = 127$, $=\text{CH-CH}_2\text{-CH}_2$); **7d**: δ 142.4 (s, C_{ipso} of Cp), 125.7, 124.4 (d, $J_{\text{C-H}} = 156$, 160, 2 $=\text{CH}$), 111.4, 111.3, 102.7, 102.1 (d, $J_{\text{C-H}} = \text{overlap}$, overlap, 179 and 174 respectively, 4 CH of Cp), 77.1 (d, $J_{\text{C-H}} = 143$, CH of *i*-Pr), 73.3 (t, $J_{\text{C-H}} = 139$, NCH₂), 35.1, 34.9 (t, $J_{\text{C-H}} = 133$ and 133 respectively, 2 $=\text{CH-CH}_2$), 30.9 (q, $J_{\text{C-H}} = 130$, CH_3 of *t*-Bu), 29.7 (t, $J_{\text{C-H}} = 130$, CpCH₂), 23.2 (q, overlap, CH_3 of *i*-Pr), 22.1 (t, $J_{\text{C-H}} = 130$, $=\text{CH-CH}_2\text{-CH}_2$), 19.8 (q, $J_{\text{C-H}} = 126$, CH_3 of *i*-Pr), C_q of *t*-Bu not observed. ^{51}V NMR (131.4 MHz, $\text{C}_6\text{D}_5\text{Br}$, 25°C): δ -521 ($\Delta\nu_{1/2} = 4300$).

Generation of $[(\eta^5, \eta^1\text{-C}_5\text{H}_4\text{CH}_2\text{CH}_2\text{N}i\text{-Pr})\text{V}(\eta^2\text{-styrene})(\text{N}t\text{-Bu})][\text{MeB}(\text{C}_6\text{F}_5)_3]$ (**7e**)

To 0.929 g of a 0.223 mM solution of **6** in $\text{C}_6\text{D}_5\text{Br}$ was added 78.4 mg (0.75 mmol) of styrene. Compound **7e** had to be measured immediately in order to prevent polymerization, which takes place even at low temperatures. Two isomers are formed (A:B ~ 4:5).

^1H NMR (500 MHz, $\text{C}_6\text{D}_5\text{Br}$, -30°C): *free olefin*: δ 7.25 (d, $J_{\text{H-H}} = 8$, 2H, CH of Ph), 7.17 (t, $J_{\text{H-H}} = 8$, 2H, CH of Ph), 7.12 (t, $J_{\text{H-H}} = 7$, 1H, CH of Ph), 6.61 (dd, $J_{\text{H-H}} = 18 / 11$, 1H, $=\text{CH}$), 5.64 (d, $J_{\text{H-H}} = 18$, 1H, $=\text{CHH}$ cis to Ph), **xxx** (d, $J_{\text{H-H}} = 11$, 1H, $=\text{CHH}$ trans to Ph); **7e**: δ 6.81^A (dd, $J_{\text{H-H}} = 17 / 10$, $=\text{CH}$), 6.73^B (dd, $J_{\text{H-H}} = 18 / 10$, $=\text{CH}$), 5.89, 5.74 (br, 2 Cp), 5.62 (shoulder of solvent, CH of *i*-Pr), 5.31 (overlap, Cp), 5.24 (m, CH of *i*-Pr), ~5.1^A (overlap with styrene, $=\text{CHH}$ cis to Ph), 5.04 (overlap, 2 Cp), 5.01, 4.93, 4.78 (br, 3 Cp), 4.53^B (d, $J_{\text{H-H}} = 17$, $=\text{CHH}$ cis to Ph), 4.48^B (d, $J_{\text{H-H}} = 10$, $=\text{CHH}$ trans to Ph), 4.36, 4.16 (m, 2 NCHH), 3.79^A (d, $J_{\text{H-H}} = 9$, $=\text{CHH}$ trans to Ph), 3.16 (dd, $J_{\text{H-H}} = 14 / 7$, NCHH), 3.09 (dd, $J_{\text{H-H}} = 14 / 8$, NCHH), 2.62 (dd, $J_{\text{H-H}} = 13 / 7$, CpCHH), 2.28 (dd, $J_{\text{H-H}} = 13 / 7$, CpCHH), 1.88, 1.73 (m, 2 CpCHH), 0.94 (s, *t*-Bu), 0.93 (shoulder, *t*-Bu), 0.88, 0.76, 0.68, -0.09 (d, $J_{\text{H-H}} = 6$, 6, 6 and 6 respectively, 4 CH_3 of *i*-Pr). ^{13}C NMR: *free olefin*

(125.7 MHz, C₆D₅Br, -30°C): δ 138.8 (s, C_{ipso} of styrene), 137.7 (d, J_{C-H} = 150, =CH), 129.3 (d, J_{C-H} = 159, CH of Ph), 128.6 (d, J_{C-H} = 160, CH of Ph), 127.0 (d, J_{C-H} = 158, CH of Ph), 114.4 (t, J_{C-H} = 158, =CH₂); **7e**: δ 142.2, 141.5 (s, 2 C_{ipso} of Cp), 135.8, 133.6, 133.3, 133.2, 132.9, 129.2, 129.1, 129.0, 128.4, 128.1 (2 =CH, 2 C_{ipso} of Ph and 6 CH of Ph), 113.5, 112.6, 111.7, 111.1, 102.2, 101.8, 101.7, 101.3 (8 CH of Cp), 86.0, 83.8 (t, J_{C-H} = 162 and 159 respectively, 2 =CH₂), 77.0, 76.0 (2 CH of *i*-Pr), 73.3, 72.6 (2 NCH₂), 30.9, 30.8 (2 CH₃ of *t*-Bu), 29.7, 29.6 (2 CpCH₂), 24.2, 24.1, 22.5, 20.6 (4 CH₃ of *i*-Pr), C_q of *t*-Bu not observed. ⁵¹V NMR (131.4 MHz, C₆D₅Br, -30°C): δ -614 (Δν_½ = 2200).

Generation of [(η⁵,η¹-C₅H₄CH₂CH₂Me)V(η²-ethene)(N*t*-Bu)][MeB(C₆F₅)₃] (**8**)

The same procedure was used as for **7a**, starting from [(η⁵,η¹-C₅H₄CH₂CH₂NMe)V(N*t*-Bu)][MeB(C₆F₅)₃]. The exact amount of ethene in solution was determined by ¹H NMR.

¹H NMR (500 MHz, C₆D₅Br, -30°C): δ 5.74 (br, 1H, Cp), 5.52 (br, 1H, Cp), 5.22 (br, 1H, Cp), 4.96 (br, 1H, Cp), 4.71 (m, 2H, =CH₂), 4.54 (m, 1H, NCHH), 4.29 (m, 2H, =CH₂), 3.79 (s, 3H, NCH₃), 3.63 (m, 1H, NCHH), 2.48 (m, 1H, CpCHH), 2.25 (m, 1H, CpCHH), 0.91 (s, 9H, *t*-Bu). ¹³C NMR (125.7 MHz, C₆D₅Br, -30°C): δ 140.8 (C_{ipso} of Cp), 109.0, 103.3, 101.5, 100.1 (4 CH of Cp), 101.3 (t, J_{C-H} = 165, =CH₂), 84.9 (NCH₃), 64.4 (NCH₂), 30.8 (CH₃ of *t*-Bu), 28.0 (CpCH₂), C_q of *t*-Bu not observed. ⁵¹V NMR (131.4 MHz, C₆D₅Br, -30°C): δ -734 (Δν_½ = 3500).

Generation of [(η⁵,η¹-C₅H₄CH₂CH₂N*i*-Pr)V(η²-ethene)(N*p*-Tol)][MeB(C₆F₅)₃] (**9**)

The same procedure was used as for **7a**, starting from [(η⁵,η¹-C₅H₄CH₂CH₂N*i*-Pr)V(N*p*-Tol)][MeB(C₆F₅)₃]. The exact amount of ethene in solution was determined by ¹H NMR.

¹H NMR (500 MHz, C₆D₅Br, -30°C): δ 6.89 (br, 4H, CH of *p*-Tol), 5.85 (br, 1H, Cp), 5.49 (br, 1H, Cp), 5.31 (overlap with free ethene, CH of *i*-Pr), 5.25 (br, 1H, Cp), 5.12 (m, 1H, Cp), 4.79 (m, 2H, =CH₂), 4.68 (m, 1H, NCHH), 4.22 (m, 2H, =CH₂), 3.50 (m, 1H, NCHH), 2.68 (m, 1H, CpCHH), 2.17 (s, 4H, CH₃ of *p*-Tol and shoulder of CpCHH), 0.99 (d, J_{H-H} = 7, 3H, CH₃ of *i*-Pr), 0.65 (d, J_{H-H} = 7, 3H, CH₃ of *i*-Pr). ¹³C {¹H} NMR (125.7 MHz, C₆D₅Br, -30°C): δ 159.3, 142.0, 141.1 (2 C_q of *p*-Tol and C_{ipso} of Cp), 123.8 (CH of *p*-Tol), 109.7, 109.3, 105.1, 104.4 (4 CH of Cp), 104.9 (=CH₂), 75.2 (NCH₂), 74.1 (CH of *i*-Pr), 29.2 (CpCH₂), 23.0 (CH₃ of *i*-Pr), 22.2 (CH₃ of *p*-Tol), 21.3 (CH₃ of *i*-Pr), 1 CH of *p*-Tol not observed (probably due to overlap with solvent resonances). ⁵¹V NMR (131.4 MHz, C₆D₅Br, -30°C): δ -600 (Δν_½ = 6500).

Generation of [(*t*-BuN)VCp(η²-cyclopentene)(N*i*-Pr₂)][MeB(C₆F₅)₃] (**10**)

The same procedure was used as for **7d**, starting from [(*t*-BuN)VCp(N*i*-Pr₂)][MeB(C₆F₅)₃].

¹H NMR (500 MHz, C₆D₅Br, -30°C): δ 6.43 (br, 1H, =CH), 5.44 (s, 5H, Cp), 4.95 (br, 1H, =CH), 4.41 (sept, J_{H-H} = 6, 1H, CH of *i*-Pr), 3.16 (br, 1H, CH of *i*-Pr), 1.47 (d, J_{H-H} = 6, 3H, CH₃ of *i*-Pr), 0.99 (s, 9H, *t*-Bu), 0.84 (d, J_{H-H} = 7, 3H, CH₃ of *i*-Pr), 0.70 (d, J_{H-H} = 6, 3H, CH₃ of *i*-Pr), 0.54 (d, J_{H-H} = 7, 3H, CH₃ of *i*-Pr), =CH-CH₂ and =CH-CH₂-CH₂ not observed. ¹³C {¹H} NMR (125.7

MHz, C₆D₅Br, -30°C): δ 128.7, 120.3 (2 =CH), 108.5 (Cp), 80.9 (C_q of *t*-Bu), 70.6, 60.4 (2 CH of *i*-Pr), 35.0, 34.8 (2 =CH-CH₂), 33.2 (CH₃ of *i*-Pr), 31.6 (CH₃ of *t*-Bu), 26.9 (CH₃ of *i*-Pr), 23.3 (=CH-CH₂-CH₂), 22.3, 19.4 (2 CH₃ of *i*-Pr). ⁵¹V NMR (131.4 MHz, C₆D₅Br, 25°C): δ -555 ($\Delta\nu_{1/2}$ = 700).

Generation of [(*p*-TolN)VCp(η^2 -cyclopentene)(N*i*-Pr₂)] [MeB(C₆F₅)₃] (13)

The same procedure was used as for **7d**, starting from [(*p*-TolN)VCp(N*i*-Pr₂)] [MeB(C₆F₅)₃].

¹H NMR (500 MHz, C₆D₅Br, -30°C): δ 6.90 (s, CH of *p*-Tol), 6.32 (s, =CH), 5.42 (s, Cp), 4.74 (s, =CH), 4.38 (br, CH of *i*-Pr), 3.22 (br, CH of *i*-Pr), 2.18 (s, CH₃ of *p*-Tol), 1.81 (=CH-CH₂), ~1.6 (overlap with free olefin, CH₃ of *i*-Pr), 1.02 (CH₃ of *i*-Pr), 0.75 (CH₃ of *i*-Pr), 0.57 (CH₃ of *i*-Pr), =CH-CH₂-CH₂ not observed. ¹³C {¹H} NMR (125.7 MHz, C₆D₅Br, -30°C): δ 160.0, 141.4 (2 C_{ipso} of *p*-Tol), 127.7, 125.8 (2 CH of *p*-Tol), 129.9, 115.6 (2 =CH), 109.4 (Cp), 69.2, 61.2 (2 CH of *i*-Pr), 35.0, 26.4 (2 CH₃ of *i*-Pr), 35.0, 33.2 (2 =CH-CH₂), 22.2 (CH₃ of *p*-Tol), 22.1 (=CH-CH₂-CH₂), 20.2, 19.5 (2 CH₃ of *i*-Pr). ⁵¹V NMR (131.4 MHz, C₆D₅Br, 25°C): δ -397 ($\Delta\nu_{1/2}$ = 2500).

Determination of K_{eq}

The K_{eq} was determined from the ¹H NMR spectra of the reaction mixtures at 25°C. The ratio olefin adduct: solvent separated ion pair was determined by integrating well separated resonances of both complexes (mostly resonances of the Cp moiety or of the ethylene bridge). In order to have reliable data, a relaxation time (d1) of 25 seconds was used during the measurement, and an average integral value of several resonances was calculated. When gaseous olefins were used, the amount of olefin in the reaction mixture was calculated from its integral.

The K_{eq} of the formation of **7a** was determined at 25°C from 4 samples with different vanadium and olefin concentrations (values: 89, 94, 105, 108). From this K_{eq} = 100 ± 10 was calculated.

The results of the variable temperature ¹H NMR measurements on the coordination of cyclopentene to **6** (Table 3), were corrected for errors in the temperature by calibration with 100% methanol (temperatures < 0°C) or 100% ethylene glycol (temperatures > 0°C). In order to compensate for the variable density of the solvent at different temperatures, the density of C₆D₅Br was determined in the range of 5 to 39 °C (measuring range of the density meter is 0 to 40 °C) and extrapolated to -10 °C and +70 °C. The equation for the solvent density is: density = 1.57 - 1.41 × 10⁻³ × T (r² = 0.996, density in g/mL, T in °C). When the temperature was decreased (starting at 30°C in steps of -10°C), the solution was kept at the new temperature for 45 minutes before the ¹H NMR measurement was started, so that the equilibrium could stabilize. In the temperature range of 30°C to 80°C (steps of +10°C) a waiting time of 30 minutes was

used. Below -10°C the K_{eq} values did no longer respond to temperature changes, and these results have not been used in the calculations.

Table 3: ¹H NMR measurements on the coordination of cyclopentene to **6**.

Temp (K)	Fraction Adduct	K_{eq}	ΔG^0 (kJ·mol ⁻¹)
260	0.557	29.4	-7.30
269	0.495	22.5	-6.96
280	0.436	17.3	-6.63
290	0.374	13.2	-6.22
300	0.323	10.4	-5.84
309	0.257	7.39	-5.14
319	0.232	6.41	-4.93
328	0.194	5.05	-4.42
338	0.165	4.14	-3.99
347	0.141	3.41	-3.54

Calculation of ΔG^0 , ΔH^0 and ΔS^0

For every value of K_{eq} , the ΔG^0 was calculated using Equation 3 (Table 3). By plotting ΔG^0 vs. T, ΔH^0 and ΔS^0 were calculated using Equation 4. The equation for ΔG^0 is: $\Delta G^0 = 0.0437 \cdot T - 18.8$ ($r^2 = 0.993$, ΔG^0 in kJ·mol⁻¹, T in K). This resulted in values of -19 kJ·mol⁻¹ for ΔH^0 and -0.04 kJ·mol⁻¹·K⁻¹ for ΔS^0 . The error in the calculations was estimated by repeating the calculations using K_{eq} values 10% higher and lower than the observed values. This resulted in errors of ± 1 kJ·mol⁻¹ for ΔH^0 and ± 0.01 kJ·mol⁻¹·K⁻¹ for ΔS^0 .

4.5 References

- (1) Shriver, D.F.; Atkins, P.W.; Langford, C.H., *Inorganic Chemistry*, 2nd edition, Oxford University Press, Oxford, **1994**, 685-686.
- (2) (a) Arlman, E.J.; Cossee, P., *J. Catal.*, **1964**, 3, 99. (B) Cossee, P., *J. Catal.*, **1964**, 3, 80.
- (3) Zirconium alkoxide complex (a) Wu, Z.; Jordan, R.F.; Petersen, J.L., *J. Am. Chem. Soc.*, **1995**, 117, 5867.
Yttrium alkyl complex (b) Casey, C.P.; Hallenbeck, S.L.; Pollock, D.W.; Landis, C.R., *J. Am. Chem. Soc.*, **1995**, 117, 9770. (c) Casey, C.P.; Hallenbeck, S.L.; Wright, J.M.; Landis, C.R., *J. Am. Chem. Soc.*, **1997**, 119, 9680. (d) Casey, C.P.; Fagan, M.A.; Hallenbeck, S.L., *Organometallics*, **1998**, 17, 287.
Other d⁰ metal olefin adducts (e) Temme, B.; Karl, J.; Erker, G., *Chem. Eur. J.*, **1996**, 919. (f) Karl, J.; Erker, G., *Chem. Ber. / Recueil.*, **1997**, 130, 12619. (g) Karl, J.; Dahlmann, M.; Erker, G.; Bergander, K., *J. Am. Chem. Soc.*, **1998**, 120, 5643.
- (4) Kress, J.; Osborn, J.A., *Angew. Chem. Int. Ed. Eng.*, **1992**, 31, 1585.

- (5) Bis-Cp complexes (a) Woo, T.K.; Fan, L.; Ziegler, T., *Organometallics*, **1994**, *13*, 432.
(b) Woo, T.K.; Fan, L.; Ziegler, T., *Organometallics*, **1994**, *13*, 2252.
Constrained geometry complexes: (c) Fan, L.; Harrison, D.; Woo, T.K.; Ziegler, T.,
Organometallics, **1995**, *14*, 2018.
- (6) de With, J.; Horton, A.D., *Organometallics*, **1993**, *12*, 1493.
- (7) The ^{13}C NMR resonance of the $\text{H}_2\text{C}=\text{CHPh}$ carbon of the coordinated styrene in **7e** could not be observed, and we expect it overlaps with resonances of the free styrene and the solvent. This means that it appears 2 - 10 ppm upfield from the corresponding resonance of the free styrene.
- (8) Sandström, J., *Dynamic NMR spectroscopy*; Academic Press, London, **1982**, 96.
- (9) Gillis, D.J.; Tudoret, M.-J.; Baird, M.C., *J. Am. Chem. Soc.*, **1993**, *115*, 2543.
- (10) Since the neutral methyl complexes used for the generation of the adducts **8** and **9** are oils, they could not be purified completely. The small amounts of impurities probably cause the slow observed polymerization of the ethene, which can influence the determination of K_{eq} . No polymer formation was observed after the K_{eq} measurement of **8** and **9**, however, after one night at room temperature the ^1H NMR spectrum shows that all ethene is polymerized. Furthermore, the equilibrium reaction of **6** with ethene stabilizes slowly, which means that leaking of ethene from the reaction mixture by polymerization may influence the determination of K_{eq} .
- (11) All calculations performed using the Gaussian 94 package (Gaussian 94, Revision E.1; Frisch, M.J.; Trucks, G.W.; Schlegel, H.B.; Gill, P.M.W.; Johnson, B.G.; Robb, M.A.; Cheeseman, J.R.; Keith, T.A.; Peterson, G.A.; Montgomery, J.A.; Raghavachari, K.; Al-Lahan, M.A.; Zakrewski, V.G.; Ortiz, J.V.; Foresman, J.B.; Cioslowski, J.; Stefanov, B.B.; Nanayakkara, A.; Challacombe, M.; Peng, C.Y.; Ayala, P.Y.; Chen, W.; Wong, M.W.; Andres, J.L.; Replogle, E.S.; Gomperts, R.; Martin, R.L.; Fox, D.J.; Binkley, J.S.; DeFrees, D.J.; Baker, J.; Stewart, J.P.; Head-Gordon, M.; Gonzalez, C.; Pople, J.A. Gaussian, Inc.: Pittsburgh, PA, 1995) using the B3LYP functional (Becke, A. D., *J. Chem. Phys.* **1993**, *98*, 5648). The small split-valence 3-216 basis (ref. a) was used for C, H and N, and the small core LANL 202 basis (ref. b) was used for V. (a) Binkley, S.; Pople, J.A.; Hehre, W.J., *J. Am. Chem. Soc.*, **1980**, *102*, 939. (b) Hay, P.J.; Wadt, W.R., *J. Chem. Phys.*, **1985**, *82*, 299.
- (12) Margl, P.; Deng, L.; Ziegler, T., *Organometallics*, **1998**, *17*, 933.
- (13) Witte, P.T.; Meetsma, A.; Hessen, B.; Budzelaar, P.H.M., *J. Am. Chem. Soc.*, **1997**, *119*, 10561.
- (14) Klotz, I.M.; Rosenberg, R.M., *Chemical Thermodynamics: basic theory and methods*, 5th edition, Wiley & Sons, New York, **1994**, 162.
- (15) Atkins, P.W., *Physical Chemistry*, 3th edition, Oxford University Press, Oxford, **1986**, 221-222.

- (16) Beck, S.; Prosenc, M-H.; Brintzinger, H.H., *J. Mol. Catal. A. Chem.*, **1998**, *128*, 41.

Chapter 5

Synthesis of di-, tri- and tetravalent vanadium complexes

5.1 Introduction

Since the initial reports of the use of Cp-amido ligands on the group 3 metal scandium,¹ most research has focused on the use of this type of ligand in catalytic olefin polymerization by group 4 metal complexes (Cp-amido)MCl₂.^{2,3} Despite numerous reported ligand variations and their influence on the catalyst performance, studies on the effect of the electronic configuration of the metal center have not been performed. Only in theoretical calculations on the insertion barrier of ethene in the M-Me bond, the cationic d⁰ [(Cp-amido)M(IV)Me]⁺ complex is compared to the neutral d¹ (Cp-amido)M(III)Me complex (M = Ti, Zr, Hf).^{4a} Just before this thesis was completed, a theoretical study was published in which the potential of complexes of the first row metals Ti, V, Cr and Mn with a d-electron count of 1-4 as olefin polymerization catalysts was discussed. Based on the study of elementary steps as ethylene binding, chain propagation, and chain termination, systems with a high oxidation state and a d-electron count up to three (for instance a d¹ vanadium(IV) complex) were considered to have the best catalytic properties.^{4b} The synthesis of d¹ (Cp-amido)VCl₂ complexes makes experimental comparison with the known d⁰ (Cp-amido)TiCl₂ complexes possible.⁵

In this chapter we describe the synthesis of the first Cp-amido vanadium(IV) di-chloro complex and initial results on its performance as an ethene polymerization catalyst precursor. This is compared to the performance of the isostructural d⁰ titanium analogue.

Since attempts to introduce the Cp-amido ligand directly on a vanadium(IV) precursor failed, the ligand was introduced on vanadium(III). After

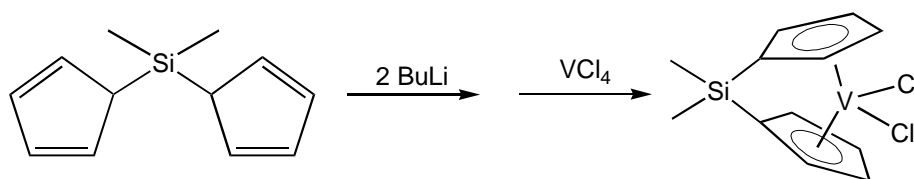
a one-electron reduction a Cp-amido vanadium(II) complex was obtained, which could be oxidized by PhICl_2 to the desired Cp-amido vanadium(IV) dichloride.

5.2 Results and discussion

5.2.1 Attempted ligand introduction on vanadium(IV) precursors

Introduction of a Cp-amido ligand on a group 4 metal center is generally performed by either salt metathesis, HCl elimination or amine elimination (see Chapter 2), starting from metal(IV) chloro or amido complexes. However, these three methods proved unsuccessful in the synthesis of Cp-amido vanadium(IV) complexes.

Salt metathesis: The *ansa*-vanadocene dichloride $\{\text{Me}_2\text{Si}(\text{C}_5\text{H}_4)_2\}\text{VCl}_2$ was synthesized in a salt metathesis reaction of the di-lithium salt of the ligand with VCl_4 in a very low yield (7%, Scheme 1).⁶ We attempted the synthesis of $(\text{C}_5\text{H}_4\text{CH}_2\text{CH}_2\text{N}i\text{-Pr})\text{VCl}_2$ in a similar way, by addition of a THF solution of the di-lithium salt of the Cp-amido ligand, $[\text{C}_5\text{H}_4\text{CH}_2\text{CH}_2\text{N}i\text{-Pr}]\text{Li}_2$ (see Chapter 2), to a pentane solution of VCl_4 at 0°C . This led to the immediate formation of a dark precipitate which was insoluble in pentane, toluene and THF, and which could not be characterized.

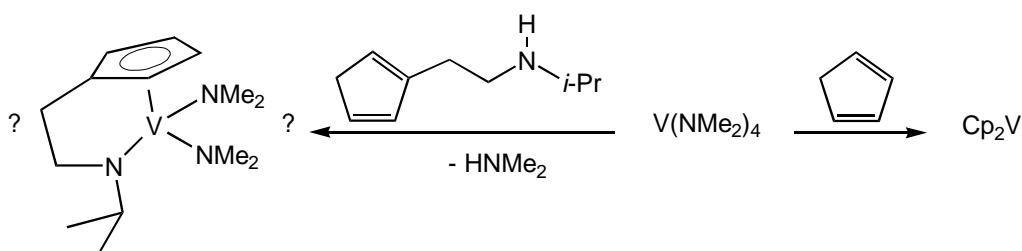


Scheme 1

HCl elimination: Introduction of the Cp-amido ligand on titanium(IV) by HCl elimination has been performed by reacting the neutral ligand precursor with TiCl_4 in the presence of a base (NEt_3).^{5a} However, VCl_4 is known to react

with tertiary amines; the reduced vanadium complex $\text{VCl}_3(\text{NMe}_3)$ is one of the complexes that has been isolated from the reaction of NMe_3 with VCl_4 .⁷ For this reason, the HCl elimination route was not attempted.

Amine elimination: The Cp-amido ligand can be introduced on vanadium(V) by amine elimination (Chapter 2, section 2.2.2). For introducing the ligand on vanadium(IV) we studied the reaction of the ligand precursor $\text{C}_5\text{H}_5\text{CH}_2\text{CH}_2\text{N}(\text{H})i\text{-Pr}$ with $\text{V}(\text{NMe}_2)_4$ (in C_6D_6), which could generate $(\text{C}_5\text{H}_4\text{CH}_2\text{CH}_2\text{N}i\text{-Pr})\text{V}(\text{NMe}_2)_2$ by amine elimination. After heating the reaction mixture for half an hour at 80°C in an NMR tube, resonances for the (diamagnetic) ligand precursor had disappeared and resonances for HNMe_2 had appeared; the color of the solution had changed from green to red. When the reaction of $\text{C}_5\text{H}_5\text{CH}_2\text{CH}_2\text{N}(\text{H})i\text{-Pr}$ with $\text{V}(\text{NMe}_2)_4$ was performed on preparative scale, a red paramagnetic oil was obtained and no products could be crystallized. Addition of Me_3SiCl to convert the supposedly generated di-amido complex to the di-chloro complex⁸ also did not yield crystalline products. The vanadium amido complex $\text{V}(\text{NMe}_2)_4$ has been used before in an amine elimination reaction. However, in the reaction with C_5H_6 (CpH) reduction occurs and the vanadium(II) complex Cp_2V was isolated (Scheme 2).⁹



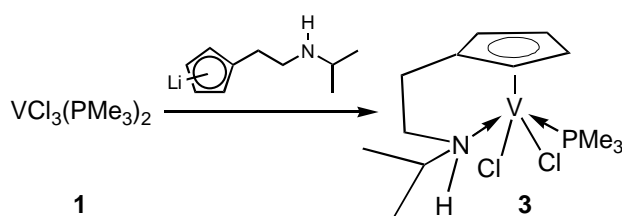
Scheme 2

5.2.2 Synthesis of vanadium(III) Cp-amido complexes

An alternative route for the synthesis of (Cp-amido)M(IV) complexes is ligand introduction on a M(III) precursor, and subsequent oxidation to the desired M(IV) dichloride. This route is used for the synthesis of $(\text{C}_5\text{Me}_4\text{SiMe}_2\text{N}t\text{-Bu})\text{M}(\text{Cl})_2$

Bu)TiCl₂, where the magnesium salt of the ligand [C₅Me₄SiMe₂N*t*-Bu]Mg₂Cl₂ is reacted with TiCl₃(THF)₃, and the Ti(III) intermediate oxidized *in situ* with PbCl₂ to the Cp-amido titanium(IV) dichloride.¹⁰ In order to investigate if such a route is possible for vanadium, we synthesized a Cp-amido vanadium(III) complex. However, attempts to synthesize this complex directly from VCl₃(PMe₃)₂ by reaction with the di-lithium salt [C₅H₄CH₂CH₂N(H)*i*-Pr]Li₂ failed. Therefore a step-wise introduction of the Cp-amido ligand was performed, starting with the attachment of the Cp moiety to the vanadium center.

Introduction of a single unsubstituted cyclopentadienyl ligand on vanadium(III) is possible by reaction of CpNa with VCl₃(PMe₃)₂ (**1**), yielding the purple paramagnetic complex CpVCl₂(PMe₃)₂ (**2**).¹¹ From the reaction of the mono-lithium salt [C₅H₄CH₂CH₂N(H)*i*-Pr]Li with **1** the Cp-amine complex (η⁵,η¹-C₅H₄CH₂CH₂N(H)*i*-Pr)VCl₂(PMe₃) (**3**) was isolated as a purple paramagnetic complex in a reasonable yield (59%, Scheme 3). The complex is well soluble in THF, but only sparingly in toluene; in both solvents slow decomposition is observed at room temperature. Single crystals were obtained by diffusion of pentane vapor into a THF solution of the complex. The crystal structure of complex **3** (Figure 1, Table 1) shows that the amine functionality of the ligand is coordinating to the vanadium center, which implies that the chelating effect of the amine functionality is strong enough to drive out one of the PMe₃ ligands. Even when the synthesis was performed in the presence of an excess of PMe₃ (5 equivalents), **3** was isolated and no evidence was found for the formation of a complex where the amine functionality is not coordinating.



Scheme 3

The Cp-amine complex **3** is essentially isostructural to the Cp complex **2**.¹¹ Both complexes have a four-legged piano stool conformation with the chlorine ligands in a trans configuration; in **3** the amine has replaced one of the phosphine ligands of **2**. This last feature has no significant effect on the V-Cl bond lengths (**2**: 2.401(1) and 2.405(1) Å), or on the V-Cg bond length (**2**: 1.973 Å; Cg = centroid of the Cp ring). Also the angles Cl(1)-V-Cl(2) (**2**: 126.1(0)°) and Cl-V-Cg (**2**: 116.0 and 117.9°) are very similar for both complexes. The coordinating amine in **3** has no effect on the V-P bond length (**2**: 2.507(1) and 2.510(1) Å), but the P-V-N angle in **3** is significantly larger than the P-V-P angle in **2** (**2**: 132.6(0)°). The V-N bond length in **3** (2.290(2) Å) is similar to that of other vanadium(III) amine complexes (average: 2.24 Å).¹²

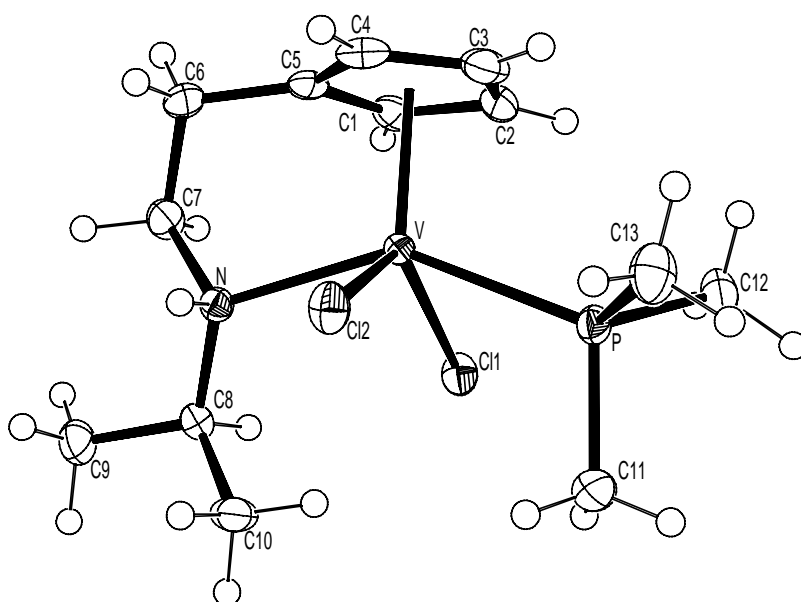


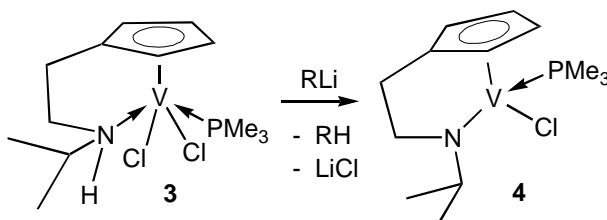
Figure 1: Crystal structure of **3**.

Table 1: Selected bond distances and angles in **3**.

V-N	2.290(2)	Cg-V-N	106.33(6)
V-Cl(1)	2.3904(8)	Cg-V-Cl(1)	116.35(3)
V-Cl(2)	2.4134(9)	Cg-V-Cl(2)	118.04(3)
V-P	2.5140(8)	Cg-V-P	111.13(3)
V-Cg	1.9662(13)	P-V-N	142.45(6)
H...Cl	2.82(3)	Cl(1)-V-Cl(2)	125.53(3)
		Cl(1)-V-P	79.08(3)
		Cl(2)-V-P	79.17(3)
		Cl(1)-V-N	86.87(6)

In the solid state **3** is associated to form a dimer, by hydrogen bridging of the N-H with a chloride ligand of a neighboring molecule (2.82(3) Å). This is probably the reason why the N-H vibration is not observed in the IR spectrum (solid **3** in nujol mull), and it can also explain the low solubility of **3** compared to **2**.

The Cp-amine rhenium complex (C₅H₄CH₂CH₂N(H)Me)Re(CO)₂, which is described in literature,^{3c} can be converted to a Cp-amido rhenium complex by deprotonation with butyl lithium, yielding [(C₅H₄CH₂CH₂NMe)Re(CO)₂]Li and generating butane. In a comparable reaction, the Cp-amine complex **3** is converted into a Cp-amido complex by reaction with an alkyl lithium reagent, generating the alkane and lithium chloride (Scheme 4).



Scheme 4

When the purple complex **3** was treated with one equivalent of Me₃SiCH₂Li, a color change to green was observed. When MeLi was used, gas evolution (probably methane) was observed together with this color change. The product of this reaction, the Cp-amido vanadium(III) complex (η^5, η^1 -C₅H₄CH₂CH₂N \dot{i} Pr)VCl(PMe₃) (**4**, Scheme 4), is paramagnetic and was identified by its crystal structure.

The structure of **4** (Figure 2, Table 2) shows slightly shorter V-Cl (2.3597(6) Å) and V-P (2.4791(6) Å) bond lengths compared to **3**, as can be expected for a complex with a lower coordination number. The V-Cg (1.9537(10) Å) distance is similar to that of **3**. As expected, the V-N(amido) bond in **4** (1.8728(17) Å) is much shorter than the V-N(amine) bond in **3**

(2.290(2) Å), caused by strong π -donation of the nitrogen atom; the V-N(amido) bond in **4** is one of the shortest found for vanadium(III) (1.83 - 1.96 Å).^{12b,13} The Cp-V-N bite angle of the Cp-amido ligand in **4** (114.07(6)°) is larger than that of the Cp-amine ligand in **3** (106.33(6)°).

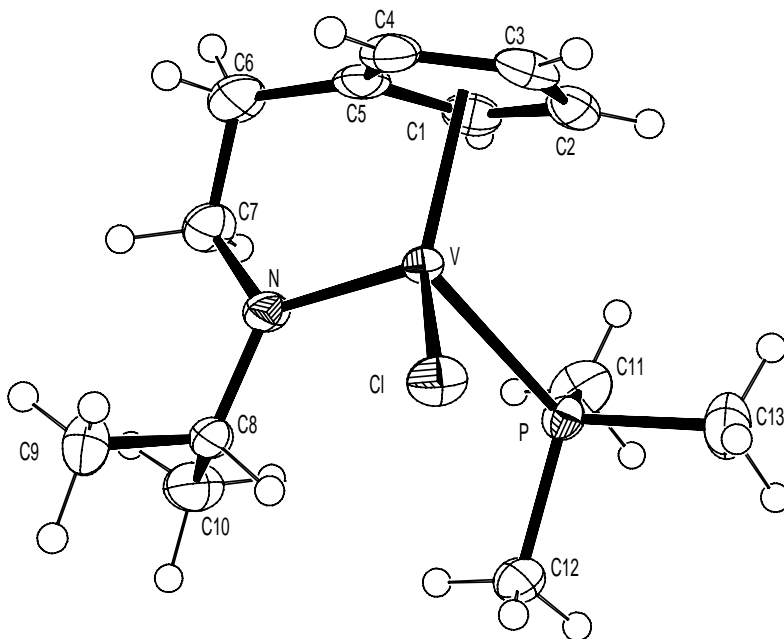


Figure 2: Crystal structure of **4**.

Table 2: Selected bond distances and angles in **4**.

V-N	1.8728(17)	Cg-V-N	114.07(6)
V-Cl	2.3597(6)	Cg-V-P	116.71(2)
V-P	2.4791(6)	Cg-V-Cl	124.54(2)
V-Cg	1.9537(10)	N-V-Cl	103.86(6)
		N-V-P	102.63(6)
		Cl-V-P	90.99(2)

5.2.3 Attempted oxidation of **4** to a Cp-amido vanadium(IV) complex

The reagent used in titanium chemistry for the oxidation of a Ti(III) complex to the desired Ti(IV) dichloride, PbCl_2 , is not suitable to oxidize the Cp-amido vanadium(III) complex **4** to a vanadium(IV) di-chloro species. Although PbCl_2 has been used in vanadium chemistry to oxidize vanadium(II) complexes to vanadium(III), subsequent oxidation to vanadium(IV) did not occur.¹⁴ Two

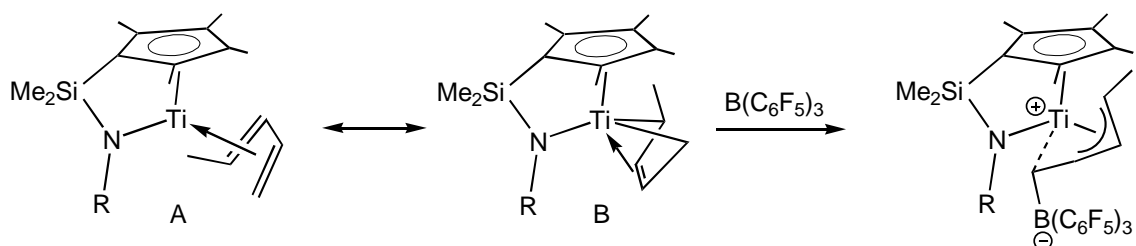
reported methods to oxidize vanadium(III) complexes to vanadium(IV) chlorides are reaction with one equivalent CuCl ¹⁵ or PCl_3 .¹⁶ We attempted both methods for the oxidation of **4** to the (Cp-amido) VCl_2 , but without success. Although both reagents react with **4**, as was seen by the formation of metallic copper in the reaction of **4** with CuCl and the change of the color of the solution from green to brown in both reactions, no Cp-amido vanadium complexes could be isolated from the reaction mixtures. It is possible that the PMe_3 ligand interferes with the oxidation of the vanadium center, since the phosphine ligand itself can also be oxidized. Therefore we attempted the synthesis of Cp-amido vanadium(III) complexes without a coordinated phosphine ligand.

Neither the reaction of $\text{VCl}_3(\text{THF})_3$ with the di-lithium salt $[\text{C}_5\text{H}_4\text{CH}_2\text{CH}_2\text{N}(\text{H})i\text{-Pr}]_2\text{Li}_2$, or a step-wise ligand introduction yielded a Cp-amido vanadium(III) complex. This is not surprising, since reaction of CpNa with $\text{VCl}_3(\text{THF})_3$ also failed to yield well-defined mono-Cp complexes.¹¹

A phosphine-free vanadium(III) Cp-amido complex was obtained when the phosphine complex **4** was reacted with an allyl-Grignard (THF, -30°C). The IR spectrum of the brown-red crystals (obtained after extraction with pentane at 0°C , and crystallization at -60°C), probably $(\eta^5, \eta^1\text{-C}_5\text{H}_4\text{CH}_2\text{CH}_2\text{N}i\text{-Pr})\text{V}(\eta^3\text{-C}_3\text{H}_5)$, clearly shows a vibration for an η^3 -allyl group (1501 cm^{-1}) while the phosphine ligand is no longer observed. However, since the allyl complex is extremely soluble and possibly thermally labile, it could not be obtained analytically pure.

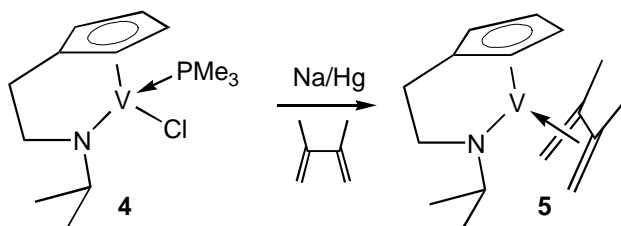
5.2.4 Synthesis of a vanadium(II) Cp-amido complex

In Chapter 3 (sections 3.2.1 and 3.2.3) the generation of cationic complexes by methyl abstraction with the Lewis acid $\text{B}(\text{C}_6\text{F}_5)_3$ is described. This cocatalyst has also been used in the group 4 chemistry to convert M(II) diene adducts into M(IV) cationic complexes. The Cp-amido titanium(II) diene adduct $(\text{C}_5\text{Me}_4\text{SiMe}_2\text{N}t\text{-Bu})\text{Ti}(1,3\text{-pentadiene})$ reacts with $\text{B}(\text{C}_6\text{F}_5)_3$ to generate a cationic titanium(IV) allyl complex, which is an active olefin polymerization catalyst (Scheme 5).¹⁷


Scheme 5

Since oxidation of the Cp-amido vanadium(III) complex **4** to a Cp-amido vanadium(IV) complex was not successful, we synthesized a Cp-amido vanadium(II) diene adduct, which could act as a precursor for a Cp-amido vanadium(IV) olefin polymerization catalyst. Furthermore, this method yields a phosphine free Cp-amido vanadium complex, thus opening the possibility for selective oxidation of the vanadium center to the desired vanadium(IV) dichloride.

One-electron reduction of the vanadium(III) complex **4** with sodium amalgam in the presence of 2,3-dimethyl-butadiene (Scheme 6) led to the formation of a dark green complex, which could be crystallized from pentane.¹⁸ The IR spectrum of this paramagnetic complex reveals the absence of a phosphine ligand.


Scheme 6

Despite conformational disorder in the ethylene bridge around a crystallographic mirror plane, crystal structure determination showed that this complex is the vanadium(II) diene adduct $(\eta^5, \eta^1\text{-C}_5\text{H}_4\text{CH}_2\text{CH}_2\text{N}i\text{-Pr})\text{V}(\eta^4\text{-C}_6\text{H}_{10})$

(**5**, Figure 3, Table 3). The diene ligand in **5** coordinates in a prone fashion, with C(8)-C(9) only 0.015 Å longer than C(9)-C(19) and V-C(9) 0.054 Å longer than V-C(8). This is in agreement with the Cp-amido titanium diene complexes (C₅Me₄SiMe₂NR)Ti(diene) (R = *t*-Bu, Ph, Scheme 5),^{17b} where the prone isomer (A) has mainly a Ti(II) diene character and the supine isomer (B) mainly a Ti(IV) metallacyclopentene character.

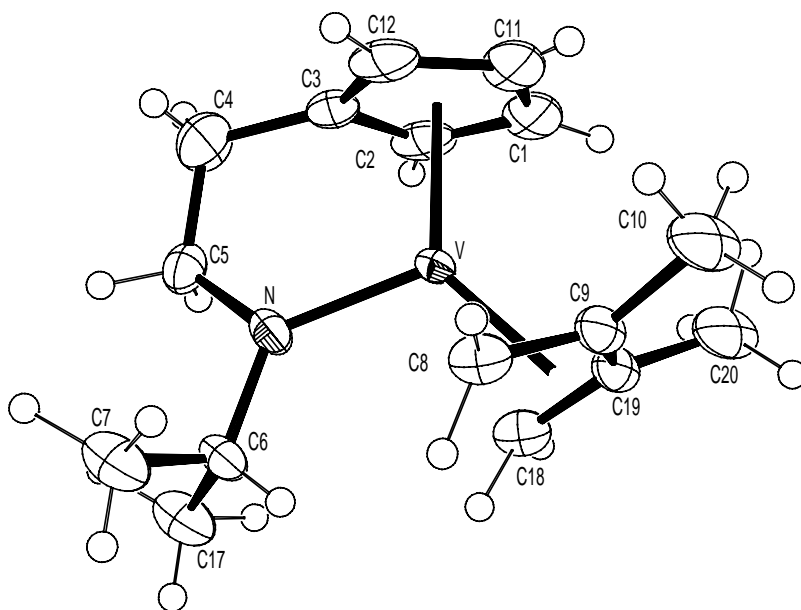


Figure 3: Crystal structure of **5**.

Table 3: Selected bond distances and angles in **5**.

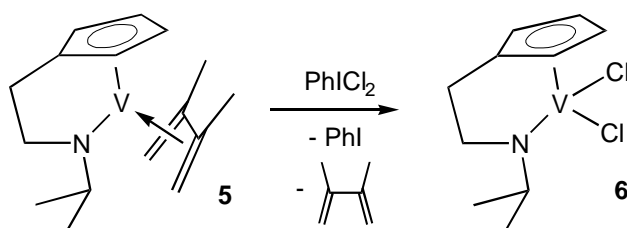
V-N	1.924(4)	Cg-V-N	110.17(6)
V-C(8)	2.192(4)	Cg-V-C(8)	133.66(11)
V-C(9)	2.246(3)	Cg-V-C(9)	117.55(10)
V-Cg	1.952(2)	N-V-C(8)	94.44(14)
C(8)-C(9)	1.412(5)	N-V-C(9)	128.30(14)
C(9)-C(19)	1.397(5)		

The vanadium(II) diene adduct **5** reacted with B(C₆F₅)₃ in pentane to form an unstable microcrystalline complex. The poor solubility of the product suggests that a zwitterionic complex vanadium(IV) allyl complex may have been formed, however, attempts to redissolve this complex in toluene only led to decomposition. The reaction of **5** with B(C₆F₅)₃ in toluene under ethene

pressure did not lead to ethene polymerization. It is possible that the expected vanadium(IV) allyl species that is generated in this reaction is too unstable (probably because of the strong oxidizing power of vanadium(IV) in combination with the stability of allyl radicals) and decomposes even in the presence of ethene. In general, vanadium(IV) allyl complexes are much less stable than their group 4 analogues, and none have been reported so far.

5.2.5 Synthesis of a vanadium(IV) Cp-amido complex

Oxidation of vanadium(II) complexes to vanadium(III) species has been reported for a variety of reagents,^{14,19} however, a possible subsequent oxidation to vanadium(IV) seems to be dependent on the ligand system. For example, decamethyl-vanadocene (Cp^*_2V) can be oxidized to the vanadium(IV) complex Cp^*_2Vl_2 using one equivalent of I_2 , whereas oxidation of vanadocene (Cp_2V) with I_2 does not go beyond the vanadium(III) complex Cp_2Vl , even with an excess of I_2 .¹⁹ The vanadium(I) complex $\text{Cp}^*\text{V}(\text{CO})_4$ can be oxidized by Cl_2 to the vanadium(IV) complex Cp^*VCl_3 .²⁰ For the synthesis of a Cp-amido vanadium(IV) dichloride from the Cp-amido vanadium(II) complex **5**, Cl_2 should be a suitable oxidizing reagent; to facilitate the addition of the correct stoichiometry, we used the crystalline PhlCl_2 as a source of Cl_2 .²¹



Scheme 7

The oxidation of **5** by PhlCl_2 is exothermic, and in order to control the reaction temperature the solvent (THF) was condensed onto a mixture of solid **5** and PhlCl_2 (liquid nitrogen temperature). After melting of the THF, the green

color of the solution changed to brown in a few seconds. In the reaction the diene and PhI are liberated (Scheme 7), as indicated by GC/MS analysis. Crystallization of the organometallic product from toluene²² yielded dark crystals of (η^5, η^1 -C₅H₄CH₂CH₂N*i*-Pr)VCl₂ (**6**) in a 57% yield.

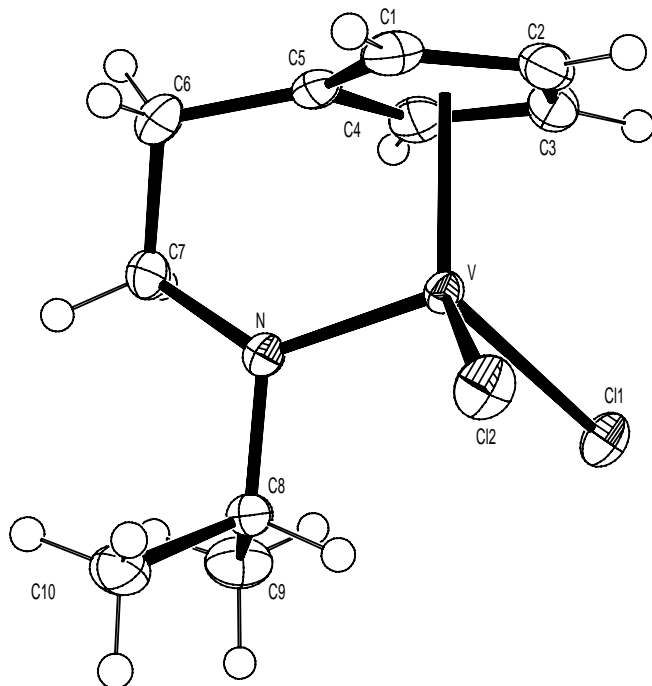


Figure 4: Crystal structure of **6**.

Table 4: Selected bond distances and angles in **6** (M = V) and **7** (M = Ti).⁵

	6	7		6	7
M-N	1.8308(13)	1.864(2)	Cg-M-N	105.11(4)	104.4(1)
M-Cl(1)	2.2879(5)	2.2752(11)	Cg-M-Cl(1)	119.90(2)	118.3(1)
M-Cl(2)	2.2958(4)	2.2996(12)	Cg-M-Cl(2)	122.09(2)	118.5(1)
M-Cg	1.9336(8)	2.008(4)	Cl(1)-M-Cl(2)	95.61(2)	103.01(2)
			N-M-Cl(1)	107.45(4)	104.98(8)
			N-M-Cl(2)	105.33(4)	106.53(7)

When the structure of the vanadium(IV) di-chloride **6** (Figure 4, Table 4) is compared to that of its d⁰ titanium analogue (η^5, η^1 -C₅H₄CH₂CH₂N*i*-Pr)TiCl₂ (**7**),⁵ the observed differences are small. The M-Cg and M-N distances are smaller for **6**, which can be explained by the smaller ionic radius of the V⁴⁺ ion. In contrast, the M-Cl distances are slightly longer for **6** (average 2.292 Å for **6**,

2.287 Å for **7**); the Cl(1)-M-Cl(2) angle in **6** ($95.61(2)^\circ$) is significantly smaller than in **7** ($103.01(2)^\circ$). These features are also observed when the crystal structures of the isostructural vanadium and titanium di-chloro complexes $(\text{MeCp})_2\text{VCl}_2$ (**8**) and $(\text{MeCp})_2\text{TiCl}_2$ (**9**) are compared.²³ EPR studies reveal that the extra electron in the d^1 complex **8** occupies an orbital in plane with the two chlorides and the metal, but perpendicular to the plane of the two Cp-centroids and the metal. The d^1 electron forces the two chlorides closer together, resulting in a more acute Cl-V-Cl angle. In order to minimize steric hindrance the V-Cl bonds are elongated. Since the structural features of the Cp-amido complexes **6** and **7** are comparable to those of the bis-Cp complexes **8** and **9**, we assume that the d^1 electron in **6** occupies an orbital with a similar orientation as described for **8** (Figure 5).

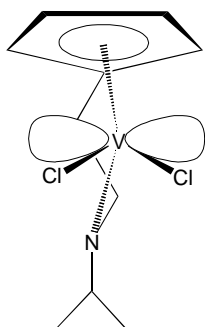


Figure 5: Orbital accomodating the d^1 electron in **8**.

5.2.6 Ethene polymerization by Cp-amido vanadium complexes

The synthesis of the Cp-amido vanadium(IV) di-chloro complex **6**, makes it possible to compare isostructural d^0 and d^1 metal complexes $(\text{Cp-amido})\text{MCl}_2$ ($\text{M} = \text{Ti}, \text{V}$) as catalyst precursors for olefin polymerization. The Cp-amido titanium(IV) di-chloro complex $(\eta^5, \eta^1\text{-C}_5\text{H}_4\text{CH}_2\text{CH}_2\text{N}i\text{-Pr})\text{TiCl}_2$ (**7**) is active in the catalytic polymerization of ethene, after activation with MAO. In order to minimize deactivation of the catalyst by reduction, the complex was injected into the autoclave after this was charged with the MAO and put under ethene

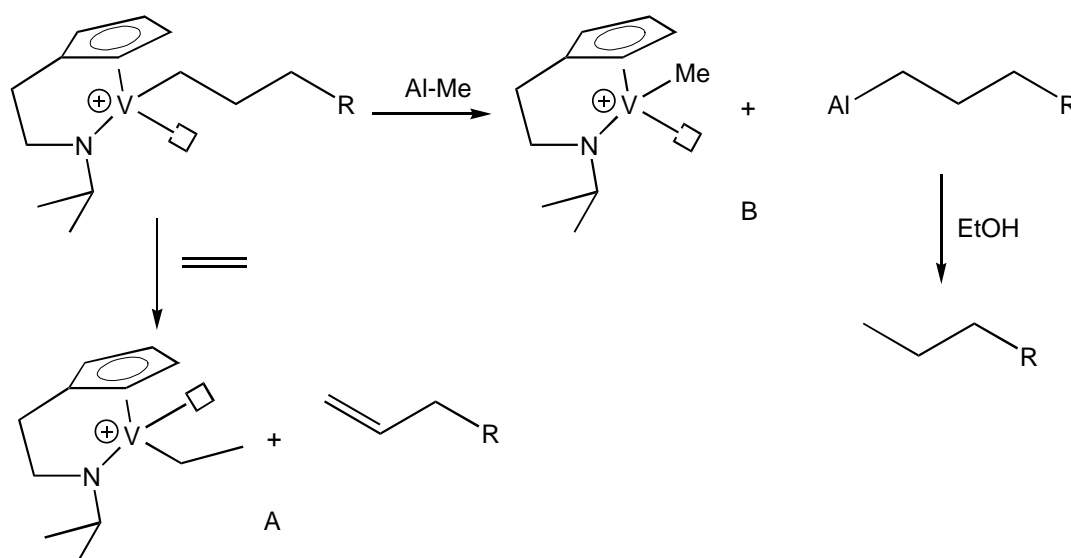
pressure.^{5b} The Cp-amido vanadium(IV) complex **6** was tested under identical conditions for comparison (Table 5).

Table 5: Ethene polymerization data for **6** and **7**.

complex	yield (g)	activity (kg·mol ⁻¹ ·h ⁻¹ ·bar ⁻¹)	M _w (g·mol ⁻¹)	M _n (g·mol ⁻¹)	M _w /M _n	melting point (°C)
6	4.7	209	14900	4900	3.0	129
7	12.0	534	139000	59500	2.3	134

15 μmol catalyst, 500 eq. MAO, 3 bar ethene, 50°C, 250 mL toluene, 30 minutes.

These first results show that the vanadium complex **6** is active in ethene polymerization after activation with MAO, although the activity is somewhat lower than that of the isostructural titanium complex **7**, and molecular weight of the produced polymer is much lower. Both catalysts are still active when the reaction is quenched after 30 minutes.



Scheme 8

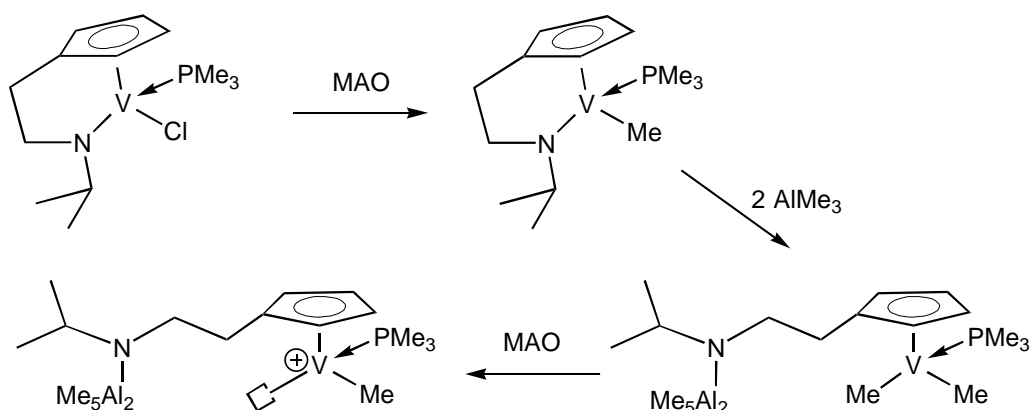
The short chain length of the polymers produced by the vanadium based catalyst allows for end group determination by ¹H NMR. The polymer has mainly vinylic end groups, indicative of termination by β-H transfer to monomer

(Scheme 8, route A). Integration of saturated and unsaturated end groups shows that about 13% of the polymer chains are fully saturated, indicative for termination by chain transfer to aluminum (Scheme 8, route B).²⁴

It is tempting to assume that the above described differences between the titanium and vanadium based catalyst are due to the effect of the extra d-electron in the [(Cp-amido)VR]⁺ cationic species, which is presumed to be the active species in the polymerization. However, from ethene polymerization experiments with Cp-amido vanadium(III) complexes activated by MAO it appears that the Cp-amido ligand is not inert towards the MAO cocatalyst.

When we tested the Cp-amido vanadium(III) complex **4** as catalyst precursor under identical conditions as used for **6** and **7**, this complex proved active in the ethene polymerization, producing polymer with remarkably similar properties as those of the polymer produced by **6**/MAO (**4**/MAO M_w : 15100; M_n : 7970; M_w/M_n : 1.9, activity of **4**/MAO is in the same range as that of **6**/MAO, but since the runs were performed with a different batch of MAO activities can not be compared). Activation of the di-chloro complexes **6** and **7** is presumed to proceed by methylation and subsequent methyl abstraction to generate the cationic [(Cp-amido)MMe]⁺ species (see Chapter 1, Scheme 1). However, when these two steps take place with the mono-chloro vanadium(III) complex **4**, the cationic [(Cp-amido)V(PMe₃)]⁺ species is generated, which will be inactive as a catalyst since it lacks a metal-alkyl bond.

A possible activation pathway is shown in Scheme 9: AlMe₃, which is always present in MAO,²⁵ is known to react with metal-amido bonds to generate metal-methyl species;²⁶ subsequent methyl abstraction could now generate a cationic vanadium(III) methyl species.



Scheme 9

5.3 Conclusions

Vanadium(IV) Cp-amido complexes are not directly available from vanadium(IV) precursors. Instead, ligand introduction on vanadium(III) is performed, followed by one electron reduction and subsequent two electron oxidation. This route not only gives entry to vanadium(IV) Cp-amido complexes, but also opens the field of vanadium(III) and (II) chemistry.

The Cp-amido vanadium(IV) complex catalyzes the polymerization of ethene after activation with MAO, although the activity is lower than that of the isostructural titanium based catalyst. The much lower molecular weight of the polymer formed by the vanadium based catalyst compared to the titanium based catalyst, is a result of faster β -H elimination by the vanadium based catalysts. Chain transfer to aluminum is a minor termination pathway. However, polymerization experiments with a Cp-amido vanadium(III) complex yield polymer with very similar properties as the polymer produced with the vanadium(IV) based catalyst. It is therefore unclear what the actual active species is in these polymerizations. More experiments on these systems, preferably polymerization reactions by well-defined cationic vanadium(IV) species, for instance $[(\text{Cp-amido})\text{VMe}][\text{MeB}(\text{C}_6\text{F}_5)_3]$, are necessary.

5.4 Experimental

General considerations

All experiments were performed under nitrogen atmosphere using standard glove-box, Schlenk, and vacuum line techniques. Deuterated solvents (Aldrich) were either dried over Na/K alloy and vacuum transferred before use (C_6D_6 , THF- d_6) or degassed, flushed with nitrogen and stored over mol. sieves ($C_2D_2Cl_4$). Toluene, THF, diethyl ether and pentane were distilled from Na or Na/K alloy before use. The following were prepared according to literature procedures: $C_5H_5(CH_2)_2NH*i*-Pr$,²⁷ (η^5, η^1 - $C_5H_4(CH_2)_2N*i*-Pr$) $TiCl_2$ (**7**),^{5a} $PhCl_2$,²¹ PMe_3 using $MeMgI$ instead of $MeMgBr$,²⁸ $VCl_3(THF)_3$,²⁹ $MeLi$ /diethyl ether (Aldrich) was used as purchased, 2,3-dimethyl-1,3-butadiene (Aldrich) was degassed, dried over $MgSO_4$ and distilled before use. Ethene (AGA 99.5%) was passed over a supported copper scavenger (BASF R 3-11) and mol. sieves (3\AA) before being passed to the reactor. NMR spectra were run on a Varian Unity-500 spectrometer. IR spectra were recorded from nujol mulls between KBr discs on a Mattson Galaxy 4020 FT-IR spectrophotometer. GC analyses were performed on a HP 6890 instrument equipped with a HP-1 dimethylpolysiloxane column (19095 Z-123). GC/MS spectra were recorded at 70 eV using a HP 5973 mass-selective detector attached to a HP 6890 GC as described above. DSC was performed on a Perkin-Elmer DSC 7 calorimeter; melting points were determined from the second heating run. Elemental analyses were performed by the Microanalytical Department of the University of Groningen. Every value is the average of at least two independent determinations. GPC measurements were carried out at the University of Groningen by high temperature GPC ($150^\circ C$), using 1,2,4-trichlorobenzene as solvent and narrow MWD polystyrene standard samples as references. The measurements were performed on a LC-1000 system (Spectra Physics) equipped with 2 PL-Gel mixed-C columns, RALLS light scattering detector, H502 viscometer (Viscotek), refractive index detector and DM400 data manager (Viscotek).

Synthesis of (η^5, η^1 - $C_5H_4CH_2CH_2N(H)*i*-Pr$) $VCl_2(PMe_3)$ (**3**)

To a suspension of 0.61 g $VCl_3(THF)_3$ (1.6 mmol) in 25 mL of THF, 0.4 mL of PMe_3 (3.8 mmol) was added. The resulting brown solution was stirred for an hour at ambient temperature, and then cooled to $-80^\circ C$. A solution of 0.15 g Me_3SiCH_2Li (1.6 mmol) in 5 mL THF was slowly added by syringe to a solution of 0.25 g $C_5H_5CH_2CH_2N(H)*i*-Pr$ (1.6 mmol) in 3 mL of THF (cooled in an ice bath) and subsequently stirred for 30 min. The solution containing the lithiated ligand was added drop wise to the cold VCl_3 -solution, after which the mixture was allowed to warm up. At $-40^\circ C$ the color of the solution changed from brown to purple. The solution was brought to room temperature and stirred overnight. The volatiles were removed *in vacuo*, and the resulting purple solid was stripped of residual THF by stirring with 20 mL of pentane which was subsequently pumped off. After extraction with warm toluene, the solvent was removed from the extract *in vacuo* and the resulting solid was redissolved in 15 mL of THF. Crystallization was achieved by slow diffusion of pentane vapor into the solution. Yield: 0.33 g (0.94 mmol, 59%) of purple crystalline **3**. These crystals were suitable for X-ray structure determination.

$^1\text{H NMR}$ (500 MHz, THF- d_8 , 25°C): δ 6.5 ($\Delta\nu_{1/2} = 820$ Hz, 6H, CH_3 of *i*-Pr), 4.0 (br, overlaps solvent), -17.8 ($\Delta\nu_{1/2} = 2150$ Hz, 9H, PMe_3). *IR*: 635 (w), 669 (m, PMe_3), 735 (s, PMe_3), 816 (s), 849 (w), 866 (w), 880 (m), 945 (s, PMe_3), 990 (s), 1040 (s), 1051 (s), 1119 (m), 1140 (m), 1157 (m), 1221 (m), 1256 (m), 1275 (m, PMe_3), 1298 (m, PMe_3), 1319 (w), 1341 (w), 1360 (sh), 1422 (m, PMe_3), 3082 (w), 3214 (m) cm^{-1} . *Anal. calcd for* $\text{C}_{13}\text{H}_{25}\text{VNPCl}_2$: C, 44.85; H, 7.24; N, 4.06; V, 14.63; Cl, 20.37. Found: C, 44.77; H, 7.30; N, 4.04; V, 14.55; Cl, 20.50.

Synthesis of (η^5, η^1 - $\text{C}_5\text{H}_4\text{CH}_2\text{CH}_2\text{N}i\text{-Pr}$) $\text{VCl}(\text{PMe}_3)$ (**4**)

From 3: To a solution of 0.71 g of **3** (2.0 mmol) in 15 mL THF, at 0°C, a cooled solution of 0.19 g $\text{Me}_3\text{SiCH}_2\text{Li}$ (2.0 mmol) in 5 mL THF was added drop wise. The color of the solution immediately changed from purple to green. After stirring for one more hour at room temperature, the volatiles were removed *in vacuo* and the green oil was stripped of residual THF by twice stirring with 10 mL pentane which was subsequently pumped off. The resulting green solid was extracted with a mixture of 2 mL pentane and 10 mL ether. Cooling this solution to -25 °C yielded 0.36 g (1.2 mmol, 58%) green crystalline **4** in two crops.

From $\text{VCl}_3(\text{THF})_3$: To a solution of 0.75 g $\text{VCl}_3(\text{THF})_3$ (2.0 mmol) in 30 mL THF, 0.45 mL of PMe_3 (4.3 mmol) was added. The solution was stirred for an hour after which it was cooled to -50 °C. A solution of 0.19 g $\text{Me}_3\text{SiCH}_2\text{Li}$ (2.0 mmol) in 5 mL THF was slowly added to an solution of 0.32 g $\text{C}_5\text{H}_5\text{CH}_2\text{CH}_2\text{N}(\text{H})i\text{-Pr}$ (2.0 mmol) in 5 mL THF, cooled in an ice bath, and stirred for half an hour. This solution was slowly added to the VCl_3 -solution at -50°C, and the color of the solution changed from brown to purple in a minute. The solution was brought to room temperature, and stirred overnight. The mixture was then cooled to 0°C and a cold solution of 0.19 g $\text{Me}_3\text{SiCH}_2\text{Li}$ (2.0 mmol) in 5 mL THF was slowly added. The color of the solution changed from purple to green. The solution was brought to room temperature and stirred for an additional hour. The volatiles were then removed *in vacuo* and the green solid was stripped of residual THF by stirring with 15 mL of pentane which was subsequently pumped off. The solid was extracted with a mixture of 5 mL pentane and 5 mL ether and cooled to -70 °C, from which **4** was obtained as green crystals in two crops, yielding 0.18 g (0.62 mmol, 31%). Recrystallization by slow cooling of a pentane/ether solution of **4** produced crystals suitable for an X-ray structure determination.

$^1\text{H NMR}$ (500 MHz, C_6D_6 , 25°C): δ 14.0 ($\Delta\nu_{1/2} = 240$ Hz, 3H, *i*-Pr Me), 7.6 ($\Delta\nu_{1/2} = 210$ Hz, 3H, *i*-Pr Me), -0.6 ($\Delta\nu_{1/2} = 260$ Hz, 9H, PMe_3). *IR*: 635 (w), 665 (s, PMe_3), 733 (s, PMe_3), 783 (m), 804 (m), 814 (s), 841 (w), 945 (s, PMe_3), 990 (m), 1038 (m), 1119 (m), 1140 (m), 1150 (m), 1171 (m), 1283 (m, PMe_3), 1298 (w, PMe_3), 1308 (w), 1319 (w), 1341 (m), 1424 (w, PMe_3), 3082 (w), 3214 (m) cm^{-1} . *Anal. calcd for* $\text{C}_{13}\text{H}_{24}\text{VNPCl}$: C, 50.09; H, 7.76; N, 4.49; V, 16.34; Cl, 11.37. Found: C, 49.95; H, 7.91; N, 4.29; V, 16.27; Cl, 11.80.

Synthesis of (η^5, η^1 - $\text{C}_5\text{H}_4\text{CH}_2\text{CH}_2\text{N}i\text{-Pr}$) $\text{V}(\eta^4\text{-C}_6\text{H}_{10})$ (**5**)

From 4: To a solution of 0.67 g of **4** (2.1 mmol) in 20 mL of THF, 2,3-dimethyl-1,3-butadiene (0.75 mL, 6.3 mmol) was added to the green solution. 49 mg of Na-sand (2.1 mmol) was added to 50 g of frozen Hg and carefully dissolved by thawing out the Hg. When the Na/Hg was at room temperature it was added to the vanadium solution, and the solution was stirred for two hours. The dark green THF solution was transferred into a new Schlenk and the residual Hg was washed twice with 5 mL THF. All THF solutions were combined, the volatiles removed *in vacuo*, and the resulting dark solid stripped twice with 10 mL pentane. The solid was then extracted twice with 30 mL pentane and crystallized by cooling to -25 °C. **5** was obtained as dark green crystals, 0.14 g (0.50 mmol, 24%).

From $VCl_3(THF)_3$: 6.59 g $VCl_3(THF)_3$ (17.6 mmol) was dissolved in 150 mL THF and 4.0 mL PMe_3 (38.6 mmol) was added. The solution was stirred for an hour after which it was cooled with an alcohol bath (bath temperature -50 °C). 20 mL 0.88 M MeLi solution in ether (17.6 mmol) was slowly added (5 minutes) to an ice-cooled solution of 2.71 g $C_5H_5CH_2CH_2N(H) i-Pr$ (17.6 mmol) in 20 mL THF and stirred for half an hour. The cooled ligand solution was slowly added to the cooled vanadium solution, and stirred at low temperature for one hour. The solution was then heated to room temperature, stirred for one night, and cooled with an alcohol bath (bath temperature -30 °C). 20 mL 0.88 M MeLi solution in ether (17.6 mmol) was slowly added (5 minutes). The solution was stirred at low temperature for half an hour, and at room temperature for two more hours, after which 2.5 mL 2,3-di-methyl-butadiene (22.1 mmol) was added. 0.40 g Na-sand (17.6 mmol) was added to 140 g of frozen Hg and carefully dissolved by thawing out the Hg. When the Na/Hg was at room temperature it was added to the vanadium solution, and the solution was stirred for four hours. The dark green THF solution was concentrated and transferred into a new Schlenk and the residual Hg was washed twice with 20 mL THF. All THF solutions were combined, the volatiles removed *in vacuo*, and the resulting dark solid stripped twice with 15 mL pentane. The solid was then extracted twice with 30 mL pentane and crystallized by cooling to -60 °C. **5** was obtained as dark green crystals in four portions, total 3.15 g (11.2 mmol, 63%). These crystals were suitable for single crystal X-ray structure determination.

1H NMR (C_6D_6 , 25 °C): δ 21.6 ($\Delta\nu_{1/2} = 900$ Hz), 4.9 ($\Delta\nu_{1/2} = 300$ Hz), -3.6 ($\Delta\nu_{1/2} = 240$ Hz). IR: 851(w), 864(w), 897(m), 955(m), 1026(s), 1053(s), 1121(m), 1146(m), 1165(m), 1230(m), 1262(m), 1379(w), 3040(w), 3090(w) cm^{-1} . Anal. calcd for $C_{16}H_{25}VN$: C: 68.07, H: 8.93, N: 4.96, V: 18.04; found: C: 65.92, H: 8.75, N: 4.95, V: 17.68. Carbon analyses, determined on several independently prepared samples of this compound, were consistently found to be too low, whereas the H, N and V values were as expected. This may be related to explosive decomposition of the compound in the analyzer.

Synthesis of (η^5, η^1 - $C_5H_4CH_2CH_2N i-Pr$) VCl_2 (**6**)

Onto a solid mixture of 0.30 g of **5** (1.1 mmol) and 0.30 g of $PhCl_2$ (1.1 mmol), 20 mL THF was condensed at liquid nitrogen temperature. Subsequently the mixture was thawed out.

Upon melting of the THF, a green solution formed which then quickly changed to brown. After reaching room temperature, the solution was stirred for an additional hour. The volatiles were removed *in vacuo* and the solid was stripped of remaining volatiles by stirring with 15 mL of toluene which was subsequently pumped off. The formation of 2,3-dimethyl-1,3-butadiene and iodobenzene as main organic reaction products was observed by GC/MS analysis of the volatiles. The solid was extracted with hot toluene. Cooling the extract to -25°C yielded 0.17 g (0.63 mmol, 57%) of **6** as red-brown crystals. Recrystallization by diffusion of pentane vapor into a THF solution yielded crystals suitable for X-ray structure determination.

$^1\text{H NMR}$ (THF- d_8 , 25°C): δ -0.8 ($\Delta\nu_{1/2} = 170$ Hz, *i*-Pr Me). IR: 629 (w), 685 (w), 723 (m), 781 (w), 810 (s), 826 (m), 845 (m), 866 (m), 945 (w), 959 (w), 974 (m), 1003 (w), 1017 (w), 1034 (w), 1053 (w), 1071 (w), 1111 (w), 1146 (m), 1163 (w), 1173 (w), 1231 (w), 1254 (m), 1314 (w), 1327 (w), 1339 (w), 3081 (w), 3177 (w) cm^{-1} . Anal. calcd for $\text{C}_{10}\text{H}_{15}\text{VNCl}_2$: C: 44.31, H: 5.58, N: 5.17, V: 18.79, Cl: 26.16; found: C: 44.36, H: 5.50, N: 5.23, V: 18.72, Cl: 25.69.

Ethene polymerization experiments

Polymerization reactions were carried out in a thermostated (electrical heating, water cooling), pressure-controlled Medimex 1l stainless steel autoclave, under batch conditions. For each run, the autoclave was charged with 250 mL toluene and 5.5 mL of a 1.4 M MAO (7.7 mmol) solution in toluene. The autoclave was heated to 50 °C and pressurized with ethene (3 bar). A catalyst precursor solution was made by dissolving 15 μmol of either **4**, **6** or **7** in 10 mL of toluene and polymerization was started by injecting this solution into the autoclave, ethene was continuously fed to the reactor. After 30 min. the runs were interrupted by the injection of 10 mL of methanol. The reactor was then vented and opened to the atmosphere. The polyethene was stirred in a mixture of 300 mL of methanol and 100 mL 0.5 M HCl in H_2O for several hours, collected on a glass frit and rinsed four times with 100 mL of methanol. The products were then dried *in vacuo* at 80 °C.

4/MAO: yield: 7.0 g; M_w : 15100; M_n : 7970; M_w/M_n : 1.9.

6/MAO: yield: 4.7 g; M_w : 14900; M_n : 4900; M_w/M_n : 3.0; melting point: 129 °C; $^1\text{H NMR}$ ($\text{C}_2\text{D}_2\text{Cl}_2$, 125°C): δ 5.97 (m, R- $\text{CH}_2\text{-CH=CH}_2$), 5.04 (d, $J = 17.1$ Hz, R- $\text{CH}_2\text{-CH=CHH}$), 4.98 (d, $J = 10.3$ Hz, R- $\text{CH}_2\text{-CH=CHH}$), 2.10 (q, $J = 7.1$ Hz, R- $\text{CH}_2\text{-CH=CH}_2$), 0.94 (t, $J = 6.9$ Hz, CH_3).

7/MAO: yield: 12.0 g; M_w : 139000; M_n : 59500; M_w/M_n : 2.3; melting point: 134 °C.

5.5 References

- (1) Shapiro, P.J.; Bunel, E.; Schaefer, W.P.; Bercaw, J.E., *Organometallics*, **1990**, *9*, 867.
- (2) Brintzinger, H.H.; Fischer, D.; Mülhaupt, R.; Rieger, B.; Waymouth, R.M., *Angew. Chem. Int. Ed. Eng.*, **1995**, *34*, 1143.

- (3) Examples of Cp-amido complexes of the group 5 metal tantalum (ref. a), the group 6 metal chromium (ref. b) and the group 7 metal rhenium (ref. c) have been reported: (a) Blake Jr., R.E.; Antonelli, D.M.; Henling, L.M.; Schaefer, W.P.; Hardcastle, K.I.; Bercaw, J.E., *Organometallics*, **1998**, *17*, 718. (b) Liang, Y.; Yap, G.P.A.; Rheingold, A.L.; Theopold, K.H., *Organometallics*, **1996**, *15*, 5284. (c) Wang, T-F.; Lai, C-Y; Hwu, C-C.; Wen, Y-S., *Organometallics*, **1997**, *16*, 1218.
- (4) (a) Fan, L.; Harrison, D.; Woo, T.K.; Ziegler, T., *Organometallics*, **1995**, *14*, 2018. (b) Schmid, R.; Ziegler, T., *Organometallics*, **2000**, *19*, 2756.
- (5) (a) Sinnema, P-J.; van der Veen, L.; Spek, A.L.; Veldman, N.; Teuben, J.H., *Organometallics*, **1997**, *16*, 4245. (b) Sinnema, P-J., *Ph.D. Thesis*, Groningen, the Netherlands, **1999**.
- (6) Klouras, N., *Z. Naturforsch.*, **1991**, *46b*, 650.
- (7) Fowles, G.W.A.; Pleass, C.M., *J. Chem. Soc.*, **1957**, 1674.
- (8) Christopher, J.J.; Diamond, G.M.; Jordan, R.F.; Petersen, J.L., *Organometallics*, **1996**, *15*, 4038.
- (9) Bradley, D.C.; Chisholm, M.H., *Acc. Chem. Res.*, **1976**, *9*, 273.
- (10) McKnight, A.L.; Masood, M.A.; Waymouth, R.M.; Straus, D.A., *Organometallics*, **1997**, *16*, 28798.
- (11) Nieman, J.; Teuben, J.H.; Huffman, J.C.; Caulton, K.G., *J. Organometallic Chem.*, **1983**, *255*, 193.
- (12) (a) Brandsma, M.J.R.; Brussee, E.A.C.; Meetsma, A.; Hessen, B.; Teuben, J.H., *Eur. J. Inorg. Chem.*, **1998**, 1867. (b) Wills, A.R.; Edwards, P.G., *J. Chem. Soc. Dalton Trans.*, **1989**, 1253.
- (13) (a) Wills, A.R.; Edwards, P.G., *J. Chem. Soc. Dalton Trans.*, **1989**, 1253. (b) Berno, P.; Gambarotta, S., *J. Chem. Soc. Chem. Comm.*, **1994**, 2419. (c) Cummins, C.C.; Schrock, R.R.; Davis, W.M., *Inorg. Chem.*, **1994**, *33*, 1448.
- (14) Luinstra, G.A.; Teuben, J.H., *J. Chem. Soc. Chem. Comm.*, **1990**, 1470.
- (15) Gerlach, C.P.; Arnhold, J., *Organometallics*, **1997**, *16*, 5148.
- (16) Dorer, B.; Prosenc, M-H.; Rief, U.; Brintzinger, H.H., *Organometallics*, **1994**, *13*, 3868.
- (17) (a) Cowley, A.H.; Hair, G.S.; McBurnett, B.G.; Jones, R.A., *Chem. Comm.*, **1999**, 437. (b) Devore, D.D.; Timmers, F.J.; Hasha, D.L.; Rosen, R.K.; Marks, T.J.; Deck, P.A.; Stern, C.L., *Organometallics*, **1995**, *14*, 3132.
- (18) In order to minimize loss of product during isolation, the diene adduct **5** can be synthesized starting from $VCl_3(THF)_3$, and by generating **1**, **3** and **4** *in situ*, in a 63% yield.
- (19) Gambarotta, S.; Floriani, C.; Chiesi-Villa, A.; Guastini, C., *Inorg. Chem.*, **1984**, *23*, 1739.
- (20) Aistars, A.; Newton, C.; Rübenstahl, T.; Doherty, N.M., *Organometallics*, **1997**, *16*, 1994.

- (21) (a) Willgerodt, C., *J. Prakt. Chem.*, **1886**, 33, 154. (b) Paquette, L.A., *Encyclopedia of reagents for organic synthesis*; Wiley, New York, **1995**, Vol. 6, pp 3984 - 3987.
- (22) Although the vanadium di-chloro complex **6** is only sparingly soluble in toluene this is still the preferred solvent for purification. Crystals obtained from THF persistently contained residual solvent, as indicated by elemental analysis. Single crystals obtained from THF/pentane were used for a crystal structure determination and did not contain solvent in the crystal lattice.
- (23) Petersen, J.L.; Dahl, L.F., *J. Am. Chem. Soc.*, **1975**, 97, 6422.
- (24) For the effect of chain termination on the end group of the polymer, see for instance: Resconi, L.; Fait, A.; Piemontesi, F.; Colonna, M.; Rychlicki, H.; Zeigler, R., *Macromol.*, **1995**, 28, 6667.
- (25) Sinn, H., *Macromol. Symp.*, **1995**, 97, 27.
- (26) Christopher, J.N.; Diamond, G.M.; Jordan, R.F.; Petersen, J.L., *Organometallics*, **1996**, 15, 4038.
- (27) Sinnema, P.-J.; Liekelema, K.; Staal, O.K.B.; Hessen, B.; Teuben, J.H., *J. Mol. Catal. A*, **1998**, 128, 143.
- (28) Luetkens Jr., M.L.; Sattelberger, A.P.; Murray, H.H.; Basil, J.D.; Fackler Jr., J.P.; Jones, R.A.; Heaton, D.E., *Inorg. Synth.*, **1989**, 26, 7.
- (29) Kurras, E., *Naturwiss.*, **1959**, 5, 171.

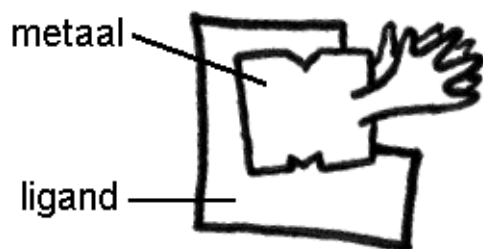
Samenvatting

Stel je voor dat je een grote kolf vult met Lego-blokjes. Iedereen weet dat deze blokjes niet spontaan aan elkaar gaan zitten, daar moet je zelf bij helpen: je moet elk blokje apart oppakken en aan het bouwwerk zetten. Zonder dat je het beseft, voldoe je op deze manier aan de drie belangrijkste voorwaarden om jezelf een katalysator te kunnen noemen. Zonder jou gaan de blokjes niet aan elkaar zitten (een katalysator knoopt moleculen aan elkaar die dat uit zichzelf niet of langzaam zullen doen), jij maakt op het einde geen deel uit van het bouwwerk (een katalysator versnelt een reactie, maar zit niet in het eindproduct) en je bent zelf aan het einde van het bouwen niet veranderd (een katalysator neemt deel aan de reactie, maar is aan het einde van de reactie onveranderd).

Er bestaan in dit verhaal nog een aantal overeenkomsten met een chemische katalysator. Tijdens het bouwen houd je met je ene hand het bouwwerk vast, terwijl je met je andere hand een blokje oppakt en aan het bouwwerk zet. Een chemische katalysator werkt niet anders, alleen spreken we nu over moleculen in plaats van blokjes en bouwwerken. Ook maken de katalysatoren die in dit proefschrift zijn beschreven geen Lego-auto's, maar plastics. Het grote verschil tussen de twee is dat een Lego-auto bestaat uit tientallen van elkaar verschillende bouwblokjes, terwijl het plastic maar bestaat uit één, twee of hooguit drie van elkaar verschillende blokjes. De katalysator pakt deze blokjes, die monomeren genoemd worden (Grieks: monos = alleen, enkel; meros = deeltje) en knoopt ze aan elkaar. Zo ontstaan lange ketens die we polymeren noemen (Grieks: polys = veel). Iedereen kent de naam PVC wel en de meesten zullen dit herkennen als die lange plastic buizen, waar je zo goed pijltjes mee kunt schieten. De afkorting PVC staat voor PolyVinylChloride: het polymeer van het monomeer vinylchloride.

Hoe zit een chemische katalysator nu in elkaar en hoe ziet hij eruit. De chemische katalysatoren die in dit proefschrift zijn beschreven bestaan uit een metaalatoom, omgeven door een ligand. Het metaalatoom heeft twee armpjes waarmee de polymeren gebouwd kunnen worden (Figuur 1). Even voor de chemici: het metaal is "vanadium", het ligand heet "amido gefunctionaliseerd

cyclopentadienyl" (of afgekort Cp-amido) en als het ligand aan het metaal gebonden zit heet het geheel "een complex". Vandaar de titel van dit proefschrift.



Figuur 1: Een katalysator.

Als je een Lego-bouwoos koopt zit daar een bouwtekening bij die beschrijft hoe het bouwwerk in elkaar gezet moet worden. In een katalysator kan het ligand vergeleken worden met een bouwtekening: het ligand geeft aanwijzingen aan het metaal welk blokje gepakt moet worden en hoe dat aan het bouwwerk gezet moet worden. Je kunt je voorstellen dat een groot ligand heel weinig ruimte overlaat voor de twee handen aan het metaal om een grote bouwsteen op te pakken of een groot bouwwerk vast te houden. Het is mogelijk om het ligand zo'n vorm te geven dat de bouwstenen slechts op één bepaalde manier vastgehouden kunnen worden, en ook maar op één bepaalde manier aan het bouwwerk gezet kunnen worden. Het ligand functioneert dan als een mal. Dit zijn belangrijke gegevens, omdat de eigenschappen van het uiteindelijke product, het plastic, afhankelijk zijn van bijvoorbeeld welk bouwblok gebruikt is en wat de ketenlengte van de polymeerketens is. Zo is het plastic dat voor boterhamzakjes gebruikt wordt heel anders dan het plastic dat voor tuinstoelen gebruikt wordt.

Veel van het huidige onderzoek heeft als doel het begrijpen van de invloed van het ligand op het uiterlijk van het polymeer of plastic. Daarbij wordt als metaalatom vooral titaan en zirkoon gebruikt, en wordt geëxperimenteerd met verschillende liganden. In mijn onderzoek gebruik ik een ligand dat al bekend is (Cp-amido), maar zet dat aan een metaal vast dat hier nog niet eerder voor gebruikt is (vanadium). In Hoofdstuk 5 beschrijf ik hoe je hier een katalysator van kunt maken en vergelijk ik mijn "Cp-amido vanadium-katalysator" met een "Cp-amido titaan-katalysator". Het blijkt dat de vanadium-katalysator iets langzamer werkt dan de

titaan-katalysator en dat hij veel kortere ketens maakt. In de Hoofdstukken 2, 3 en 4 heb ik een Cp-amido vanadium complex gemaakt dat maar één hand heeft in plaats van twee. Het kan nu wel een bouwsteen oppakken, maar kan daar niks mee bouwen. Op die manier kon ik kijken hoe het metaal de bouwsteen precies vasthoudt en welke bouwsteen hij het liefste vastheeft. Het hele onderzoek gaat dus over fundamentele principes in de polymerisatie. Het is niet de bedoeling geweest om een katalysator te maken die commercieel gebruikt kan worden, maar om meer inzicht te krijgen in het werken van een katalysator.

Summary

Since the discovery of olefin polymerization catalysts based on titanium and aluminum by Ziegler, polyolefins have grown to become one of the most important group of plastics. Millions of tons of polyolefins are produced every year, and the production is still expanding. Soluble single-site catalysts, that were once used as simple models for the heterogeneous Ziegler catalysts, have now developed into a new and independent group of catalysts. Most of these catalysts are based on the group 4 metals titanium and zirconium in combination with linked bis-Cp ligands or amido functionalized Cp (Cp-amido) ligands. By tuning of the ligands the catalysts can produce various types of polymer, and new polymer structures that can not be produced by the Ziegler catalysts, have become available.

Despite the increasing number of metals that are tested as possible single-site catalysts, vanadium, which is an important metal in the Ziegler-Natta catalysis, is mostly neglected. This thesis describes the synthesis of vanadium complexes with Cp-amido ligands, with the aim of developing the organometallic chemistry of these complexes, and to compare isostructural d^0 and d^1 (Cp-amido) MCl_2 complexes ($M = Ti$ and V) as catalyst precursors.

In Chapter 2 the synthesis of vanadium(V) Cp-amido complexes is discussed. Different routes have been studied to introduce the Cp-amido ligand on a vanadium(V) imido compound. Amine elimination gives the best results when an ethylene bridged Cp-amido ligand is used; a propylene bridged ligand can only be

introduced in a salt metathesis reaction. Ligand introduction was performed on a vanadium complex with a *t*-Bu imido ligand, variation in the imido substituent is possible by imido exchange after introduction of the Cp-amido ligand. Alkylation yielded one of the first structurally characterized vanadium(V) methyl complexes.

Starting from the methyl complexes synthesized in Chapter 2, Chapter 3 describes the generation of well-defined cationic Cp-amido vanadium(V) complexes. Methyl abstraction performed with Lewis acidic borane ($\text{B}(\text{C}_6\text{F}_5)_3$) or borate ($[\text{Ph}_3\text{C}][\text{B}(\text{C}_6\text{F}_5)_4]$) reagents, generated the expected $[(\text{Cp-amido})\text{V}(\text{NR})]^+$ species. Protonation with the Brønsted acid $[\text{PhNMe}_2\text{H}][\text{B}(\text{C}_6\text{F}_5)_4]$ showed an unexpected activation of the amido substituent of the Cp-amido ligand. The cationic $[(\text{Cp-amido})\text{V}(\text{NR})]^+$ species were reacted with 2,3-dimethyl-butadiene and 2-butyne, and based on NMR experiments, insertion of these substrates into the vanadium-amido bond is proposed.

Reaction of the cationic $[(\text{Cp-amido})\text{V}(\text{NR})]^+$ species with mono-olefins results in the reversible coordination of these olefins. Chapter 4 describes the characterization of these adducts, which are the first adducts of d^0 metal centers with simple olefins like ethene and propene. Theoretical calculations on a model compound predicts a strong vanadium-olefin bond strength, although the reason for this strong bonding is not completely clear. The equilibrium constant for the coordination of the olefins is largely dependent on the steric properties of the coordinating olefin; the coordination is exothermic with small ΔH^0 and ΔS^0 values.

Chapter 5 describes the synthesis of Cp-amido vanadium complexes, where the vanadium center is in the oxidation state +2, +3 or +4. Ligand introduction on vanadium(III) was performed by a step-wise salt metathesis. One electron reduction yields a Cp-amido vanadium(II) complex, which can be oxidized to a Cp-amido vanadium(IV) di-chloride. The use of the Cp-amido vanadium(IV) complex in ethene polymerization is tested and compared to the isostructural titanium analogue. The activity of the vanadium catalyst is lower than that of the titanium catalyst, and the produced polymer has a much lower molecular weight. The ^1H NMR spectrum of the produced polymer indicated that β -elimination is the major termination pathway in the vanadium catalyzed ethene polymerization, although chain transfer to aluminum also takes place. A problem in these polymerizations is that the active species is

unknown, and it is possible that the Cp-amido ligand is not inert towards the MAO cocatalyst.